RECRYSTALLIZATION OF FRACTURE-INFILLING CALCITE: EVIDENCE FROM $\delta^{18}O$, $\delta^{13}C$, U/Th AGES AND FLUID INCLUSIONS

A Thesis Submitted to the Committee on Graduate Studies

in Partial Fulfilment of the Requirements for the

Degree of Master of Science

in the Faculty of Arts and Science

TRENT UNIVERSITY

Peterborough, Ontario, Canada

Watershed Ecosystems M.Sc. Program

June 2000

ABSTRACT

Recrystallization of fracture-infilling calcite: Evidence from $\delta^{18}O$, $\delta^{13}C$, U/Th ages and fluid inclusions

Andrew Robert Bukata

The origin of fracture-infilling calcite from the fractured crystalline rock on the Precambrian shield at the Chalk River, Ontario properties of Atomic Energy of Canada Limited was investigated using $\delta^{18}O$, $\delta^{13}C$, U/Th ages and fluid inclusion micro-thermometry. A U/Th extraction-separation technique was developed using the commercially available UTEVA™ resin (EiChrom Industries). The method gave yields of >70% U and >80% Th, and did not introduce isotopic fractionation. Using this method, U-series ages of <9 to >350 ka were measured in the calcites. Open-vein calcites tended to have more ^{18}O-enriched and ^{13}C-depleted values (15 to 22‰ and -11 to -6‰) than sealed-vein calcites (14 to 20‰ and -9 to -5‰). Most fluid inclusions had homogenization temperatures between 70 and 90°C, and salinities of <6 wt. % NaCl. The geochemical characteristics of the fracture-infilling calcites indicate alteration or recrystallization of a metamorphic calcite by modern meteoric recharge, with statistically more calcite precipitation occurring between periods of continental glaciation.

ACKNOWLEDGEMENTS

A large debt of gratitude is owed to many people who have assisted me throughout the completion of this project. First and foremost, the Cornett Family. Jack for the supervision, encouragement, and support, without which this project would not have been possible, and Janice for her kindness and hospitality on my many trips to Chalk River. Tom Kotzer was generous with both his time and geochemical expertise, and brought an infectious curiosity which caused me to delve deeper into the material than I may have without the encouragement. Mel Gascoyne was generous with both standards and spike as well as radiochemical expertise. Abdel El-Shaarawi took time from his busy schedule to assist me with the statistical analysis, although he should not be held responsible for any far-reaching interpretations made as a result. The thesis and project benefitted from the critical input of Doug Evans.

Many people helped with the technical aspects of the project. I would like to thank Kerry Klassen for performing the stable isotope analysis and Kurt Kyser for making the analyses possible. I would also like to thank Kurt for his hospitality on my trips to Queen's to perform the fluid inclusion analysis. Jim Young, Tammie Eve and Ragu Rao all assisted with the radiochemical analysis. Richard Hughes performed the ICP-MS analysis at Trent University. Jerzy Adwent prepared thin-sections for fluid inclusion analysis. The staff at the University of Western Ontario and the University of Ottawa must be thanked for performing the XRD analysis.

I would like to thank my family for their endless support of all my endeavours. Most importantly, I would like to thank Jennifer Surtees for her love and support throughout the project and beyond. Jennifer not only married me and made me infinitely happy, but also kept me focussed on the task at hand when this project seemed to be beyond completion.

TABLE OF CONTENTS

LIST OF FIGURES

LIST OF TABLES

1 - INTRODUCTION

Carbonate minerals are currently found in the fractures of crystalline rocks of the Canadian Shield. These precipitated from one of three mechanisms: 1) precipitation from an ascending hydrothermal fluid; 2) precipitation from a descending low temperature fluid; or 3) re-crystallization or alteration of a previously deposited calcite by a subsequent ascending or descending fluid. The geochemical characteristics of the calcite will reflect the physico-chemical characteristics of the groundwater or groundwaters involved in calcite formation. If systematic variations exist between the geochemical characteristics of calcite in fractures currently open and sealed with respect to groundwater flow, these characteristics may be used to determine the long term hydrogeology and hydrogeologic characteristics of the groundwater flow in the crystalline rock.

This thesis examines the stable isotopic composition ($\delta^{13}C$ and $\delta^{18}O$), the physico-chemical characteristics of fluid inclusions, and the $^{230}Th/^{234}U$ ages of the fracture-infilling calcite from the properties of the Chalk River Laboratories (CRL), Chalk River, Ontario, of Atomic Energy of Canada Limited (AECL). These measurements were used to constrain the timing, temperature, salinity and stable isotopic composition of the fluids responsible for calcite formation in the fractures. The stable isotopic composition of the calcites, fluid inclusion salinities and homogenization temperatures, and U-series ages of the calcites were compared to the ranges of values characteristic of typical ascending and descending fluids to test the alternative formation scenarios of these fracture-infilling calcites.

1.1 - OVERVIEW AND OBJECTIVES OF THIS STUDY

The stable isotope (^{13}C and ^{18}O) composition, U/Th geochemistry including U-series dating, fluid inclusion formation temperature and salinity of fracture-infilling calcite from this investigation were combined with geochemical data previously gathered at Chalk River (Bottomley, 1987; Bottomley, 1988; Bottomley and Veizer, 1992, and Lee et al., 1998 and references therein) to constrain the conditions of calcite formation and the geochemical progression of fluids at Chalk River. This investigation integrates the results of stable isotope, fluid inclusion, and U-series measurements on the same samples; previous investigations at Chalk River and elsewhere had only used one or two of these tools. Integrating the results of these geochemical techniques allows the stable isotopic composition, temperature, salinity and age of the fluid responsible for fracture-infilling calcite to be established. The specific objectives of the investigation are listed below.

1) To determine whether there are systematic differences in the geochemistry of calcite from fractures characterized as open or sealed with respect to groundwater flow.

2) To establish whether any depth trends exist in the fracture-infilling calcite with respect to $\delta^{13}C$, $\delta^{18}O$, U/Th geochemistry or U-series age.

3) To determine whether the calcite precipitated from one of the five major fluid "events" as established by the regional geologic history of the Canadian Shield.

4) To establish whether fluid inclusion formation temperature and melting points can be used to constrain the temperature and salinity of the fluid responsible for fracture-infilling calcite formation.

5) To develop a column extraction/separation method for rapid chemical preparation for

U-series dating and to verify the technique with standards.

6) To perform $^{230}Th/^{234}U$ dating on the fracture-infilling calcite.

7) To use the fluid inclusion, stable isotope and U-series ages to construct the history of the geochemistry of calcite precipitating fluids in the Chalk River area.

8) To determine whether the timing of calcite precipitation is linked with the glacial history of the region.

The results of this investigation will allow the geochemical characteristics of the calcite to be used to determine whether the calcites formed from an ascending hydrothermal fluid, a low temperature descending fluid, or have been altered by ascending or descending fluids since initial deposition. The specific work in this thesis lead to the development of a new U/Th extraction/separation technique applicable to U-series dating. The measurements were integrated with the stable isotopic and fluid inclusion analysis in this thesis to provide a more robust examination of the fracture-infilling calcites than previously undertaken. Previous investigations preformed on fracture-infilling calcite have only made use of one or two of the analytical methods. The integration of the results from all three techniques performed in this investigation allowed information about the timing, temperature and isotopic composition of the calcite precipitating fluids to be obtained from the same samples.

1.2 - BACKGROUND THEORY

Background information regarding the interpretation of the stable isotope, fluid inclusion and U/Th data is discussed in the following sections.

1.2.1 - STABLE ISOTOPES IN CALCITE (^{13}C and ^{18}O)

Isotopes are atoms of the same element which have different numbers of neutrons, but the same number of protons in the nucleus. As a result, isotopes exhibit the same chemical behaviour, but have slightly different reaction kinetics due to their small mass difference (Kyser, 1987). Any physical or chemical reaction which results in a phase transformation or the formation of a new compound will result in the fractionation of isotopes, such that the heavier isotope will tend to be concentrated in the lower energy, more condensed phase.

Isotopic fractionation is temperature dependent, with the degree of isotopic fractionation decreasing as the temperature of the system is increased. The temperature dependency of the fractionation results because the difference between energy levels of molecules or bonds involving heavy isotopes compared to those involving only lighter isotopes becomes less significant at high temperatures. At low temperatures, the energy difference is large relative to the total energy of the system, whereas at higher temperatures, the relative energy difference decreases. The theory and application of stable isotope analysis to environmental science is extensively covered elsewhere (Faure, 1986; and Kyser, 1987).

"Isotopic fractionation" and "isotopic composition" have very specific definitions. The mathematical definitions and relationships between the terms are given as equations 1-1 to 1-4 (Faure, 1986; and Kyser, 1987). The isotopic fractionation (α) between two phases (A and B) is defined as:

$$\alpha_{A-B} = \frac{R_A}{R_B} \qquad (1-1)$$

Where R_A represents the ratio of rare (heavy) to common (light) isotopes in phase A, and R_B is the same for phase B. As it is easier to measure the relative differences between the isotopic ratios of two substances than it is to measure the absolute ratio, the value of isotopic composition is normally reported in delta (δ) notation relative to a standard. This is calculated as:

$$\delta_A = \frac{R_A - R_{Std}}{R_{Std}} * 1000 \qquad (1-2)$$

Where R_{std} is the absolute ratio in a standard. The delta value (δ_A) is then reported as a per mil (‰) value relative to the standard used. The fractionation factor between the two phases may then be given as:

$$\alpha_{A-B} = \frac{1 + \delta_A/1000}{1 + \delta_B/1000} = \frac{1000 + \delta_A}{1000 + \delta_B} \qquad (1-3)$$

or

$$1000\ln\alpha_{A-B} = \delta_A - \delta_B = \Delta_{A-B} \qquad (1-4)$$

In this investigation, the isotopic compositions of the calcium carbonate mineral calcite ($CaCO_3$) were determined.

1.2.1.1 - OXYGEN ISOTOPES

There are three stable isotopes of oxygen, ^{16}O, ^{17}O and ^{18}O. Of interest to this study are the heavy (^{18}O) and light (^{16}O) isotopes. The greater mass difference and higher abundances of ^{18}O and ^{16}O than ^{17}O make the $^{18}O/^{16}O$ ratio most widely used in isotopic investigations. The natural abundances of the stable isotopes of oxygen are;

$$^{16}O = 99.763\ \%$$
$$^{17}O = 0.0375\ \%$$
$$^{18}O = 0.1995\ \%$$

$\delta^{18}O$ values in this thesis are reported relative to the V-SMOW standard. v-SMOW is an acronym for Vienna Standard Mean Ocean Water. V-SMOW, has a ratio of $^{18}O/^{16}O$ of $2005.2*10^{-6}$ (Baertschi, 1976). SMOW is assigned a $\delta^{18}O$ value = 0, anything with $\delta^{18}O$ value > 0 is referred to as "enriched relative to SMOW," and anything with $\delta^{18}O$ value < 0 is referred to as "depleted relative to SMOW."

The fractionation of ^{18}O during the precipitation of calcite is very temperature dependent and follows the relationship:

$$1000\ln\alpha_{calcite-water} = 2.78 * \frac{10^6}{T^2} - 3.39 \quad (O'Neil\ et\ al.,\ 1969) \qquad (1-5)$$

The temperature (T) in the fractionation factor is in Kelvin. Given the temperature dependent fractionation of ^{18}O in the calcite-water system, the $\delta^{18}O$ value of the calcite ($\delta^{18}O_{calcite}$) will be largely affected by both the oxygen isotopic composition of the water ($\delta^{18}O_{water}$) and the temperature of calcite formation. As there are two unknowns in the equation, without constraining either the temperature of formation or the $\delta^{18}O_{water}$,

interpretation of the $\delta^{18}O$ values in the calcite is speculative at best.

1.2.1.2 - CARBON ISOTOPES

There are two stable isotopes of carbon, ^{12}C and ^{13}C. The relative abundances are;

$$^{12}C = 98.89\ \%$$
$$^{13}C = 1.11\ \%$$

$\delta^{13}C$ values in this thesis are reported relative to a Belemnite from the Pee Dee formation (V-PDB) standard. The $\delta^{13}C$ of V-PDB is set to zero, with a $^{13}C/^{12}C$ ratio of $1123.75*10^{-5}$ (Craig, 1957). The fractionation factor for ^{13}C between calcite and bicarbonate is defined as:

$$1000\ln\alpha_{calcite-bicarbonate} = 0.095 * \frac{10^6}{T} + 0.9 \text{ (Deines et al., 1974)} \qquad (1-6)$$

The small fractionation and the small temperature dependency of the fractionation factor allow the $\delta^{13}C$ of the calcite ($\delta^{13}C_{calcite}$) to be interpreted as indicating the source of the carbon in the calcite. Biological activity in the soil zone depletes the $\delta^{13}C_{HCO3}$- to between -23 and -15‰ at the Chalk River site (Lee et al, 1998). This will have a considerably larger effect on the $\delta^{13}C_{calcite}$ than temperature of calcite formation. For this reason, the $\delta^{13}C_{calcite}$ will be interpreted as an indication of the carbon source, rather than the formation temperature of the calcite.

1.2.2 - FLUID INCLUSION ANALYSIS

Fluid inclusions are small imperfections (1 to 50 μm) in a crystal matrix which trap a small amount of fluid from which the crystal is precipitating. As a result, the fluid

inclusion has physical and chemical properties which reflect the fluid from which the crystal formed. The theory and application of fluid inclusion analysis is extensively covered by Roedder (1984), Shepherd et al. (1985), and Goldstein and Reynolds (1994).

Minerals which have not undergone post depositional alteration may contain fluid inclusions which yield information about the formation temperature, salinity, chemical composition of the crystallization fluid, and the pressure of the system during crystal precipitation. However, in this study, neither micro-sampling of fluid inclusions for analysis of the chemical composition of the precipitating fluid, nor determination of the system pressure was performed, so they will not be discussed further.

The minimum temperature at which the crystal formed is determined by heating multi-phase fluid inclusions until the phases homogenize. The temperature at which this occurs is recorded as the temperature of homogenization (T_h) and represents the lowest possible formation temperature of the fluid inclusion, which is by extension, the lowest possible temperature at which that section of the crystal precipitated. The actual temperature of formation may have been higher if fluid inclusion formation occurred at a higher pressure. As the formation pressure was not determined, the T_h can only be interpreted as the minimum temperature of formation.

If the fluid inclusion is observed to be one phase (all liquid) at room temperature and atmospheric pressure, it may have formed from one of two possible origins. If the mineral has not undergone post depositional alteration, the fluid inclusion formed either at or below room temperature, or is meta-stable. A meta-stable inclusion is formed at < 50°C, and is too small to nucleate a vapour bubble due to internal pressure. In either case,

nothing more conclusive than T_h <=50°C can be recorded about a single-phase, all liquid fluid inclusion (Goldstein and Reynolds, 1994).

Freezing point depression is known to occur in solutions containing dissolved ions. To determine the salinity of the fluid inclusion, the fluid inclusion is cooled until the liquid freezes and then slowly heated to melt the inclusion. The temperature of final melting (T_m) is recorded. The degree of freezing point depression can then be converted to a weight percent NaCl equivalent (wt. % NaCl) using the following relationship:

$$\textit{Salinity (wt. \% NaCl)} = 0.00 + 1.78\Theta - 0.0442\Theta^2 + 0.000557\Theta^3 \qquad (1-7)$$

(*Bodnar et al*, 1992 *a+b*, *in Goldstein and Reynolds*, 1994),

Θ is the depression of the freezing/melting point below zero in degrees Celsius.

Given the possible origins for fluid inclusions in a crystal, it is important to characterize the fluid inclusion petrographically prior to analysis to ensure that the fluid inclusion was incorporated into the matrix during precipitation of the crystal, and not as the result of post depositional alteration of the crystal. The shape of the fluid inclusion and the fluid inclusion's petrographic relationship to the crystal matrix are used to characterize the fluid inclusion's origin.

A fluid inclusion may be characterized by petrographic examination of the thin section, as one of four possible types: I) Primary; II) Secondary; III) Pseudo-Secondary; or IV) Unknown. Only those fluid inclusions classified as primary by Roedder (1984), Shepherd et al. (1985), and Goldstein and Reynolds (1994) were analysed in this investigation. Primary fluid inclusions occur in growth bands in the crystal and have rounded to negative crystal shapes. A group of primary fluid inclusions in the same

growth band will have the same liquid to vapour ratio.

The T_h and T_m of primary fluid inclusions in this investigation were used to determine the minimum formation temperature and salinity of the fluids responsible for calcite precipitation. These parameters, along with the U-series ages and stable isotope ratios will be used to assess the palaeohydrology of the region.

1.2.3- URANIUM-SERIES DATING

Radiometric dating involves using the relative amounts of parent and daughter atoms, and the decay rates of the parent and daughter, to calculate the amount of time required for decay of the parent to accumulate the amount of daughter atoms present. The applicability of radio-isotopic dating techniques to a substance is contingent on whether the parent and daughter in the decay chain are physically or chemically isolated during formation of the material. If daughter ingrowth, or the unsupported decay of a daughter occur, information about the half life and initial activity of the sample can be used to determine the amount of time which has passed since the event which isolated the parent from the daughter. The use of the uranium decay series for dating samples is most easily applied to systems which exclude either U or Th during their formation and remain closed systems throughout their existence (Ivanovich and Harmon, 1992).

1.2.3.1 - U AND Th GEOCHEMISTRY

The redox chemistry of uranium and thorium in aqueous solution is the primary reason why these two nuclides are isolated from each other in the environment, and as a result form a useful dating pair. Uranium exists in one of four oxidation states, III, IV, V and VI, with IV and VI being the most common. Thorium has only one oxidation state,

IV. Both U(IV) and Th(IV) are relatively insoluble in water, with the high ionic potential of each species causing them to become adsorbed to the charged surfaces of particles (Faure, 1991). In the presence of molecular oxygen U(IV) is oxidized to U(VI), to form the soluble uranyl ion. The uranyl ion has lower ionic potential and thus is not scavenged by small particles in solution. Thus, in oxidizing aqueous environments, U is mobile as an aqueous ion, while Th is only mobile as a colloid. The uranyl ion can replace Ca^{2+} in calcite and aragonite precipitation, and Th^{4+} is strongly excluded. As a result, a freshly deposited calcite which is free of detrital contamination will include U and negligible Th. Following this, any thorium measured in a calcite is present as a result of either detrital contamination, or ingrowth of the radioactive daughter from U decay. Detrital contamination can be corrected for, allowing calcite to be used for U-series dating.

Carbonate minerals generally contain approximately 2 ppm U and negligible Th, with Th content correlated to detrital contamination (Gascoyne, 1992). Table 1-1 contains concentration ranges for U and Th in the natural environment.

1.2.3.2 - RADIOACTIVE DECAY OF U AND Th

All the decay series for U and Th end with the stable element lead. The U and Th decay series relevant to this investigation are ^{238}U and ^{232}Th, and are shown in Figure 1-1. α-decay occurs at a constant decay rate, and the α-particle emitted in each decay has a characteristic energy or characteristic energies.

While each radio-nuclide of the same element has a different α-decay energy, there are decay energy interferences from different elements in the same decay chain. Figure 1-2 shows the α-decay energies for the U and Th decay series. The α-decay

TABLE 1-1 - Summary of the concentration ranges of U and Th, and the Th/U ratios found in the natural environment.

	U (ppm)	Th (ppm)	Th/U	Reference
Igneous granite	2.2-6.1	8-33	3.5-6.3	Gascoyne, 1992
Metamorphic gneiss	2.0	5-27	1-30	Gascoyne, 1992
Sedimentary limestone	~2	0-2.4	<1	Gascoyne, 1992
Stream water	$4 X10^{-5}$	$<1 X10^{-4}$		Faure, 1991
Seawater	$3.1 X10^{-3}$	$6 X10^{-8}$		Faure, 1991

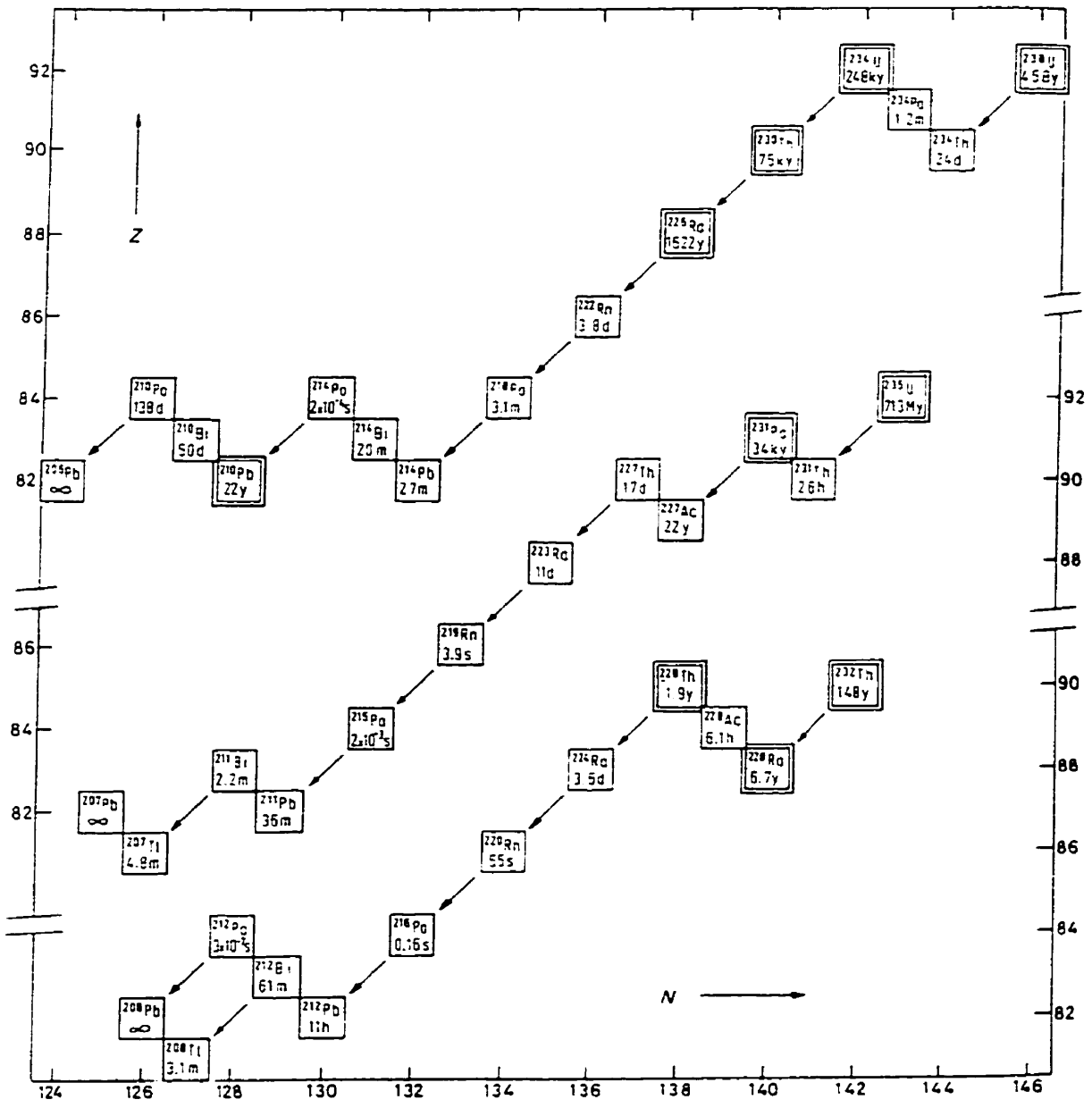

FIGURE 1-1 - The decay series of ^{238}U, ^{235}U, and ^{232}Th taken from Dicken (1992). α-decay is indicated by arrows downward to the left and β-decay is represented by boxes upward to the left. The half-life of each nuclide is also presented in the box. Z is the atomic number, or number of protons in the atom, and N is the number of neutrons in the nucleus.

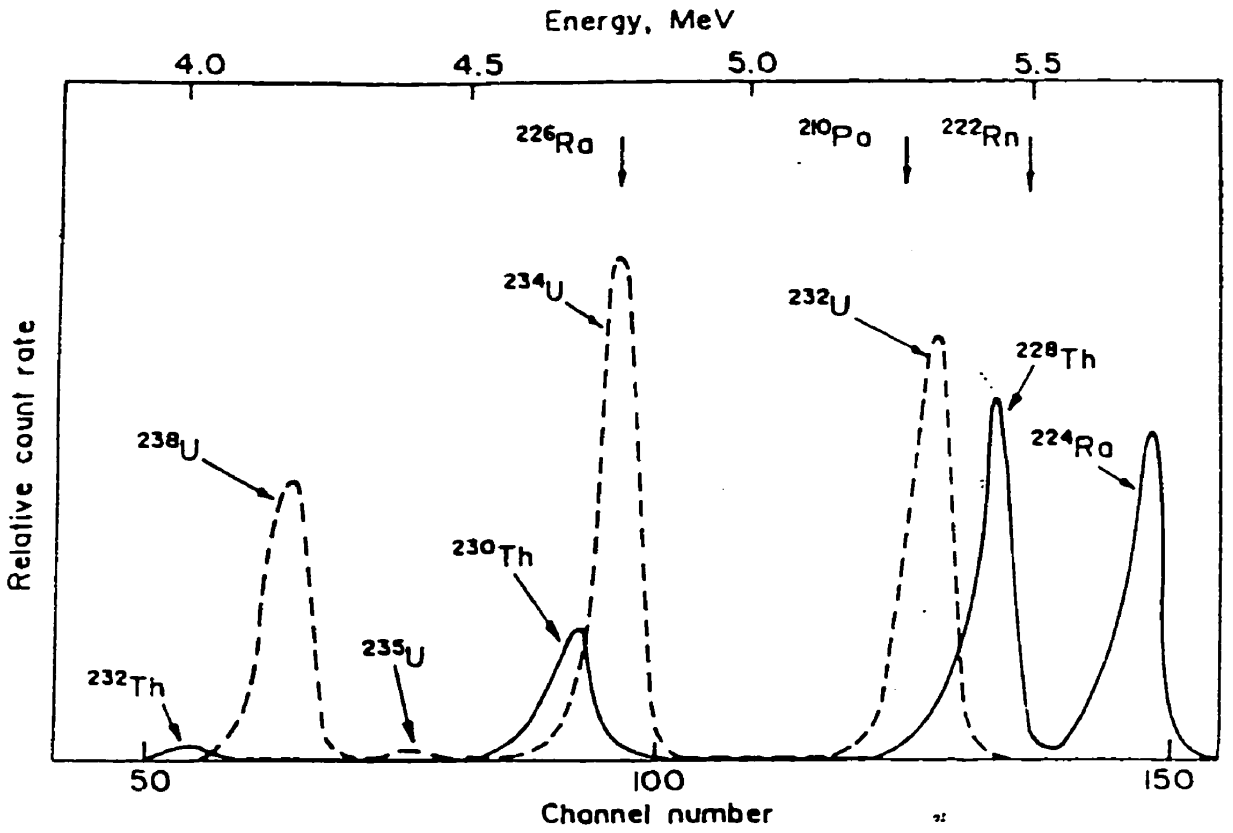

FIGURE 1-2 - The characteristic α-decay energies for the U-series actinides. Taken from Dicken (1992). The α-decay energy interferences between U and Th nuclides necessitate their separation prior to analysis by α-spectrometry.

energy interferences indicate that to measure U and Th accurately by α-spectrometry, it is necessary to separate U and Th chemically prior to their measurement.

U/Th Dating

The different solubility and mobility of U and Th in the environment, as well as the difference in their incorporation mechanism into calcite, make it possible to use the U/Th system to determine the crystallization age of a calcite. At formation, a pristine calcite should include U free of its daughter Th. Therefore, it is possible to use ingrowth of Th to calculate the age of a calcite. In this investigation, the parent-daughter pair $^{234}U/^{230}Th$ was used. ^{234}U has a half-life of 247,000 years and ^{230}Th has a half-life of 80,000 years; this allows for the dating of samples up to 350,000 years (350 ka) before present, with confidence using α-spectrometry (Gascoyne, 1992).

1.3 - CALCITE AS AN ENVIRONMENTAL MARKER

The chemical composition of calcite and its occurrence in a wide variety of geologic environments make it well suited to delineate numerous geochemical and physical processes. Stable isotope (^{13}C and ^{18}O) analysis, U-series dating and fluid inclusion analysis of calcite can yield information about the isotopic composition and salinity of the fluid which precipitated the calcite, the time of calcite crystallization, and the minimum temperature at which the calcite precipitated. This information and the ubiquitous nature of calcite in many geologic terrains make it useful in the study of a wide variety of geological processes.

Among the most widely studied environmental calcite deposits are speleothems or "cave calcites." Speleothems are banded calcite deposits which form from water seeping

into a cave after becoming saturated with respect to calcite in the overlying rock mass. The nature of the depositional process and the source of the fluids precipitating calcite have made speleothems widely used for both regional and global palaeoclimate reconstruction (Gascoyne, 1979; Gascoyne et al., 1980; Gascoyne et al., 1983; Li et al., 1989; Goede et al., 1996; Lauriol et al., 1997; and Bar-Matthews et al., 1999). As calcite deposition on the speleothem ceases if the cave is flooded, growth hiatuses in speleothem deposits from caves at or near sea level have been used to construct records of sea level fluctuations (Harmon et al., 1981; and Richards et al., 1994). Here, a speleothem growth hiatus represents a time when the speleothem was below sea level. In equatorial caves, this occurs during interglacial periods as a result of glacial meltwater entering the oceans.

The isotopic composition of fluid inclusions in speleothem carbonates has been analysed by destructive means (breaking the fluid inclusion to extract the fluid) in an attempt to develop a long term record of precipitation, and to calculate the temperature of the calcite formation using the temperature dependent fractionation of ^{18}O between water and calcite (Schwarcz and Young, 1980; and Harmon and Schwarcz, 1981). In addition to being used to determine the formation temperature of the calcite, non-destructive (heating and cooling) fluid inclusion analysis has been used to trace the thermal history of calcite during burial diagenesis (Goldstein, 1990) and the thermal alteration of a calcite cement (Muchez et al., 1991). These are only a few of the many studies of speleothem as an environmental marker.

Coral deposits are used in many of the same ways as speleothems and, in many cases, to study the same processes. The annual carbonate growth bands and U

incorporation by corals make them applicable to detailed palaeoclimate investigations. For example, Smith et al. (1997) found evidence of the Younger Dryas event in a submerged coral. The Younger Dryas event was a climatic reversal to colder conditions which existed in Europe between 11 and 10 ka. In addition, the growth bands have been used to develop a long term record of the atmospheric carbon isotope ratios (Nozaki et al., 1978), and coupled with high resolution U-series dating, corals have been used to estimate the atmospheric ^{14}C input function (Bard et al., 1990a). The calibration of atmospheric production of ^{14}C has also been performed with speleothems (Vogel and Kronfeld, 1997; and Gentry and Massault, 1997) In a manner similar to that used with speleothem determinations of palaeo-sea level, periods of coral growth have been correlated to sea level changes in equatorial regions (Bard et al., 1990b; Muhs et al., 1994; Muhs and Szabo, 1994; Szabo et al., 1994a; Bard et al., 1996; and Chappell et al., 1996).

In the late 1980's, a large banded calcite vein was discovered in Devils Hole, Nevada. It has been verified with U-series dating that the calcite has been deposited continually for the last 500 ka (Winograd et al., 1988; and Ludwig et al., 1992). This has allowed for the isotopic composition of carbon and oxygen in the calcite to be used in conjunction with the U-series age to develop a continental record of palaeoclimate comparable to the marine isotope record (Winograd et al., 1988; Ludwig, 1992; Winograd et al., 1992; Coplen et al., 1994; Crowley, 1994; Riggs et al., 1994; and Szabo et al., 1994b). Trends in the $\delta^{18}O$ values measured in the Devils Hole calcite have been used to determine the duration and structure of glacial and interglacial periods (Winograd et al.,

1997). In addition to the palaeoclimatic interpretation of the Devils Hole record, the geochemistry of the fracture coating calcite has been used to argue both for (Hill et al., 1995) and against (Stuckless et al., 1991) an upwelling component of deep-seated ground water involved in the precipitation of regional calcite deposits. If the depositional environment is stable over geologically meaningful time periods, the geochemical characteristics of deposited calcite can be used as a record of palaeoclimate, as is the case with the vein deposit at Devils Hole.

Surface deposits of calcium carbonates such as travertine and tufa are also used as proxy records of environmental conditions. Tufa deposition at a lake margin is dependent on the water level in the lake. This fact has allowed for U-series dating of tufa deposition to be used as a record of lake water level (Szabo et al., 1996). In arid regions, periods of travertine deposition have been dated and used as evidence of wetter periods in the regional palaeoclimate (Clark et al., 1991). The stable isotopic compositions of travertine deposits have also been used as records of the source and composition of the groundwater recharge responsible for calcite precipitation (Sultan et al., 1997).

Stable isotope measurements on calcite precipitated in the soil zone as pedogenic concretions in arid climates have been used as an indicator of palaeoclimate (Mack et al., 1994) and as a record of monsoon activity (Wang and Follomer, 1998).

The isotope and trace element composition of marine carbonates which have not undergone diagenesis have been used as a record of the seawater chemistry at the time of carbonate precipitation (Carpenter et al., 1991; Major and Wilber, 1991; and Whittaker et al., 1994). Similar information is generated by the analysis of freshwater lacustrine

carbonates. Stable isotopes are often used to analyse lacustrine carbonates to determine the source of water input, as well as to reconstruct the climate of the region (Fontes et al., 1996; Li et al., 1997; Anderson et al., 1997; and Menking et al., 1997). Many organisms, particularly marine and freshwater molluscs, precipitate carbonate shells. The isotopic and trace element composition of shell carbonates has been used to reconstruct the composition of both palaeo-sea (Azmy et al., 1998) and palaeo-lake waters (Lemeille et al., 1980; Rea et al., 1994; and Holmes et al., 1995). However, there are metabolic (vital) effects which fractionate ^{13}C during incorporation into shell carbonate and affect their usefulness as an environmental marker (Veinott and Cornett, 1998).

In addition to the information available from primary carbonate minerals, the stable and trace element composition of carbonates is useful in studies of diagenesis. Stable isotope and trace element analysis has been used to establish the source of water responsible for formation of diagenetic calcite in sandstone (Lundergard, 1994), calcretions in sand (Budd and Land, 1990) and limestone (Saller and Moore, 1991; and Quinn, 1991) environments.

Systematic variations in the stable isotope and trace element composition, U-series age and fluid inclusion analysis are powerful tools in the examination of the formation conditions, or diagenetic history of calcite. The ubiquitous nature of calcite makes it a useful proxy for analysis of a wide range of geochemical and physical processes.

Previous Investigations of Fracture-Infilling Calcite

There have been many investigations of the geochemical compositions of fracture-

infilling calcite. Most often the investigations are undertaken in conjunction with the geologic characterization of a region's suitability for hosting a long-term high level nuclear waste repository. The proposal to locate such a facility at Yucca Mountain, Nevada has led to many investigations of the geologic stability and palaeohydrology of the area. Szabo and Kyser (1990) performed a stable isotope (^{13}C and ^{18}O) and U-series dating study of secondary calcites in fractures from the vicinity of Yucca Mountain. They found isotopic and age evidence for episodic calcite precipitation in the fractures from meteoric recharge. Marshall et al. (1992) used Sr and stable isotope data to establish that the calcites formed from a pedogenic fluid at low temperatures. Hill et al. (1995) used a combination of their own data and the data from other investigations to argue that the origin of some of the recent (Pleistocene) calcites may be from an upwelling deep seated hydrothermal fluid. Such a scenario would raise serious concerns about siting a nuclear waste storage facility in the area because it implies that the facility could be flooded. A subsequent investigation of the micromorphology of the calcites by X-Ray Diffraction (XRD), scanning electron microscopy and cathodoluminescence indicate that the secondary calcites are more similar to pedogenic (soil-derived) deposits than phreatic (saturated zone) deposits. Thus they appear to be precipitating from recharging ground water (Monger and Adams, 1996). This debate indicates the difficulties in interpreting stable isotope data, particularly in open systems. Systems are considered open if they can freely exchange materials with external sources. Stable isotopic compositions can be affected by many variables and it is difficult to eliminate any formation scenario with a stable isotope investigation alone.

The potential for a high level nuclear waste storage facility location in Hungary was studied using the stable isotope (^{2}H, ^{13}C and ^{18}O) composition of shallow groundwater, site water (deep-seated fluids), carbonate veins and microthermometric information from fluid inclusions (Demeny et al., 1997). The stable isotopic composition of the ground water indicated meteoric recharge as the source, and the site water suggested earlier recharge during the Pleistocene. The stable isotopic composition of the carbonate veins and the fluid inclusions suggested that the carbonate formed during warmer periods in the Pleistocene. It was concluded that the groundwater had a long residence time, despite evidence for meteoric recharge at the site.

The fracture-infilling calcite from a volcanic environment in Italy was examined using U/Th, stable isotopes (^{13}C and ^{18}O) and fluid inclusion analysis (Voltaggio et al., 1997). The U-series ages constrained two main calcite precipitation events, one at 25 ka, and the other at 50 ka. The stable isotopic compositions of the calcite eliminated meteoric recharge as the source water, and the fluid inclusion analysis eliminated the possibility of seawater involvement in calcite precipitation. This led to the conclusion that the origin of the calcite was a hydrothermal crustal fluid.

Natural uranium deposits are frequently studied as analogues for nuclear waste storage facilities. Fracture calcite from the vicinity of a uranium deposit in Spain was analysed to determine the long term hydrogeology of the region. U and Th concentrations and activity ratios in the water and the minerals were measured. The results were used to date the time of calcite formation and to validate a proposed mass-balance rock/water interaction model (Ivanovich et al., 1994). Stable isotopes (^{13}C and ^{18}O) and petrographic

relationships in the calcites indicate that they were formed by mixtures of hydrothermal and supergenic (formed near the surface by descending fluids) waters (Reyes et al., 1998). Such findings are useful in determining the palaeohydrology of an area and the potential hydrologic transport of actinides from underground storage facilities.

Stable isotopic composition (^{13}C and ^{18}O), non-destructive and destructive fluid inclusion analyses were performed on secondary carbonates from a shale sequence in Central Asia to constrain the origin of two distinct calcite deposits (Yakovlev, 1998). The analysis indicated that one deposit formed from an ascending fluid, and the other formed from a low salinity, low temperature descending fluid, probably meteoric in origin. The combination of these techniques provided a powerful tool for deciphering the origin of geochemically distinct calcite deposits, and can give an indication of the fluid history of an area.

The proposal to construct nuclear waste storage facilities in the deep crystalline bedrock of Shield terrain has led many countries to study fracture-infilling calcite. Studies have been performed in Switzerland, Germany, Finland, Sweden and Canada. A study using a combination of ground water and fracture calcite analysis was performed in northern Switzerland (Balderer et al., 1987). The isotopic compositions of sulfur and oxygen, ^{36}Cl, and ^{14}C in dissolved inorganic carbon (DIC) from the groundwater and the stable isotopic (^{13}C and ^{18}O) compositions of the calcite were analysed. The fracture system was found to be open with respect to both ^{18}O and ^{13}C. The ^{14}C ages of the groundwater yielded residence times of 2 to >20 ka. The stable isotopic composition of the calcite was consistent with formation from the existing groundwater at temperatures

equal to the ambient temperature at the sample depth. Evidence for both calcite precipitation and calcite dissolution was found in the fractures.

A study of the fracture-infilling calcite from a nuclear siting task force borehole in Germany indicated the presence of three types of calcite, metamorphic, crack-filling and replacement (Komor, 1995). Trace metal and stable isotopic (^{13}C and ^{18}O) analysis of the crack-filling calcite indicated that the calcite was in chemical and isotopic equilibrium with the water than in the borehole. Komor found that chemical and isotopic re-equilibration of crack-filling calcite eliminates its use for analysing the geochemistry of fluids at greater than 120°C.

Frape et al. (1992) compiled and compared $\delta^{13}C$, $\delta^{18}O$, fluid inclusion and U-series data from several sites on the Canadian and Fennoscandian Shields. They found similar trends in the data from both shields and concluded that similar geochemical processes were controlling fracture-infilling calcite precipitation at both sites. McDermott et al. (1995) compiled all the U-series dating of fractures from both shields and found that the precipitation of fracture-infilling calcite is coincident with the end of interglacial periods. They concluded that the termination of recharge by the formation of permafrost in the overburden may be linked to the precipitation of fracture-infilling calcite.

A stable isotope (^{13}C and ^{18}O) and fluid inclusion study of fracture-infilling calcite in Finland was performed by Blyth et al. (1998). Four fluids were found to be responsible for the formation of fracture-infilling calcite, two high temperature/low salinity fluids with different isotopic compositions, a high temperature fluid of moderate salinity, and a

low temperature fluid of high salinity. Unfortunately radiometric ages were not determined on any of the calcites, so at best the chronology of the fluid events could only be inferred from the geologic history of the area.

A fluid inclusion and stable isotope (^{13}C and ^{18}O) analysis of fracture-infilling calcite from Sweden was performed by Larson and Tullborg (1984). They found that there were three fluids responsible for the formation of fracture-infilling calcite: 1) a hydrothermal fluid; 2) a fluid more $\delta^{18}O$ enriched than the water presently in the fractures; and 3) a mixture of these two fluids. Another fluid inclusion investigation of fracture-infilling calcite by Lindblom (1987) found there were three fluid events recorded in the fluid inclusions based on salinity measurements, two separate high temperature, moderate to high salinity fluids, and a low temperature low salinity alteration event fluid. The high temperature events were determined to be quite old by considering the geologic history of the region. The low temperature, low salinity event was determined to be recent.

A series of studies was performed on fractures from the proposed radioactive waste research site at Stripa, Sweden. Milton (1987) performed U-series analysis on the fracture-infilling calcite and concluded that the ages recorded the minimum ages of calcite precipitation and could be used to infer the palaeohydrology of the site. Clauer et al. (1989) performed stable isotopic (^{13}C and ^{18}O) as well as Sr analysis on the fracture-infilling calcite and identified three possible origins for calcite: metamorphic, meteoric, and post depositional alteration involving methanogenesis. Fritz et al. (1989) examined the isotope geochemistry of carbon in the groundwater at Stripa. They found that the fracture-infilling calcite provided a good record of the history of inorganic and organic

carbon sources and evolution of carbon in recharging ground water.

In association with the Nuclear Waste management program in Canada, several projects investigating fracture-infilling calcite on the Canadian Shield have been performed. Gascoyne et al. (1997) do an excellent job reviewing the projects, specifically those performed at the Underground Research Laboratory (URL) at Pinawa, Manitoba. In addition, Gascoyne et al. (1997) presented U-series dating on the fracture calcites and found that most of the calcites with low U and Th concentrations crystallized during the Pleistocene, whereas calcites with high U and Th concentrations were crystallized >350 ka. Jones et al. (1987) performed stable isotopic (^{13}C and ^{18}O) as well as mineralogic and trace element geochemical analysis on fracture-infilling calcite from the URL. They found that the fracture-infilling calcite recorded water-rock interaction, fluid mixing and changing physical conditions during calcite precipitation. They argued that the most probable fluid source was a mixture of meteoric recharge and a "Canadian Shield Brine," a highly saline fluid of unknown origin observed at depth throughout the shield.

The isotope geochemistry of fracture-infilling calcite at Chalk River, Ontario has been characterized by Bottomley (1987, 1988) and Bottomley and Veizer (1992). The studies presented stable isotopic (^{13}C and ^{18}O), Sr, mineralogic and trace element data from the fracture-infilling calcites. The investigations found that the calcites had a "hydrothermal" origin and had undergone subsequent recrystallization during conditions with variable water to rock ratios. None of the calcites measured were in chemical or isotopic equilibrium with groundwater currently in the fractures. A study of U/Th geochemistry of fracture-infilling calcite and groundwater in the same fractures

determined that the calcites are not in equilibrium with the U in the groundwater (Milton and Brown, 1983; and Milton, 1985). Milton and Brown (1987) performed U-series dating on the fracture-infilling calcite and found that the ages ranged from 50 to 300 ka. They concluded that the ages represented the most recent groundwater flow in the fracture. Lee et al. (1998) have prepared an excellent review of the geochemical and isotopic investigations performed at Chalk River. All of the studies cited here show that considerable information about the palaeohydrology of a fracture-flow dominated system can be obtained by an isotopic and geochemical investigation of fracture-infilling calcite. especially if a combination of stable isotope and other geochemical analysis is performed.

1.4 - U AND Th EXTRACTION AND RADIO-CHEMICAL ANALYSIS

Uranium and thorium analysis by α-spectroscopy requires their complete chemical separation to remove peak interferences in the spectra. Due to the low abundance of some of the U and Th nuclides, the extraction/separation procedure requires high chemical yields to ensure that all the nuclides in the sample are recovered at detectable levels. Procedures for extraction of U and Th from natural samples prior to chemical separation exist, and they are summarized in Lally (1992). Most of these methods, including the most commonly used DOWEX column method developed by Edwards (1986/87), involve liquid-liquid extraction or precipitation-scavenging steps to remove the U and Th from the matrix, and to chemically separate them from one another. These steps are time consuming and can lead to losses in recovery and variable yields.

Ion-selective resins for actinide extraction/separation have been developed and are commercially available through EiChrom Industries (Darien, IL). The extractant resins

retain actinides with affinities that vary with acid and with acid concentration. This allows the resin to be used either to extract the actinides from the matrix during a sample "clean-up" step, or to separate each actinide by sequentially eluting them with different acids or acid concentrations. EiChrom has developed many different resins, each specific to a certain element or group of elements. The EiChrom U/TEVA Spec™ resin (hereafter referred to as UTEVA) with an affinity for U and tetravalent actinides has been used to develop this protocol. The chemistry of the resin has been presented in the literature (Horwitz et al., 1992; Horwitz, 1993; Burnett et al., 1996; and EiChrom-Industries, 1997), and the characteristics of the resin appeared promising for the development of a quick and simple method for U/Th extraction and separation from calcite for the purposes of U-series dating. Therefore, the suitability of UTEVA resin was investigated as part of this study.

Application of UTEVA Resin to U/Th Extraction/Separation

Previous investigations have used the UTEVA resin for the analysis of U and Th in environmental samples. Adriaens et al. (1992) compared SIMS (Secondary Ion Mass Spectrometry) to TIMS (Thermal Ionization Mass Spectrometry) preparing the samples by two different methods, using a Bio-rad extractant, and using the UTEVA resin to extract the U and Th. In their investigation, the UTEVA resin was used in a sample clean-up step to remove the matrix prior to chemical separation of the U and Th on a Bio-rad column. Adriaens et al. (1992) found that the U fraction prepared with a Bio-Rad column after initial sample clean-up with the UTEVA gave spectra free of matrix interferences, but that the U fraction contained a larger amount of Th than when the

UTEVA was not used in a clean-up step. However, the presence of Th in the U fraction is a function of the subsequent column separation and should not be attributed to the pre-separation sample clean-up with the UTEVA resin.

Cadieux and Reboul (1996) modified the EiChrom UTEVA method for actinide analysis to separate a series of actinides from water and soil samples, as well as environmental quality assurance standards prior to analysis by PEARLS (Photon-Electron Rejecting Alpha Liquid Scintillation). They found good agreement with the reference values for U, but did not analyse the Th. Burnett et al. (1996) used the UTEVA resin to extract and separate U and Th from a series of standard soil and sediment samples. They found consistently high yields of U (60-85%), but had poor Th yields (6-32%). They observed good separation of the U and Th based on peak resolution and shape, but did not compare activity ratios measured in the samples to the standard reference values; instead they compared total activity.

An investigation by Goldstein et al. (1997) used the UTEVA resin to extract and separate U and Th from a series of human and environmental samples (soil, air filter, urine and water), in an attempt to use the $^{234}U/^{238}U$ ratio as a signature of the source of the U in the sample (anthropogenic, or nuclear industry U is more depleted in ^{234}U than natural U). Their results suggest that the UTEVA resin can be used to characterize the activity ratios of the actinides, rather than strictly being used to analyse total concentrations. Goldstein et al. (1997) observed trends in the $^{234}U/^{238}U$ ratio consistent with expected sources (anthropogenic versus natural), however, they did not present the data from any standard reference materials to verify that the resin is non-fractionating

with respect to the U nuclides.

The UTEVA resin has been used to separate U and Pu from soil samples to determine from the U nuclide ratios whether the source of the nuclides is natural or anthropogenic (nuclear industry). The technique was very successful for a wide range of natural samples and standards (Croudace et al., 1998). Apostolidis et al. (1998) used the UTEVA resin to extract and separate U and Pu from nuclear materials with high yields (>95%). Thorium, Pu, and Am were extracted and separated from bone ash using a combination of the TRU and UTEVA resins with high yields (>76%) (Pilvio and Bickel, 1998).

Removal of the calcite matrix

Experiments conducted by Horwitz et al. (1992) indicate that the majority of matrix constituents are eluted from the first 5-10 free column volumes (10 to 20 mL) at 2 N HNO_3. The matrix constituents include Ca^{2+}, Mg^{2+}, Fe^{2+} and most of the trace or minor elements that may be present in the natural calcite. The complete removal of the matrix by an acid rinse of the column ensures that the U and Th fractions will be free from ions which may interfere with the generation of a thin source for alpha spectrometry.

2 - STUDY AREA

2.1 - SITE LOCATION

Chalk River Laboratories (CRL) of Atomic Energy of Canada Limited (AECL) are located in Chalk River, Ontario. CRL are located on 100 km^2 of land 200 km northwest of Ottawa on the south side of the Ottawa River. The area is situated within the Algonquin Territory of the Central Gneiss Belt of the Grenville Province of the Canadian Shield. Figure 2-1 shows the location of CRL on a map of Ontario.

2.1.1 - CHALK RIVER REGION

2.1.1.1 - GEOLOGY OF CHALK RIVER AREA

Bedrock Geology

The bedrock in the Chalk River area is lithologically heterogeneous and structurally complex (Raven, 1986). The Chalk River area is underlain by rocks of the Grenville Province of the Canadian Shield, and is situated in the Ottawa-Bonnechere graben system, a northwesterly striking fault system. The early tectonic-metamorphic history is that of polyphase deformation, causing the formation of large-scale recumbent antiformal-synformal structures (Brown and Rey, 1984). This has led to the formation of a highly complex fracture system with faults and fracture zones ranging from the cm to km scale in the Chalk River area (Raven, 1986).

The Chalk River Pluton is situated on the northeast edge of the Algonquin Terrain within the Central Gneiss Belt of the Canadian Shield (Figure 2-2). The Algonquin Terrain is underlain by the Algonquin Batholith, a large pluton which was emplaced 1.4-1.5 Ga, and is linked to a period of transcontinental anorogenic plutonism in North

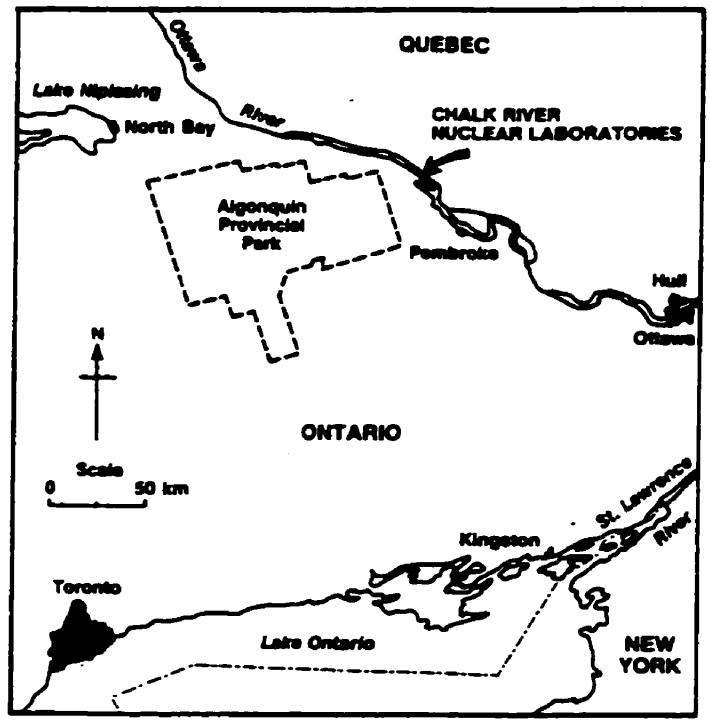

FIGURE 2-1 - Regional map showing the location of Chalk River Laboratories. Taken from Bottomley et al. (1984).

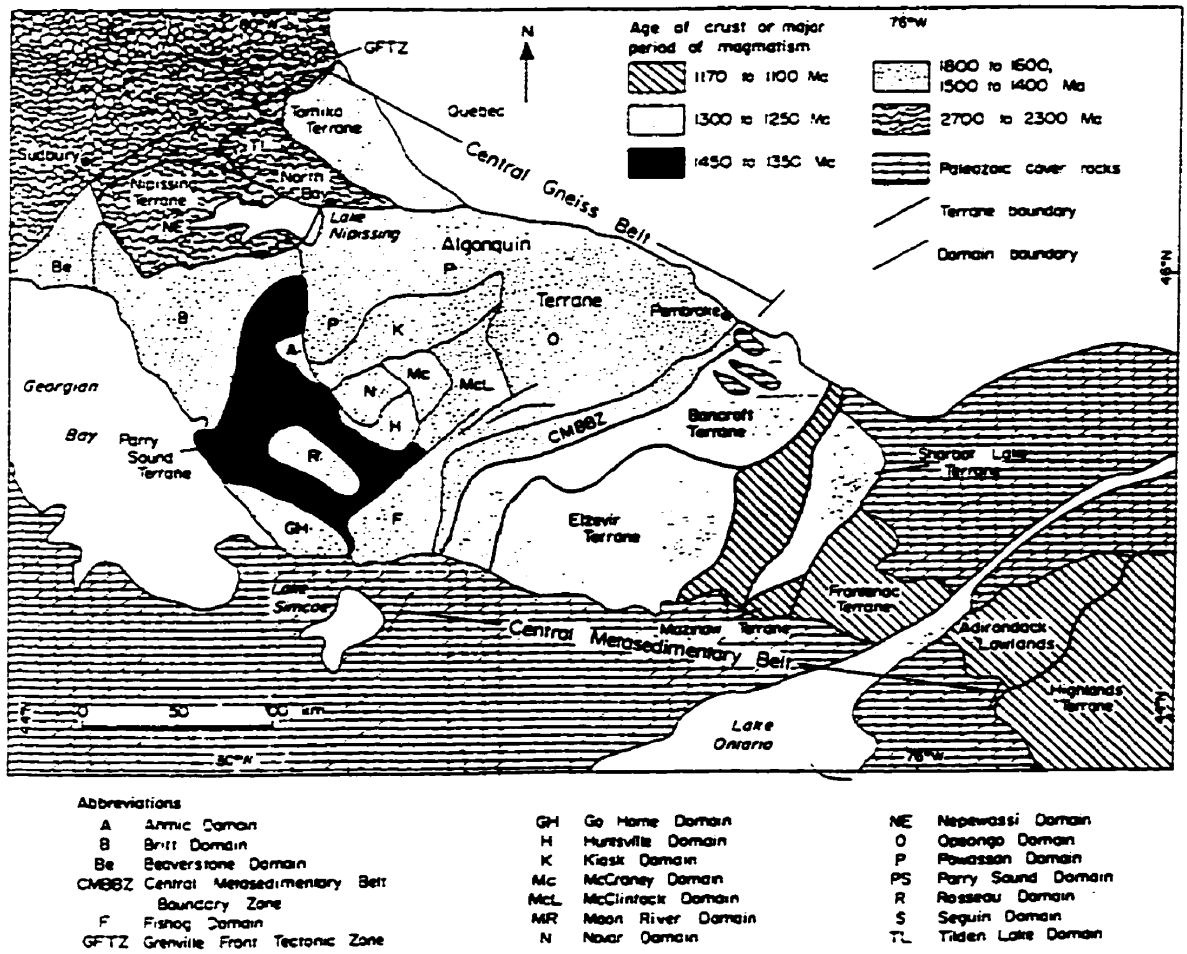

Abbreviations

A	Ammic Domain	GH	Go Home Domain	NE	Nepewassi Domain
B	Britt Domain	H	Huntsville Domain	O	Opeongo Domain
Be	Beaverstone Domain	K	Kiosk Domain	P	Pawassan Domain
CMBBZ	Central Metasedimentary Belt Boundary Zone	Mc	McCraney Domain	PS	Parry Sound Domain
		McL	McClintock Domain	R	Rosseau Domain
F	Fishog Domain	MR	Moon River Domain	S	Seguin Domain
GFTZ	Grenville Front Tectonic Zone	N	Novar Domain	TL	Tilden Lake Domain

FIGURE 2-2 - Map indicating the location of the Algonquin Terrane within the Central Gneiss Belt of the Grenville Structural Province. Chalk River is ~40 km north-west of Pembroke on the Ottawa River. Taken from Easten (1992).

America (Bottomley, 1988). The batholith forms a domal mass with meta-sedimentary gneisses wrapping around the pluton (Easten, 1992). The entire structure is cut by the Ottawa-Bonnechere Graben System and the related Grenville Swarm diabase dikes (Easten, 1992).

Geologic History of the Central Gneiss Belt (CGB) of the Grenville Province

Between 1780 and 1680 Ma (based on Nd model ages), there was a major period of crustal development in the Algonquin Terrain of the Central Gneiss Belt (Easten, 1992). The latter portion of that period, from 1740 to 1680 Ma, was a period of magmatic activity which formed most of the Algonquin Terrain, reworking crust derived from the mantle between 1800-1700 Ma (Easten, 1992).

Felsic magmatism (Lumbers and Vertolli, 1991) with associated metamorphism reaching granulite facies conditions (Culshaw et al, 1991) occurred between 1450 and 1420 Ma in the Algonquin Terrain. The result of this magmatism was to stabilize the continental crust (Easten, 1992).

The main event of the Grenville Orogeny occurred between 1100 and 1070 Ma and involved northwest directed thrusting and imbrication of the entire crust, presumably the result of the terminal collision with the continental landmass (Easten, 1992). This caused granulite facies metamorphism to occur in the central Algonquin Terrain (Easten, 1992) which corresponds to the Ottawa or classic Grenville Orogeny. This time period represents the end of regional orogenic activity in the Grenville Province of the Canadian Shield. Post-1000 Ma activity in the Grenville Orogeny consisted of cooling, uplift and erosion. By the Early Paleozoic (~570 Ma), the Grenville orogenic belt was essentially a

peneplain (Easten, 1992). Extension renewed in the Late Proterozoic, with faulting occurring along the Ottawa-Bonnechere Graben.

There have been dike swarms in the region at 900, 570, and 180 Ma, many related to the development of, and later reactivation along the Ottawa-Bonnechere Graben System, a seismically active north-west striking fault system (Easten, 1992). The main dike swarm in the Algonquin Territory was the Grenville Dike Swarm which occurred between 590 and 550 Ma (Easten, 1992). An Ar-Ar age of 570 +/-3 Ma for a dike near Chalk River, Ontario has been recorded (Easten, 1992). The cooling history of the Grenville Province is summarized in Table 2-1.

Ottawa-Bonnechere Graben System

The Ottawa-Bonnechere graben system is 60 km wide, 700 km long and displays a rift valley morphology (Easten, 1992). The system is bounded to the northeast by the Laurentian Highlands, and to the southwest by the Madawaska Highlands. The Ottawa River follows the Mattawa River fault which defines the northern boundary of the graben (Bottomley, 1988).

Composition of Chalk River Bedrock

The bulk of the Central Gneiss Belt is a 1.8-1.6 Ga gneiss intruded by 1.5-1.4 Ga granitic and monzonitic plutons (Easten, 1992). As a result, there are three main types of rock in the Chalk River area, monzonitic orthogneiss, metagabbro, and paragneiss (Milton, 1985).

Fracture-infilling Minerals

The average fracture frequency for the boreholes at CRL is 14.5/m (Dugal and

TABLE 2-1 - Summary of the formation conditions and timing of the Grenville Orogeny.

	Value	Reference
Uplift Rate	0.07-0.14 km/Ma	Cosca, 1989
Cooling Rate -Grenville	2-4 °C/Ma	Cosca, 1989
- N. Algonquin	1.4-2.7 °C/Ma	Cosca et al., 1990; Anderson, 1990
Temperature	700-800 °C	Culshaw et al., 1991
	650-750 °C	Dugal and Kamineni, 1983
Pressure	8-10 kbar	Culshaw et al., 1991
	4-5 kbar	Dugal and Kamineni, 1983
Metamorphic Peak	1100 Ma	Baer, 1981

Kamineni, 1983). Weathering is generally evident in the shallow core, and the amount of carbonate and clay minerals infilling fractures decreases with depth (Milton, 1985). The dominant fracture-filling minerals at CRL are chlorite and calcite; minor minerals include pyrite, sericite, epidote, iron oxides and clay minerals (Bottomley, 1988).

2.1.1.2 - QUATERNARY GEOLOGIC HISTORY OF THE CHALK RIVER AREA

Catto et al. (1982) reconstructed the glacial history of the Chalk River area and found evidence for the presence of the Champlain Sea in the area during a brief period of glacial retreat between 11 and 10.5 ka. During the Wisconsin glaciation, the lithosphere underwent isostatic subsidence due to glacial loading on the crust. During the post-glacial period prior to isostatic rebound, seawater entered the depression to form a saline water body called the Champlain Sea. The Champlain Sea was an initial intrusion of Atlantic ocean water forming a water body which was then fed by glacial meltwater. Because of the mixing of ocean water, glacial meltwater recharge, and local meteoric precipitation, the Champlain Sea had a composition ranging from seawater to glacial meltwater.

Catto et al. (1981 and 1982) based the existence of the Champlain Sea on the CRL properties on sedimentological, geochemical and paleontological evidence. Catto et al. (1982) found a layer of till deposited on the bedrock (pre-11.5 ka) capped by a clay layer. On the basis of elevated boron and vanadium concentrations in the clay, it was suggested to be marine in origin. The occurrence of this clay horizon immediately above the glacial till indicated that a marine incursion occurred immediately following deglaciation in the region. Likewise, a layer of till above this clay indicated a glacial re-advance in the area

(Catto et al., 1982). Fossil evidence of the foraminifera *Elphidium subarticum* and *Elphidium clavatum* in the clay strengthens the argument that the clay is of marine origin, as both species of foraminifera live in shallow brackish environments (16-22‰ salinity) at temperatures below 4°C. These conditions are consistent with the suggested composition of the Champlain Sea (Catto et al., 1982). The boron and vanadium concentrations indicate a salinity of 12-16‰ for the water, which is consistent with the foraminiferal evidence.

During the final retreat of the glacier, meltwater discharge from North Bay persisted throughout the Ottawa Valley until 5 ka when the North Bay outlet closed. This reduced volume of glacial discharge led to many elevated terraces in the Chalk River area (Catto et al., 1982). When the outlet closed, the Ottawa River level at Chalk River fell to its present elevation of 111 m above sea level (Catto et al., 1982). Figure 2-3 is reproduced from Catto et al. (1982), and schematically depicts the glacial history of a transect along the Ottawa River from Amprior to Rapides-Des-Joachims.

2.1.1.3 - REGIONAL GEOGRAPHY

The present day climate of the Chalk River region is humid continental, characterized by warm summers and cold winters (in Noack, 1995). The mean daily air temperatures range from -12°C in January (<-30°C overnight), to 19°C in July (in Noack, 1995). The region receives an average of 830 mm/yr precipitation (rain equivalent), evenly distributed throughout the year (in Noack, 1995). The annual evapotranspiration rate is approximately 530 mm (in Noack, 1995), leaving 300 mm/yr available for infiltration and runoff.

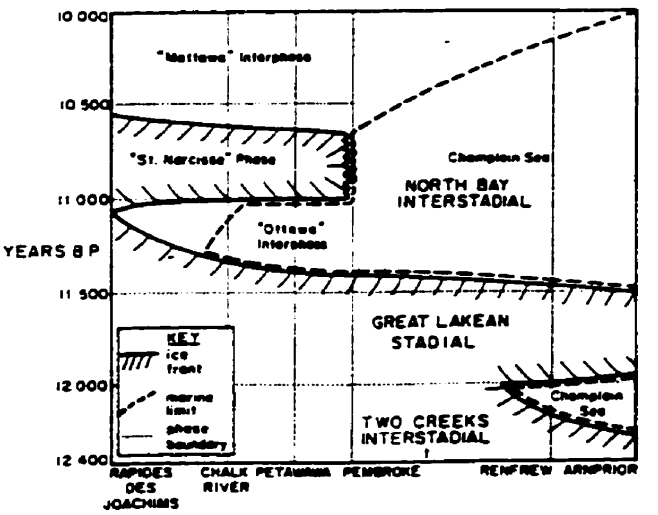

FIGURE 2-3 - A schematic representation of the Wisconsin glacial history of the region around Chalk River. Taken from Catto et al. (1982).

Overburden

Unconsolidated sediments of glacial and post-glacial origins cover 95% of the bedrock on the CRL properties (Killey and Devgun, 1986). The thickness of the overburden is generally less than 30 m (Killey and Devgun, 1986), and the water table is only a few metres below the surface, except beneath sand dunes where it can be up to 15 m below the surface (Noack, 1995).

2.1.2 - GROUNDWATER CHARACTERIZATION

Physical Hydrology

The overburden is the principal zone of groundwater migration in Canadian Shield environments. Except in areas of fractured bedrock, the till-bedrock interface is considered to be the lower boundary of active groundwater flow at CRL (Killey and Devgun, 1986). In general, the hydraulic conductivity of the till is 1.5-2 orders of magnitude lower than the aeolian sands which constitute most of the hydrologically active overburden, and the hydraulic conductivity of the bedrock is 4-5 orders of magnitude lower than that of the sands (Killey and Devgun, 1986).

Groundwater flow through the crystalline metamorphic and granitic rocks (bedrock) occurs primarily through fractures in the rock. As a result, the hydraulic conductivity is primarily a function of aperture spacing, fracture continuity and interconnectivity (Bottomley, 1988). At CRL, the equivalent rock mass hydraulic conductivity has been determined by borehole hydraulic testing to range from 2.4×10^{-4} m/s to 2.9×10^{-12} m/s, and the effective equivalent fracture aperture was calculated to be between 1 to 500 μm (Raven, 1980). The most permeable groundwater pathways occur

along discrete fracture zones associated with faulting of the bedrock (Bottomley, 1988).

Groundwater Chemistry

Groundwater recharge entering fractures in bedrock in the vicinity of Chalk River has been well characterized, and has been found to have increasing pH, Ca^{2+}, Mg^{2+}, HCO_3^- and $\delta^{13}C$ with increasing residence time in the overburden (Fritz et al., 1978). Mineral saturation indices calculated by using an equilibria modelling software program (MINTEQ) and the chemical concentration of cations and anions in overburden groundwater indicate that the groundwaters are slightly saturated to saturated with respect to calcite and iron oxides upon entry to the fracture system (K. King - personal communication).

The groundwater chemistry at CRL has been characterized by detailed examination of the hydrogeology of an air percussion drilled borehole CR13 (Bottomley et al., 1984). The shallow groundwater (<50 m) is dominated by Ca and HCO_3 which evolves to Na and HCO_3 rich groundwater at depths of 200-250 m due to water-rock interaction and exchange reactions with clay minerals. The groundwater is saturated with respect to calcite at both depth intervals. Between 250-350 m, Bottomley et al. (1984) documented a dilute Na/Cl water which is believed to be residual Champlain Sea water. Below 350 m, the groundwater is Na/HCO_3 dominated. The meteoric water which enters the fractures as recharge chemically evolves through water rock interaction in both the overburden and in the fractures to become a brackish Na/HCO_3 water at depth.

2.2 - LOCATION OF BOREHOLES

The drill core material used in this investigation was sampled from previously

drilled boreholes on the properties of the CRL. Core samples were taken from boreholes E1, RH1, RH3, CR9 and CR18. The location of the boreholes is shown on Figure 2-4, and Table 2-2 gives additional information regarding each of the boreholes.

2.2.1 - BOREHOLE SELECTION

Boreholes were selected for core sampling based on the following criteria: 1) the geochemical systematics of the present day groundwater in the borehole has been well characterized; 2) the present-day nature of the groundwater flow at the borehole is known (hydrology); and 3) the core was accessible for sampling. The cores listed in Table 2-2 satisfied these criteria and were sampled during the fall of 1996 and 1997.

2.2.2 - BOREHOLE HYDROGEOLOGY

Previous investigators have made hydraulic head elevation measurements with depth on all the boreholes used in this investigation. The results indicate that for all the boreholes except CR18, the groundwater is recharging. At CR18, the hydraulic head increases with depth, indicating upward groundwater flow or groundwater discharge is occurring at that borehole (Lee et al, 1998).

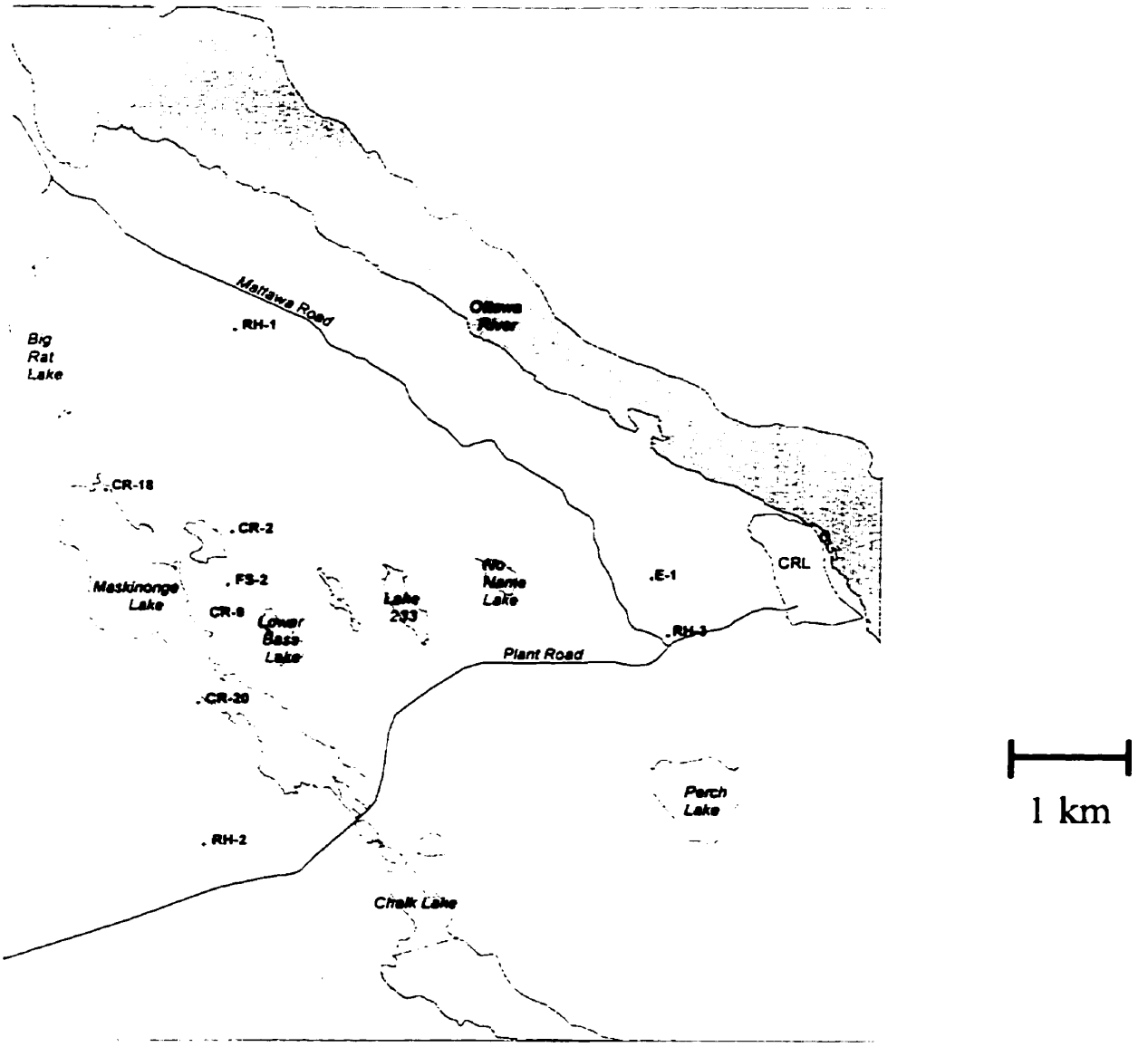

FIGURE 2-4 - Map of the Chalk River Properties of Atomic Energy of Canada Limited showing the location of the boreholes sampled. Direction is not indicated on the map, but the top of the page is North.

TABLE 2-2 - Summary of the drill-core information.

Borehole	Date Drilled	Length (m)	Depth (m)	Starting Trend/Plunge	Reference
E1	1994	~200	181.3	220 / 65	Davison et al, 1995
RH1	1994	201.2	192.4	039 / 73	Golder Associates, 1995
RH3	1994	200.9	193.1	109 / 74	Golder Associates, 1995
CR9	1979	704.25	571.50	245 / 75	Dugal and Kamineni, 1989
CR18	1982	~60	~60	/ 90	Lee, 1989

3 - ANALYTICAL METHODS

3.1 - SAMPLE CHARACTERIZATION

Prior to geochemical analysis, samples of the core were characterized by visual inspection, along with information from the core-logs, as open or sealed with respect to groundwater flow.

3.1.1 - OPEN-VEIN Vs. SEALED-VEIN CALCITE

The drill core sample was determined to contain "open-vein" calcite if it was sampled from a fracture identified as water-bearing in the core log, or if a visual inspection of the calcite indicated either vuggy calcite (open space crystallization) or open channels in the mineral which could serve as a groundwater flow path. The sample was characterized as a "sealed-vein" calcite if calcite was occurring in a fracture from an interval in the core which was not listed as water bearing, or if a visual inspection of the calcite indicated that it was completely sealing the fracture, making the fracture unavailable for groundwater flow. Examples of calcite samples characterized as open-vein and sealed-vein are given in Figure 3-1. In cases where drill logs did not exist (CR18 and E1), or when the drill log did not indicate whether the fracture was water-bearing, the characterization was based entirely on the visual inspection of the core.

3.2 - VERIFICATION OF SAMPLE COMPOSITION

Prior to geochemical analysis, X-Ray Diffraction Analysis (XRD) was performed on a sub-sample of all the carbonate mineral samples taken from the fractures to verify the composition was predominantly calcite. Verification of mineral composition was necessary to correctly interpret the $\delta^{13}C$, $\delta^{18}O$ values as the isotope fractionation factors

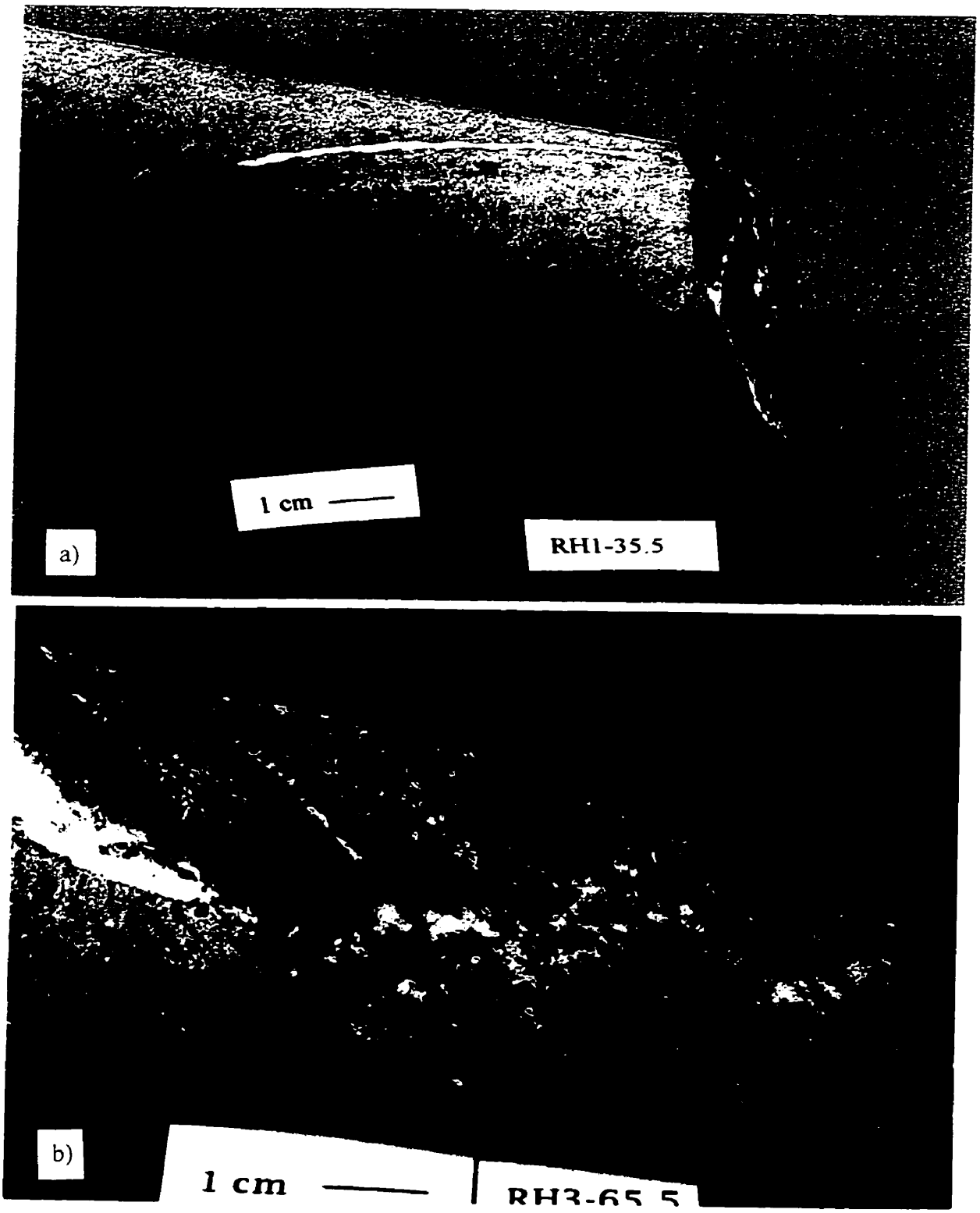

FIGURE 3-1 - Examples of a) sealed-vein and b) open-vein calcite samples from Chalk River boreholes.

are mineral specific.

Samples were sent to the XRD facilities at the University of Western Ontario or the University of Ottawa for analysis. Each sample was ground to a fine powder, homogenized, and XRD analysis was performed on a few mg of this powder. A thin layer of the sample was adhered to a glass slide using ethanol. The slide was bombarded by a monochromatic X-ray beam with the detector recording the intensity of the X-ray beam at varying angles of incidence. Due to mineral structure and atomic composition, each mineral has characteristic X-ray diffraction angles which coincide with interplanar spacings and can be used to identify minerals. The identification of characteristic peaks in the spectra and the absence of any other peaks was taken as verification that the sample was predominantly calcite (>95%), within the confidence of the technique.

3.3 - STABLE ISOTOPE ANALYSIS ($\delta^{18}O$ and $\delta^{13}C$)

The stable isotope composition of oxygen and carbon was measured in the Stable Isotope Lab at Queen's University using a Finnigan Mat 252 IRMS (Isotope Ratio Mass Spectrometer). The $^{13}C/^{12}C$ and $^{18}O/^{16}O$ isotope ratios were measured on CO_2 evolved by reacting 10-30 mg of sample with H_3PO_4, according to the standard method for isotopic analysis of calcium carbonates (McCrea, 1950).

The $\delta^{13}C$ values were reported as per mil (‰) relative to V-PDB with an associated error (2-σ) of 0.1‰, and the $\delta^{18}O$ values were reported as ‰ relative to V-SMOW with an associated error (2–σ) of 0.2‰.

3.4 - FLUID INCLUSION ANALYSIS

To constrain the formation temperature of the calcite and the salinity of fluids

from which the calcite precipitated, fluid inclusions in the carbonate minerals were examined.

3.4.1 - THIN SECTION PREPARATION

Fluid inclusions in calcite can range from 1 to 100 μm in diameter, with the majority below 10 μm. To prepare thin section slides without destroying the fluid inclusions it was necessary to prepare the thin sections between 50 and 100 μm thick. The thin sections were highly polished on both sides so they could be removed from the glass slide mount to fit into the fluid inclusion microscope stage for analysis. The samples were then sent to the thin section lab at Queen's University to be prepared professionally. The thin sections were cut perpendicular to the fracture surface to allow for more easily interpretable petrography of the calcite crystals infilling the fractures.

3.4.2 - ANALYSIS AND PRECISION

The petrography of the thin sections was characterized using a petrographic microscope at low magnification. Once the fluid inclusion had been petrographically characterized (primary, secondary, pseudo-secondary or unknown), the homogenization temperature (T_h) and the temperature of final melting (T_m) were measured using a Reynolds-type (Shepherd et al., 1985) heating/cooling stage at Queen's University. The stage was calibrated with a series of pencils with different melting points, and was accurate to within 0.5°C. The T_m is recorded with an error of +/-0.5°C, and the T_h has an associated error of +/-2°C.

Leakage or post depositional shape change of the fluid inclusion could lead to highly variable T_h and T_m from the same population of fluid inclusions. As a result,

populations or groups of fluid inclusions were used whenever possible. An additional check for leakage or deformation of the fluid inclusion is to make duplicate measurements of the T_h. If there is a breach in the fluid inclusion wall, an increasing value for T_h will be recorded for each successive measurement. This would also be observed if the walls of the fluid inclusion were being stretched during the heating of the fluid inclusion.

3.5 - RADIOCHEMICAL ANALYSIS

The time of calcite precipitation in the fracture was determined using $^{230}Th/^{234}U$ age dating by α-spectrometry. Prior to analysis by α-spectrometry, U and Th must be extracted from the sample to prevent matrix interferences in α-spectrometry, and separated from one another to prevent decay energy overlap in their spectra. The method of chemical extraction and separation was developed as a component of this thesis. Verification of the method is presented in Chapter 4. The method separates U and Th, allowing for chemical precipitation and analysis by α-spectrometry.

3.5.1 - EXTRACTION-SEPARATION PROTOCOL

EiChrom Industries provided a standard procedure for the extraction and separation of U and Th from soil samples using the UTEVA resin (EiChrom-Industries, 1994) . The procedure is based on the retention characteristics of the resin given in the literature (Horwitz et al., 1992; Horwitz, 1993; and EiChrom-Industries, 1997), and is very similar to the method used by Burnett et al. (1996) to analyse U and Th in soils and sediments. Both the Burnett et al. (1996) and EiChrom-Industries (1994) procedures were modified, with attention given to the retention characteristics of the UTEVA resin

given in Horwitz et al. (1992), to develop a method for U/Th extraction and separation from calcite for the purposes of U-series dating. Existing methods for the chemical extraction-separation of U and Th for analysis are time consuming, labour intensive, and can lead to variable recoveries. The objective of this protocol is to adapt the commercially available pre-packed EiChrom UTEVA column to the extraction-separation of U and Th from calcite.

Characteristics and Chemistry of Pre-packed UTEVA Resin Columns

The active compound in the UTEVA resin is Diamyl amylphosphonate, the structure of which is given in Figure 3-2a. In the presence of nitrate, U and tetravalent actinide ions form nitrato complexes with the phosphate group in the resin. The chemical equilibria for both the U(VI) and Th(IV) ions are given in Figure 3-2b. The presence of nitrate causes the actinides to form nitrato complexes with the diamyl amylphosphonate which moves the equilibrium to the right, and strong chemical complexes are formed in the presence of concentrated nitric acid (Horwitz et al., 1992; and EiChrom-Industries, 1997).

U and Th can be extracted by the UTEVA resin due to differences in the resins' affinity for U and Th as a function of acid concentration. The affinity of diamyl amylphosphonate has been shown to increase with increasing molarity of both HNO_3 and HCl for the UTEVA resin (Horwitz et al., 1992). This is expected given the nature of the chemical equilibrium for extractant-actinide binding (Figure 3-2b). There are differences in the relationship between extractant affinity and acid concentration, and extractant affinity and acid composition for U and Th (Horwitz et al., 1992). These differences in extractant affinity were used to create an extraction-separation protocol for U and Th

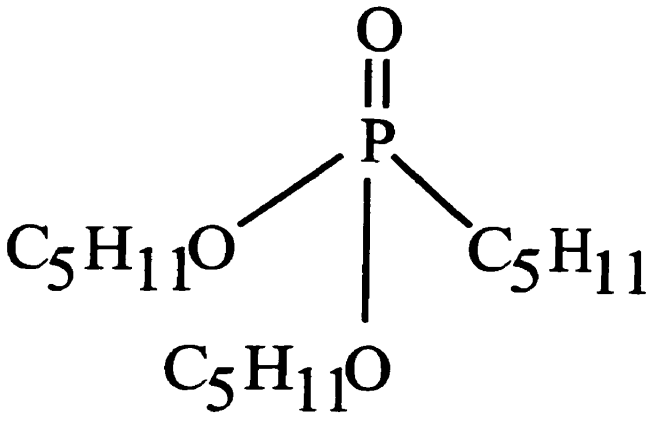

A) Structure of diamyl amylphosphonate.

$$UO_2^{2+} + 2NO_3^- + 2E \leftrightarrow UO_2(NO_3)_2E_2$$

$$Th^{4+} + 4NO_3^- + 3E \leftrightarrow Th(NO_3)_4E_3$$

E = diamyl amylphosphonate

B) Chemical equilibria of U(VI) and Th(IV) with diamyl amylphosphonate in nitric acid.

Figure 3-2 - A) Diagram of the molecular structure of diamyl amylphosphonate, the active extractant in the EiChrom UTEVA resin. Actinides form nitrato complexes with the phosphate group in the diamyl amylphosphonate. **B)** The chemical equilibria of U and Th with diamyl amylphosphonate in the presence of nitric acid. The higher the concentration of nitric acid, the further to the right the equilibria are driven, and the more tightly bound the U and Th are by the extractant.

from calcite using the UTEVA resin.

Development of the extraction/separation protocol

The extraction of U and Th from the calcite matrix required sample digestion in concentrated nitric acid. The dissolved sample was loaded onto the column in 5 M HNO_3. In 5 M HNO_3, the extractant affinity for both U and Th is high (Horwitz et al., 1992). Separation of the U and Th with the UTEVA resin required acid conditions that generate large differences in the extractant affinity for U and Th. In nitric acid the extractant affinities of U and Th are too similar at all acid concentrations to allow for a complete chemical separation of U and Th (Horwitz et al., 1992). The relationship between extractant affinity and acid strength in hydrochloric acid is different for U and Th. Thus HCl was used to facilitate chemical separation of the U and Th. At 5 M HCl, the extractant affinity is high for U, and lower for Th. This allowed for the Th to be eluted with 5 M HCl while the U remained bound to the column. The extractant affinity for U is low in 0.01 M HCl, and therefore the U on the column can be eluted by HCl of this molarity.

Extraction/Separation of U and Th from calcite using the ion selective UTEVA Resin

The 2 mL pre-packed UTEVA column was preconditioned prior to sample loading. The tip of the column was clipped and the packing solution drained. The column was then rinsed with 10 mL of 1 M NaOH, followed by 10 mL of double-distilled de-ionized (DD-DI)-H_2O, and converted to nitric form by washing with 10 mL of 2.5 M HNO_3. The pre-packed columns have a frit which ensures that the column will not run

dry if the reservoir is drained. This allows for the column to be left unattended while eluting without concern that the resin will be exposed to air which could cause channelling within the column.

Approximately 1 gram of calcite was placed in 8-10 mL DD-DI-H_2O and concentrated (15.9 N) Environmental Grade HNO_3 was added drop-wise to gently dissolve the calcite, bringing the solution to a final volume of 15 mL. This was done to gently dissolve the calcite, thus avoiding the dissolution of any detrital component which may be present in the samples. As the detrital Th would be present as contamination, this gentler dissolution process is used to ensure that only the calcite is dissolved (Gascoyne, 1979; Milton, 1985). The sample was then centrifuged and the supernatant fraction was used for analysis. The solution was passed over the column and subsequently washed with 10 mL of 5 M HNO_3 (an additional 10 mL per gram of calcite was used if more than 1 g of calcite was loaded on the column). The calcite eluent may be collected and saved if any additional chemical analysis of the sample is to be performed, otherwise, this fraction is waste. The U and Th were retained on the column resin, completely separated from the matrix.

Thorium was eluted first with 40 mL of 5 M HCl. HCl converts the column to chloride form, lowering the resins' ability to retain Th by several orders of magnitude. Uranium was then eluted with 15 mL of 0.01 M HCl. Thorium and uranium fractions were collected in sterilized plastic containers. A schematic representation of the extraction /separation protocol is given in Figure 3-3.

Low yields of U and Th were experienced in initial runs. This was attributed to

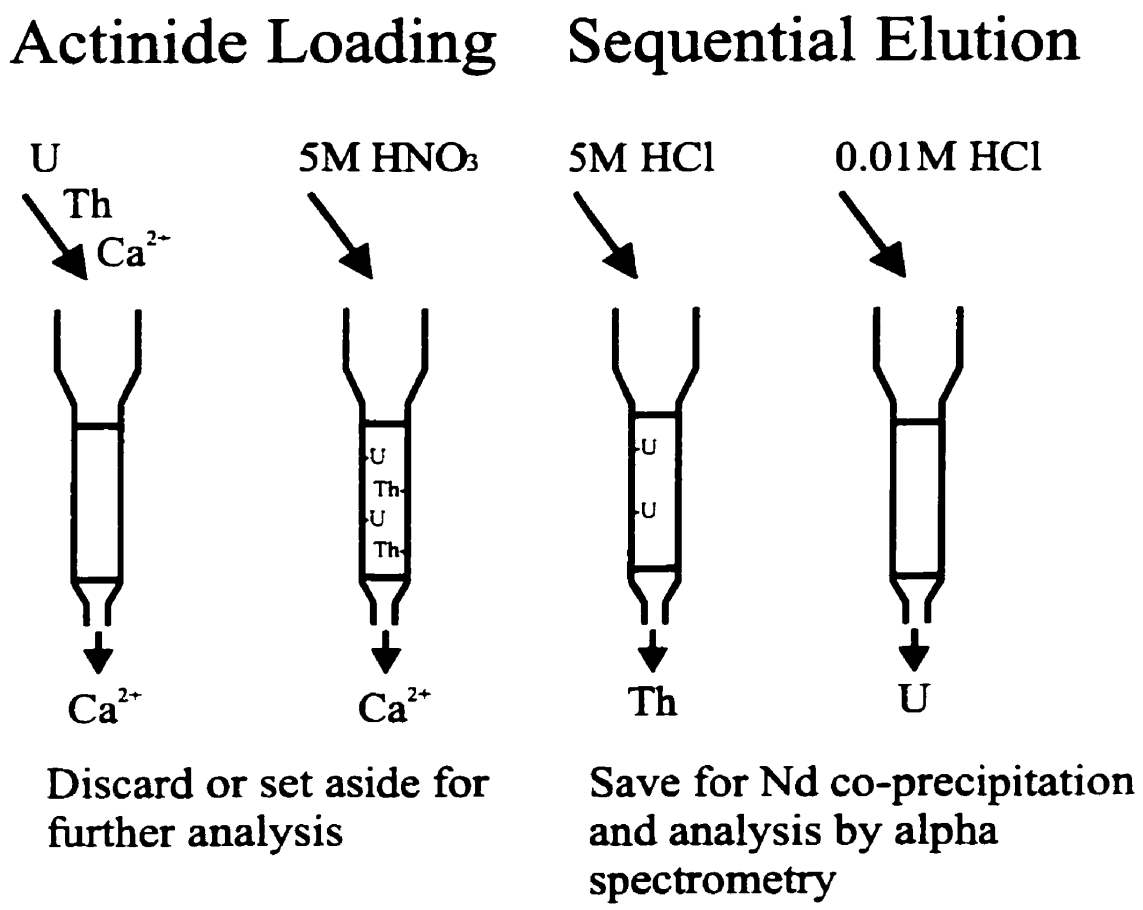

Figure 3-3 - A schematic representation of the U/Th extraction/separation protocol developed by modification of the EiChrom (1994) and Burnett et al. (1996) standard procedure for U and Th measurement in soil and sediment. The figure is a modification of a figure from Bukata et al. (1998a).

possible leaching of the organic resin materials into the U and Th fractions. The resin would then adhere to the wall of the plastic container and bind with the U and Th, removing them from solution. To eliminate this, the eluted fractions were subjected to two oxidation steps, first with concentrated HNO_3 followed by concentrated HCl, which served to break the C-C bonds, volatilize the organic resin materials and release the bound U and Th back into solution.

The separated fractions of U and Th were transferred to clean Pyrex beakers on a hot plate at a low boil, and evaporated to near dryness in a fumehood. The U and Th fractions then had 10 mL of 15.9 M HNO_3 added to them, and were re-evaporated to near dryness. This was done 3 times. 10 mL of 12.1 M HCl was added to the sample which was then evaporated to near dryness. This was also done 3 times. The organic resin materials in each fraction had now been destroyed and the U and Th fractions made available for radio-analytical analysis. Radio-analytical analysis involved co-precipitation of the U and Th separates with neodymium on planchets for detection using alpha spectrometry.

3.5.2 - ALPHA SPECTROSCOPY

Source Preparation

A source suitable for high resolution alpha spectrometry must have the following characteristics: a) the radio-nuclides must be uniformly distributed on the source; b) the source must be as thin as possible, preferably a monatomic layer; and c) the source must be a flat disk (Lally, 1992). If these criteria are not met, an alpha particle ejected from an actinide on the source may lose energy to the source during escape. This would lead to

peak tailing toward lower energies in the spectra. The peaks will be broader, resulting in lower spectral resolution. The source must be stable and must be free of all traces of acid or solvent which may cause damage to the surface barrier detector in the α-spectrometer (Lally, 1992). The method selected for U and Th source preparation was the neodymium co-precipitation method developed by Hindman (1986) and used by Rao and Cooper (1995) on environmental samples. Trial precipitations of dissolved uranyl nitrate and thorium nitrate salts indicated that the Nd co-precipitation method for alpha spectrometry source preparation was an appropriate method for use in this study.

For neodymium co-precipitation the U and Th fractions were dissolved in 10 mL of 1 M HCl. One mL of a solution of 100.68 μg Nd per mL of 1 M HCl was added, followed by 3-4 drops of a 20% titanium trichloride solution. One to two mL of HF was added to co-precipitate the actinides. The actinide/Nd solution was poured into the reservoir of the filtration apparatus, and was precipitated on a 0.1 micron Tuffryn Membrane Filter preconditioned by filtration of 1 mL of the Nd solution in 10 mL of 1 M HCl with a few drops of HF added. The actinide/Nd solution was allowed to stand for 2 minutes before vacuum filtering. The filter was washed with 5 to 10 mL of DD-DI H_2O with 1-2 drops of HF added. The filter was then air dried and mounted on a stainless steel planchet with a double-sided adhesive, for analysis by α-spectrometry. Due to the low activities of the samples, the U fractions were counted for one week, and the Th samples were counted for two to three weeks to improve the counting statistics.

Alpha Detection

Six "Nucleus" Alpha Spectrometers, model 5300 operated by the Environmental

Research Branch of AECL were used to perform the analysis. The detectors share a common vacuum line, and were controlled with Version 3.10 of EG & G ORTEC's Maestro software (1995) on an IBM Personal Computer.

Alpha Spectrometer Calibration and Background Determination

Prior to use, the alpha detectors were calibrated to an external source and the detectors were then inter-compared. The energy calibrations of the alpha detectors were determined using a dual spike radio-nuclide source (^{243}Am and ^{236}Pu) of known activity. ^{243}Am and ^{236}Pu each have specific decay energies. The detector channel of each peak was recorded, and the Maestro software used the number of channels separating the peaks to linearly calibrate the relationship between energy and channel for the detector. The detector efficiencies were calculated by dividing the measured ^{243}Am and ^{236}Pu count rates by the initial source activity corrected for decay since the preparation of the source. A record of the detector calibration dates and calculated detector efficiencies is given in Table 3-1.

The background of each detector was frequently measured by counting a stainless steel disc with the same geometry as the precipitated source. The counts in the energy ranges for each nuclide in the U series decay chain were then integrated and recorded. The background activity was subtracted from the activity recorded in each sample. The long term stability of the background was monitored by frequent background analysis.

Detector Intercomparison

As part of the quality control program, the energy calibration and detector efficiency determination were checked by counting an ^{241}Am source on each detector.

Table 3-1 - Record of detector calibration dates and calculated detector efficiencies.

Detector	Calibration Date	^{243}Am Efficiency	^{236}Pu Efficiency	Average Efficiency
1	01/97	27.8	25.1	26.5
	not used post 04/98			
2	01/97	26.1	25.3	25.7
	05/29/98	29.8	26.6	28.3
3	01/97	29.1	28.6	28.9
	05/07/98	30.9	32.2	31.6
4	06/11/98	36.0	35.0	35.5
	06/03/98	35.5	30.0	32.8
5	06/01/97	21.5	20.6	21.0
	05/10/98	27.1	32.7	30.0
6	01/97	27.9	25.4	26.7
	05/15/98	27.0	29.3	28.4

The measured activity was corrected for the counter efficiency according to equation 3-1.

$$A_{corrected} = A_{measured} * (\frac{100}{E}) \qquad (3-1)$$

E = detector efficiency as a %

The corrected activity and α-decay energy of the sample in each detector is presented in Table 3-2. The average activity of the source was determined to be 1.46 +/- 0.12 Bq (2-σ). The activities determined for the source by each detector agree within the 95% confidence interval. The average α-decay energy of 5.53 (2-σ = 0.02) MeV compares well with the expected α-decay energy of 5.49 MeV for ^{241}Am. The agreement in the activity determination among the detectors for the ^{241}Am source indicated that the calculated detector efficiencies were in agreement, and the agreement within 2-σ of the α-decay energy reported for the peak indicated that the calibrations are in agreement. Table 3-2 also indicates that the activities measured for the unknown ^{241}Am source in each detector agree within the error on each measurement due to counting statistics alone.

3.5.3 - DETERMINATION OF CHEMICAL YIELD AND RADIO-NUCLIDE ACTIVITY

The chemical yield was determined using as a yield tracer a spike of ^{232}U in secular equilibrium with its daughter ^{228}Th for the radiochemical analysis. Several mL of a concentrated spike with a total activity of 22.8 Bq (11.4 Bq of both ^{232}U and ^{228}Th) were supplied by Mel Gascoyne at AECL-Whiteshell. The spike activity had been well established by the Uranium Dating lab at AECL-Whiteshell. The concentrated spike was diluted 100 times with 1 N HNO_3 prior to use. The diluted spike was used in all

Table 3-2 - Summary of the analysis of standard ^{241}Am source of unknown activity. Sample was run as a verification of detector calibration, and as an inter-comparison of calculated detector efficiencies.

Detector	Date Counted	^{241}Am Peak Energy (MeV)	Peak FWHM (MeV)	Efficiency corrected Activity (Bq)	Error 1-σ (Bq)
2	05/03/98	5.52	0.03	1.32	0.07
3	05/15/98	5.53	0.02	1.45	0.08
3	05/15/98	5.52	0.03	1.47	0.04
3	05/31/98	5.53	0.04	1.41	0.07
3	09/11/98	5.53	0.04	1.48	0.04
4	09/11/98	5.51	0.05	1.50	0.05
5	05/15/98	5.55	0.02	1.50	0.08
5	09/11/98	5.54	0.04	1.50	0.04
6	05/16/98	5.54	0.05	1.44	0.05
6	05/31/98	5.53	0.05	1.48	0.06
6	09/11/98	5.53	0.03	1.47	0.04
AVERAGE		**5.53**		**1.46**	**0.06**

experiments reported in this investigation. The activity of the spike was verified by spiking 1 mL of 1000 ppm U Atomic Absorption secondary standard and running it through the extraction/separation protocol. The sample had a calculated U concentration of 1006.16 +/- 9.79 (1-σ) ppm, well within the error range of the certified 1000 ppm for the standard. Between 0.1 and 1 mL of the spike was added to each of the samples prior to radiochemical analysis.

The precision and accuracy of the radiochemical analysis were tested by running well characterized natural calcite samples (Gascoyne, 1979 and Li et al., 1989) through the protocol and comparing the results to the published values for the samples. The results of these analyses are presented in Chapter 4.

The chemical yield and corrected count rates were determined using a modified spreadsheet program supplied by the Uranium Laboratory at AECL-Whiteshell.

Radiochemical Calculations and $^{230}Th/^{234}U$ Age Determination

The radiochemical calculations performed in this investigation are summarized in Appendix I and the method used for determination of the $^{230}Th/^{234}U$ age is presented in Appendix II.

3.6 - ICP-MS ANALYSIS OF U AND Th

Sample Preparation

For ICP-MS (Inductively Coupled Plasma Mass Spectrometrometry) analysis, 0.020 to 0.060 g of the calcite sample was dissolved in 1 mL of concentrated (15.9 N) Environmental Grade Nitric Acid and the solution was brought to a final volume of 50 mL with DD-DI-H_2O. A 1 mL aliquot of each sample was taken and diluted to 10 mL by

DD-DI-H_2O. Both dilutions were analysed, to provide duplicate analysis of each sample. The sample replicates, and replicates prepared at half the concentration, were included for analysis as an internal check of laboratory reproducibility.

ICP-MS Analysis

Analysis was performed at Trent University's ICP-MS Facilities. The analyses were performed on an Elan 5000 in direct injection-ion counting mode. Standard laboratory protocols (Hughes and Evans, 1996) were used for element analysis in the samples. The lower limit of detection for U in solution was 0.005 ppt, and was 0.006 ppt for Th.

4 - VERIFICATION OF U/Th EXTRACTION-SEPARATION TECHNIQUE

The ability of the developed protocol to extract U and Th from a calcite matrix and chemically separate them was determined in three stages. The first stage involved using synthetic lab grade reagent calcite spiked with U and Th to test the chemical separation. The synthetic calcite experiments were also used to crudely verify the chemical yields of U and Th. The second stage of experiments involved using spiked natural calcite samples which have been previously U-series dated using alternative U/Th extraction-separation techniques. This was done to verify that the method is non-fractionating with respect to each of the U and Th radio-nuclides and therefore applicable to $^{230}Th/^{234}U$ dating. The spike used was a radio-chemical yield tracer for α-spectroscopy. This allowed the U and Th yields to be accurately determined using this protocol. The final stage of the protocol verification involved using the measured system blank to determine the range of calcite ages which can be calculated, and lower limits of U concentrations which can be measured, using this technique.

4.1 - SYNTHETIC CALCITE SAMPLES

Synthetic calcite experiments were designed to provide a rapid test of the protocol during development, prior to analysis of natural calcite samples. The majority of the analytical time involved in α-spectroscopy investigations of U-series actinides in environmental samples is spent counting the sample, due to the low actinide concentrations in the sample and long half-lives of the U-Th decay series. To shorten the counting time, the synthetic calcites were spiked with concentrations of U and Th which had been calculated to give approximately 4000 decays per day. Assuming a detector

efficiency of 25%, this meant the samples would require only 1 day of counting to achieve 3% relative error. Stock U (1 ppm) and Th (10 ppm) solutions were prepared from uranyl nitrate and thorium nitrate salts. Synthetic lab grade calcium carbonate was spiked with each of these solutions prior to extraction/separation using the described protocol. The samples were not spiked with a yield tracer, and therefore only a crude chemical yield based on mass U detected relative to the total mass of U and Th added by the stock solutions could be determined.

Degree of Chemical Separation and Removal of Matrix

The degree of chemical separation of U and Th was determined by examination of the α-spectroscopy spectra. Complete chemical separation of the U and Th was determined by examining the U-fraction spectra for the absence of Th peaks, and the Th-fraction spectra for the absence of U peaks. Once the final protocol had been developed, the U-fraction was determined to be free of Th, and the Th-fraction was determined to be free of U.

It is important to remove all the matrix prior to co-precipitation of U and Th with NdF_3. The co-precipitation of compounds, specifically CaF_2, during source preparation for analysis by α-spectroscopy, leads to the preparation of a thick source. A thick source will cause broad peaks and lower resolution in the spectra. The U and Th spectra observed using the developed protocol had well formed, well-resolved peaks. This indicated that the procedure was effective in extracting the U and Th completely from the matrix.

The U and Th spectra for one of the well-characterized calcites are shown in

Figure 4-1 The spectra of a well-characterized calcite are shown rather than one of the synthetic calcite samples because the radio-chemical yield tracer spike ($^{232}U/^{228}Th$) was used in the natural samples, but was not used with the synthetic calcites. In addition to demonstrating the effectiveness of the protocol in extracting and separating the U and Th naturally present, the spectra from a spiked natural calcite indicate that the protocol is effective in separating the U and Th in the spike as well. It is evident in Figure 4-1 that the U and Th are completely separated, and the well formed and resolved peaks of the individual nuclides indicate that both the U and Th fraction are free of matrix constituents.

The ^{228}Th peak in Figure 4-1b has a slight shoulder on its low energy side. This shoulder is not the result of the presence of another radio-nuclide (^{232}U), but rather is the result of the fact that ^{228}Th has two primary α-decay energies. The majority (71%) of ^{228}Th decays with an α-particle energy of 5.427 MeV, while a smaller fraction (28%) decays at an energy of 5.344 MeV (Ivanovich et al., 1992). To ensure that no U was present in the Th fraction and no Th was present in the U fraction, the initial samples underwent prolonged counting. The shoulder on the ^{228}Th peak is the result of prolonged counting making the contribution from the secondary decay energy apparent. The absence of any other U in the Th fraction is taken as evidence that there was no U breakthrough in the Th elution.

Chemical Yield

In this series of experiments, the synthetic calcite was spiked with a known mass of U and Th. As no yield tracer was used, the yield had to be calculated by converting the

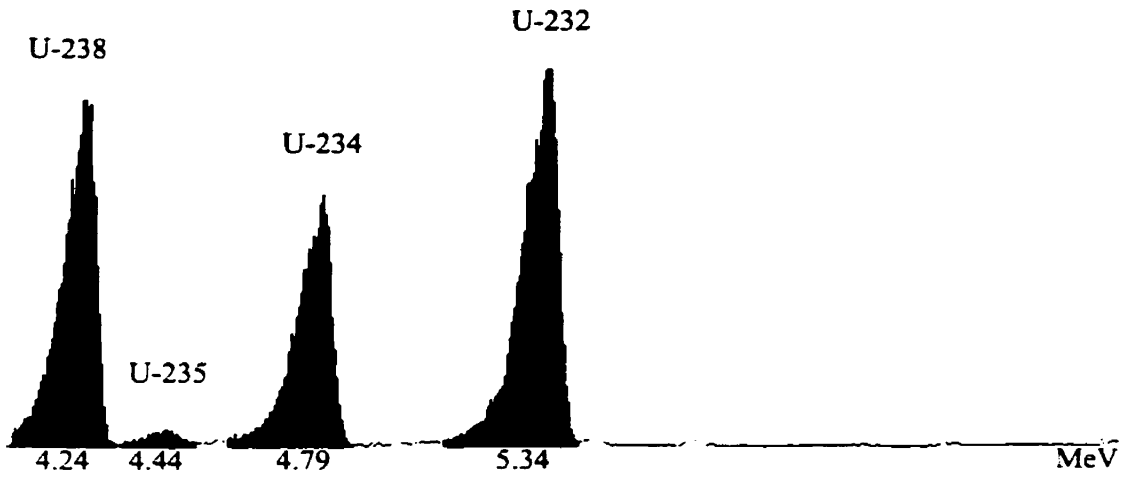

a) Uranium Fraction of C14 - 76126 with 1 mL spike, detector #1

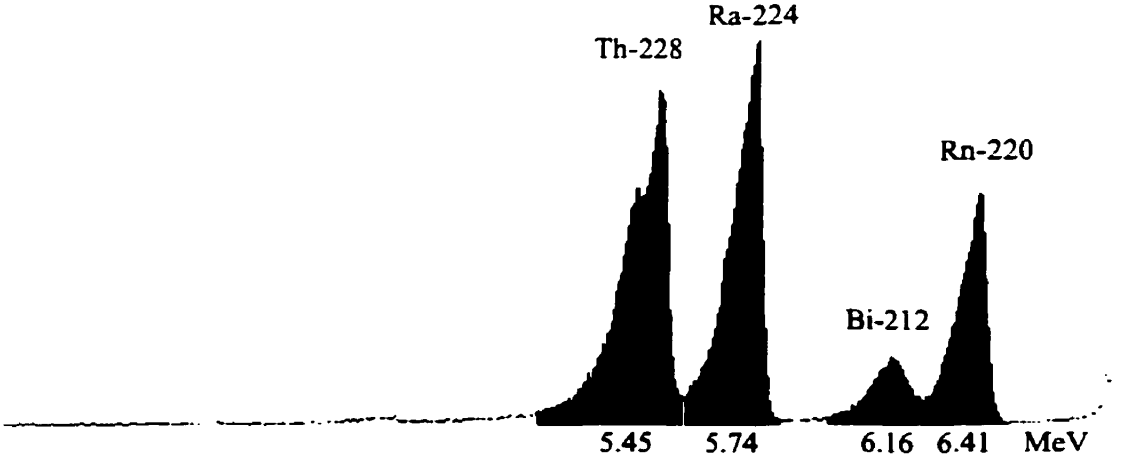

b) Thorium Fraction of C14 - 76126 with 1 mL of spike, detector #2

FIGURE 4-1 - α-spectra for the U (a) and Th (b) fractions of the speleothem standard 76126. Approximately 1 g of calcite was spiked with $^{232}U/^{228}Th$ for analysis. The U and Th fractions were extracted and separated using the UTEVA column method as described in the text. This figure is a modification of a figure from Bukata et al. (1998a).

detector efficiency corrected activities for all U and Th nuclides into total atoms present using the nuclide's decay constant. The total number of atoms were then converted into masses and summed. The yields of U and Th were then calculated according to the following equation:

$$Yield\ (\%) = \frac{mass\ calculated}{mass\ in\ spike} * 100 \qquad (4-1)$$

The error was determined by propagating the error on counting statistics through the same calculations and is reported as a percent. This crude yield was calculated to ensure that high yields of both U and Th were obtained from the protocol, prior to the analysis of standards or natural samples.

The yields determined for the spiked synthetic calcites are summarized in Table 4-1 The yields reported are for samples which did not result in further refinement of the protocol. An average U yield of 94.9 +/- 14.2% (2-σ), and an average Th yield of 83.0 +/-25.4% (2-σ) was observed using the spiked synthetic calcite. It is important to note that the main objective of the spiked synthetic calcite series of experiments was to develop a reliable separation technique. Therefore, the crude yields were only important to establish that the technique gave high recoveries.

4.2 - NATURAL CALCITE STANDARDS

The synthetic calcite experiments established that the developed protocol gave an excellent separation of U and Th, removed any interfering matrix from the fractions, and appeared to give high chemical yields. It was important next to verify that the protocol worked on natural calcite samples spiked with a radio-chemical yield tracer. Two

TABLE 4-1 - Summary of the U and Th obtained by spiking synthetic lab grade calcium carbonate with U (1 μg) and Th (10 μg). The method was being developed during the runs, as a result, the average percent yield can only be considered as an indicator of overall success of the technique.

RUN #	YIELDS (%) *			
	Uranium	Error (1-σ)	Thorium	Error (1-σ)
1	95.9	1.6	**	**
2	98.9	1.0	68.9	0.8
3	101.8	1.7	99.6	0.9
4	83.1	1.9	80.5	0.9
AVERAGE	94.9	1.6	83.0	0.9
STD DEV (1-σ)	7.1	-	12.7	-
STD DEV (2-σ)	14.2	-	25.4	-

* The U and Th yields were calculated as percent mass recovery.
** fraction lost due to human error (dropped beaker)

previously well characterized natural calcite samples were used to perform this series of experiments.

There were three main objectives in this series of experiments. The first was to verify that the protocol gave high chemical yields of U and Th from a natural calcite by using a $^{232}U/^{228}Th$ yield tracer. The second objective was to verify that the activity ratios of the U-series nuclides were not altered during the column extraction/separation protocol, and the final objective was to compare the ages calculated for the calcite standards by this procedure to the published ages in the literature using different extraction/separation protocols. Although objectives two and three are related, objective three is a more strict verification that all the activity ratios are not altered because for the correct ages to be calculated, all the U and Th ratios in the sample must be unaltered or a different age would be calculated. For the developed extraction/separation protocol to be useful in this investigation, the ages calculated using the U and Th fractions have to be correct.

4.2.1 - DESCRIPTION OF STANDARDS

Two natural calcites which have been previously dated using U-series disequilibrium (Gascoyne, 1977; Gascoyne et al., 1983; and Li et al., 1989) and are used as lab standards were graciously supplied by M. Gascoyne (AECL-Whiteshell) to be used as the standards in this investigation. The standards are McMaster University Standard Speleothems 76001 and 76126.

76001

This is a homogenized flowstone collected from Sumidero Tenejepa, Chiapas,

Mexico in January 1976 by M. Gascoyne. This calcite is used as a laboratory reference at McMaster and has been extensively dated by α-spectroscopy (Gascoyne, 1977 and 1979) and by TIMS (Li et al., 1989). The sample has a low U concentration (0.8 ppm) and an age of 47.7 +/- 2.2 ka by α-spectroscopy, and 47.58 +/- 1.17 ka using TIMS (both errors are 1-σ).

76126

This is a non-homogenized stalagmite from Northwest England. The speleothem has a high (13.3 to 13.7 ppm) U content and has been dated at 9.7 +/-0.3 ka at the base and 0.8 +/-0.1 ka at the top (Gascoyne et al., 1983). The details of the sample can be found in Gascoyne et al. (1983). As the sample is not homogenized, the age calculated using this sample was expected to fall within the range of deposition ages determined by Gascoyne et al. (1983). This sample was used to verify that the protocol developed was applicable to samples with a wide range of U concentrations.

4.2.2 - VERIFICATION OF YIELD AND U CONCENTRATION

The U and Th yields were calculated as the activity of the spike measured in the sample divided by the total activity of the spike added to the sample prior to analysis. The U and Th yields for both the natural calcites and a 1000 ppm Atomic Absorption Spectroscopy (AA) standard are summarized in Table 4-2. Consistently high U and Th yields, with the exception of one anomalously low yield, were observed for both the natural calcite standards and the AA standard, although the yields for the AA-standard were slightly lower than the calcite standards. The reason for the low yield with the AA-standard is unknown. These yields are consistent with the less rigorous high yields

Table 4-2 - U and Th yields for natural calcite samples (standards 76001 and 76126) and a 1000 ppm Atomic Absorption Spectroscopy standard.

Sample	Run #	Mass (g)	Yield (%)				Concentration (ppm)	
			U	Error	Th	Error	U	Error
76001	18	1.1080	88.89	0.72	70.74	0.21	0.81	0.04
	22	1.0588	34.29	0.29	84.51	0.29	0.72	0.08
	23	1.0082	85.13	0.26	74.72	0.21	0.78	0.03
	42	0.1357	77.80	0.42	95.27	1.13	0.64	0.18
	Avg.		**71.53**	**21.86**	**81.31**	**9.49**	**0.74**	**0.06**
76126	14	1.1508	91.09	0.57	72.61	0.29	12.99	0.18
	15	1.0505	82.49	0.53	79.31	0.57	12.41	0.19
	Avg.		**86.79**	**4.30**	**75.96**	**3.35**	**12.70**	**0.29**
AA-std	17	0.06	63.55	0.43	54.48	0.18	1006.16	9.79

note - error on the average was determined as the standard deviation in the average (1-σ)

calculated for the synthetic calcite samples. It was determined that the protocol developed for the extraction and separation of U and Th from natural samples gave high yields.

The $^{232}U/^{228}Th$ spike was also used to calculate the U concentration in the sample. These values are also given in Table 4-2. The U concentration measured in the natural calcite samples agree well (within 1-σ) with the concentrations given in the literature. In addition, the developed protocol determined the concentration of the 1000 ppm AA standard within analytical error (1-σ). It was concluded that the U concentration calculated by the protocol agreed well with the concentrations established by other methods, and therefore the technique could be used to determine the U concentration of environmental samples.

4.2.3 - VERIFICATION THAT THE ACTIVITY RATIOS IN THE SAMPLE ARE PRESERVED BY THE CHEMICAL PROCEDURE

The activity ratios measured in the standards were compared to the activity ratios for the standards published in the literature. The results are summarized in Table 4-3. The $^{230}Th/^{234}U$ and the $^{234}U/^{238}U$ activity ratio ranges measured in this investigation overlap the ranges of values published in the literature for both the low U standard (76001) and the high U standard (76126). The $^{230}Th/^{234}U$ ratio measured for 76001 overlaps the range published in the literature, and the average falls at the low end of the published range, but it does fall within the range of published values. The $^{234}U/^{238}U$ ratio also overlaps the published range and the average falls slightly outside the range, but within 1-σ of the upper limit. The agreement between the activity ratios measured using

Table 4-3 - Activity ratios determined for the calcite standards.

Sample	Run #	Measured Ratios		Published Ratios	
		$^{230}Th/^{234}U$	$^{234}U/^{238}U$	$^{230}Th/^{234}U$	$^{234}U/^{238}U$
76001	18	0.33 (0.01)	1.97 (0.07)		
	22	0.39 (0.01)	2.00 (0.07)		
	23	0.35 (0.01)	1.95 (0.04)		
	42	0.32 (0.02)	2.14 (0.12)		
	Avg.	**0.35 (0.03)**	**2.02 (0.07)**		1.867 (0.065)*
	Range	0.32 - 0.39	1.95 - 2.14	0.349 - 0.382*	1.748 - 1.970*
76126	14	0.02 (0.00)	0.74 (0.01)		
	15	0.01 (0.00)	0.75 (0.01)		
	Avg.	**0.02**	**0.75**		
	Range	0.01 - 0.02	0.74 - 0.75	0.007 - 0.085**	0.713 - 0.719**

note - numbers in brackets represent the errors, and error on the average is 1-σ
* - taken from Gascoyne, 1979
** - taken from Gascoyne et al., 1983

the developed protocol and the published values for the activity ratios suggest that the columns are non-fractionating with respect to the U-series radio-nuclides.

4.2.4 - CALCULATED $^{230}Th/^{234}U$ AGES FOR THE STANDARDS

The activity ratios measured in this investigation were used to calculate the $^{230}Th/^{234}U$ age for the standards. The calculated ages are presented in Table 4-4. The average age calculated for the flowstone (76001) is 44.7 +/- 4.2 ka (1-σ); this agrees within 1-σ with the published ages summarized in Table 4-4. The stalagmite (76126) gave an age range of 1.1 to 3.3 ka, these fall within the range of deposition ages measured for the same sample (0.8 to 9.7 ka, Gascoyne et al., 1983). The agreement in ages calculated for both the low U (76001) and high U (76126) standards between this method and the published ages for the standards indicates that this protocol can be applied to $^{230}Th/^{234}U$ dating of natural calcites. Sample 76001-42 used a smaller mass of standard (0.10 g as opposed to 1.00 g) and gave the lowest $^{230}Th/^{234}U$ activity ratio and the highest $^{234}U/^{238}U$ activity ratio; both ratios also have the highest associated errors. Further analyses of lower masses of standards must be run before it can be determined whether this sample is anomalous or if a minimum mass of standard must be used to adequately verify the technique.

4.3 - DETECTION LIMIT AND REAGENT BLANK CONSTRAINTS ON THE APPLICABILITY OF THE TECHNIQUE TO $^{230}Th/^{234}U$ DATING

The applicability of the developed protocol to $^{230}Th/^{234}U$ dating of natural samples will be determined by the detection limit for U and Th. The lower limit of detection (LLD) of the method with respect to both the U and Th concentrations and the minimum

Table 4-4 - The $^{230}Th/^{234}U$ ages determined for the natural calcite standards in this study and the ages reported in the literature.

Sample	Run #	Calculated Ages in this Study (ka)	Ages in Literature (ka)
76001	18	42.1 (+1.4 / -1.6)	
	22	51.3 (+1.7 / -2.0)	
	23	45.1 (+1.4 / -1.6)	
	42	40.4 (+3.0 / -3.0)	
	Avg.	**44.7 (4.2)**	**47.35 (2.85) *1 47.58 (1.17) *2 47.7 (2.2) ****
	Range	**40.4 - 51.3**	**44.50 - 50.20 *1 46.40 - 48.75 *2 45.00 - 50.20 ****
76126	14	2.2 (0.1) a	
	15	1.1 (0.2) a	
	Avg.	**1.7 (0.6) a**	
	Range	**1.1 - 2.2 a**	**0.8 (0.1) - 9.7 (0.3) *****

() - error (1-σ)
a - corrected for ^{232}Th
*1 - Li et al. (1989) by α-spectrometry
*2 - Li et al. (1989) by TIMS (Thermal Ionization Mass Spectrometry)
** - Gascoyne, 1979
*** - Gascoyne et al., 1983

age was examined. The detectable range of calcites was found to be restricted by the amount of the spike used and the LLD of ^{234}U. This method requires at least 0.08 μg U in the sample and the datable range is limited only if >0.5 mL of spike are used. The development and presentation of the LLD for this method are given in Appendix III.

4.4 - SUMMARY OF PROTOCOL VERIFICATION

The results of the protocol verification indicate that a high degree of U and Th separation is seen in both synthetic and natural calcite systems. High chemical yields (>70 % U, and >80% Th) are obtained from natural calcite using a yield tracer. No isotopic fractionation is observed for the U and Th isotopes during extraction and separation using the developed protocol, and the developed protocol can therefore be used to $^{230}Th/^{234}U$ date natural samples accurately. However, analysis of the lower limit of detection indicates that there are restrictions on the U concentration and age of calcites analysed using this protocol.

5 - RESULTS AND DISCUSSION

Fracture-infilling calcite in crystalline rock can form from ascending hydrothermal fluids, or descending recharge fluids, or may have been recrystallized by ascending or descending fluids since initial deposition. The stable isotopic composition, fluid inclusion microthermometry and salinity, and U-series geochemistry of fracture-infilling calcites from the properties of CRL were used to discern the origin of the calcites.

5.1 - STABLE ISOTOPES ($\delta^{18}O$ and $\delta^{13}C$)

Several major fluid events may have occurred in the geologic history of the Grenville Structural Province, each of which would precipitate calcite with different geochemical characteristics. The stable isotope ratios of oxygen and carbon in the calcites in this investigation were interpreted with respect to the ranges of values expected if calcite precipitated in isotopic equilibrium with one or more of these proposed fluids.

5.1.1 - RANGE OF MEASURED ISOTOPE RATIOS

Histograms of the measured $\delta^{18}O$ and $\delta^{13}C$ values of the calcites from this investigation (Figures 5-1a and 5-2a), and the combined data set from Bottomley (1988) and this thesis (Figures 5-1b and 5-2b), defined as either "open-vein" or "sealed-vein" calcites (Section 3.1) indicate the ranges of isotopic values observed in the calcites.

5.1.1.1 - STATISTICAL ANALYSIS OF THE STABLE ISOTOPE DATA

Test for the Validity of Pooling Data

The stable isotope data ($\delta^{13}C$ and $\delta^{18}O$) from calcite samples identified as open-vein or sealed-vein in this thesis were compared to the open-vein and sealed-vein isotope data from fracture-infilling calcites in Bottomley (1988) to establish the validity of using

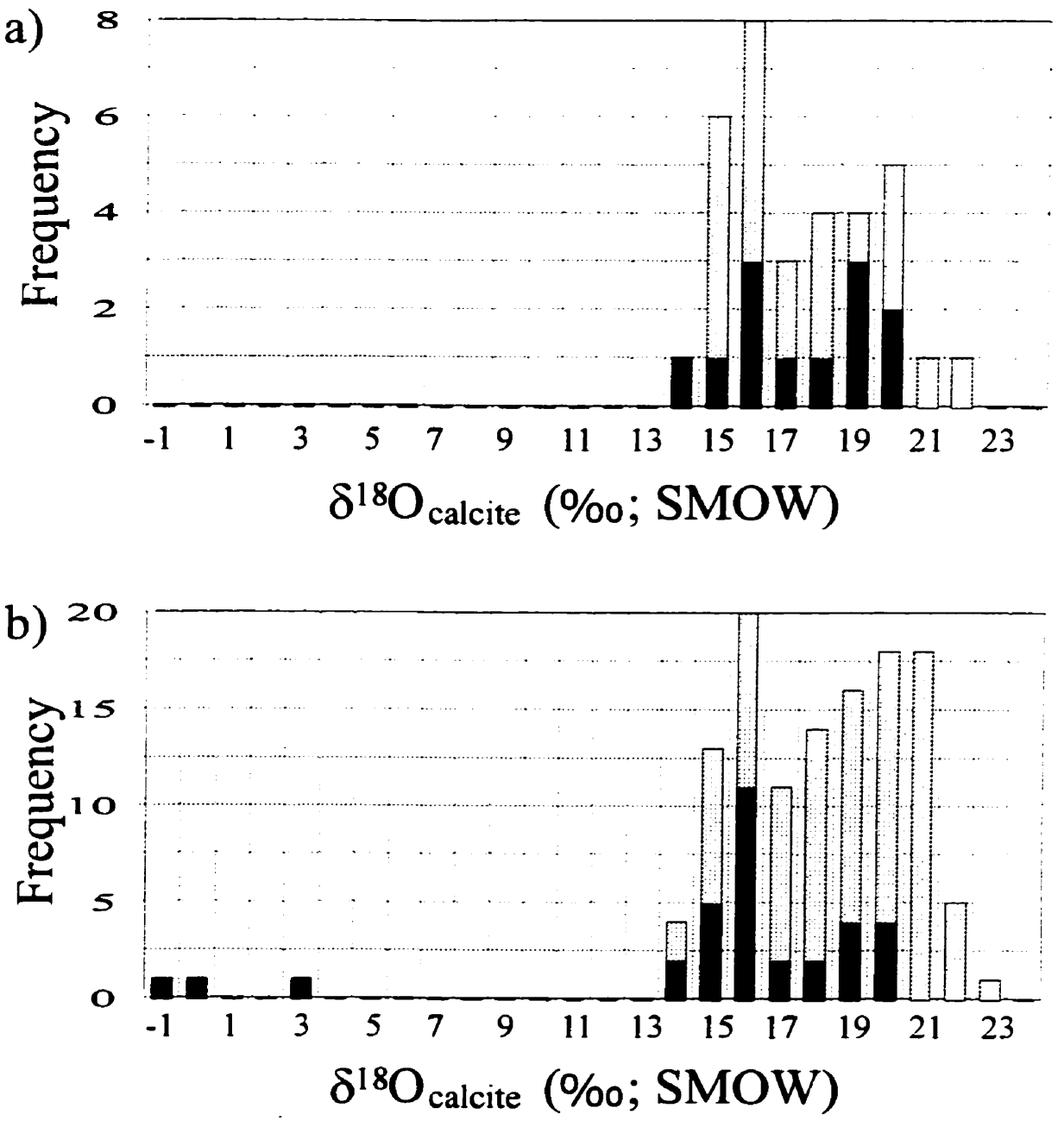

FIGURE 5-1 - Histogram of measured $\delta^{18}O$ values from fracture-infilling calcite on the Chalk River properties of AECL. The darker areas represent sealed-vein calcites, and the lighter areas represent open-vein calcites. a) data measured in this investigation; b) Combined data sets, the $\delta^{18}O$ values measured in this investigation and samples from Bottomley (1988) identified as open-vein or sealed-vein calcites.

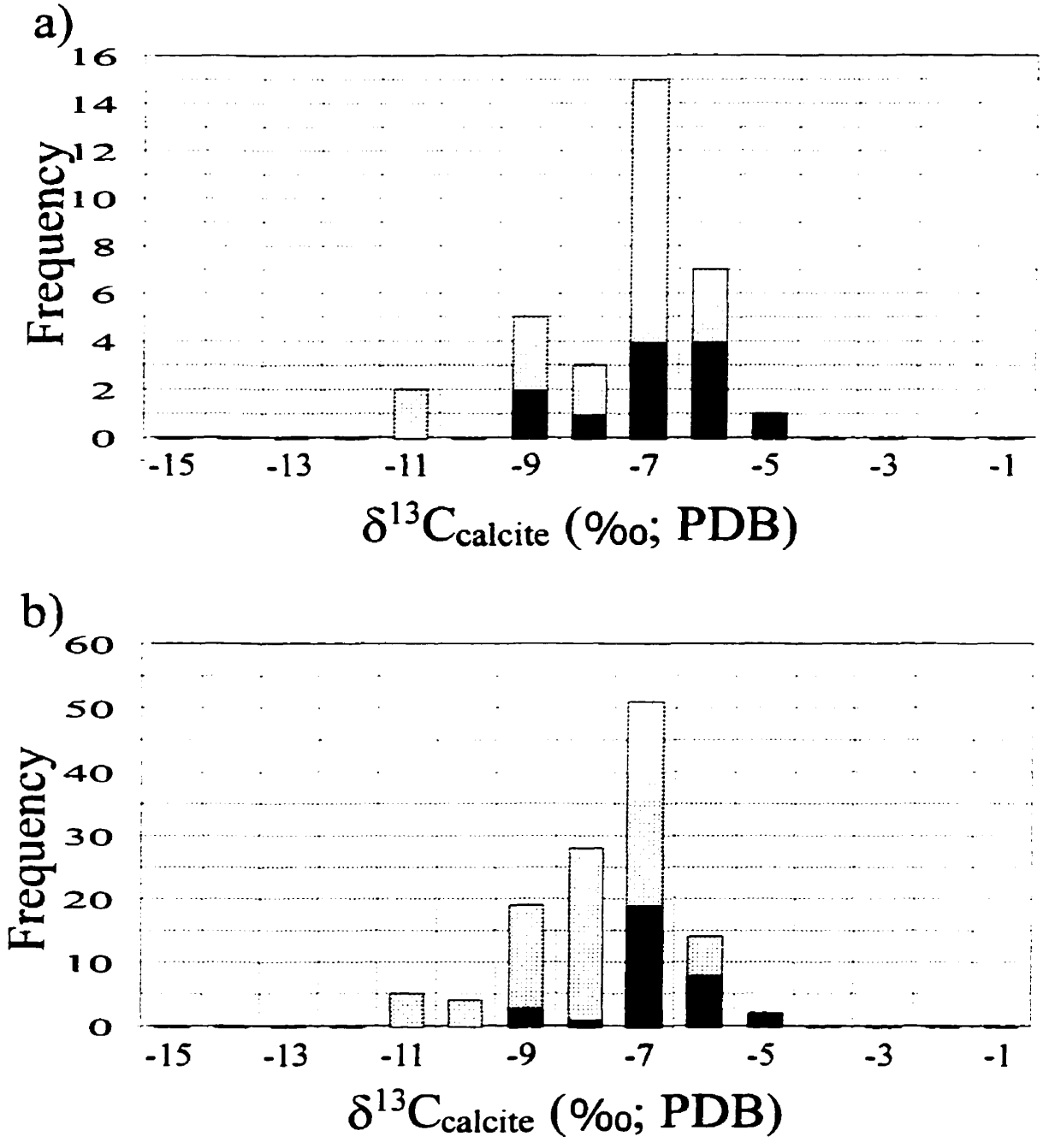

FIGURE 5-2 - Histogram of measured $\delta^{13}C$ values from fracture-infilling calcite on the Chalk River properties of AECL. The darker areas represent sealed-vein calcites, and the lighter areas represent open-vein calcites. a) data measured in this investigation; b) Combined data sets, the $\delta^{13}C$ values measured in this investigation and samples from Bottomley (1988) identified as open-vein or sealed-vein calcites.

a combined data set. An F-test was performed which compared the $\delta^{18}O$ of open-vein calcite from this investigation (mean = 18.0‰, variance = 4.6‰, and n = 21) to Bottomley's (1988) open-vein calcite $\delta^{18}O$ data (mean = 19.6‰, variance = 4.3‰, and n = 69), and found the data sets had equal variances ($F_{calc} = 1.07 < F_{crit} = 1.67$). The subsequent two-tailed t-test ($\alpha = 0.05$) indicated that there was no difference between the means of the two data sets ($t_{calc} = 1.81 < t_{crit} = 1.99$). The $\delta^{18}O$ values of sealed-vein calcite from this investigation (mean = 17.8‰, variance = 3.8‰, and n = 12) were compared to the $\delta^{18}O$ values of sealed-vein calcite from Bottomley (1988) (mean = 16.8‰, variance = 2.7‰, and n = 18) and were determined to have equal variances ($F_{calc} = 1.38 < F_{crit} = 2.15$). The subsequent two-tailed t-test ($\alpha = 0.05$) indicated that there was no difference between the means of the two data sets ($t_{calc} = -1.51 < t_{crit} = 2.05$), and thus it was acceptable to pool the $\delta^{18}O$ data from both investigations of fracture-infilling calcite from the properties of the CRL.

An F-test of the $\delta^{13}C$ data from open-vein calcites in this investigation (mean = -7.3‰, variance = 1.6‰, and n = 21) was compared to the open-vein $\delta^{13}C$ data from Bottomley (1988) (mean = -7.5‰, variance = 2.3‰, and n = 69) and it was determined that the data had equal variances ($F_{calc} = 1.29 < F_{crit} = 1.93$). The two-tailed t-test ($\alpha = 0.05$) indicated that there was no difference between the means of the two data sets ($t_{calc} = -0.69 < t_{crit} = 1.99$). An F-test of the $\delta^{13}C$ data from sealed-vein calcites in this investigation (mean = -6.5‰, variance = 1.5‰, and n = 12) was compared to the sealed-vein $\delta^{13}C$ data from Bottomley (1988) (mean = -6.4‰, variance = 0.8‰, and n = 18) and

it was determined that the data had equal variances ($F_{calc} = 1.95 < F_{crit} = 2.15$). The two-tailed t-test ($\alpha = 0.05$) indicated that there was no difference between the means of the two data sets ($t_{calc} = 0.15 < t_{crit} = 2.05$), and thus it was acceptable to pool the $\delta^{13}C$ data from both investigations of fracture-infilling calcite from the properties of the CRL.

Testing the Difference Between Open-Vein and Sealed-Vein calcite

A) This Investigation

The $\delta^{13}C$ and $\delta^{18}O$ values of sealed-vein and open-vein calcite measured in this investigation were compared to determine whether there were statistically significant differences between the means. The $\delta^{18}O$ values of open-vein calcites (mean = 17.9‰, variance = 4.6‰, and n = 21) were compared to the $\delta^{18}O$ values of sealed-vein calcites (mean = 17.8‰, variance = 3.8‰, and n = 12) measured in this investigation. The data were found to have equal variances ($F_{calc} = 1.22 < F_{crit} = 2.65$) and to have the same mean ($t_{calc} = 0.15 < t_{crit} = 2.05$ with $\alpha = 0.05$). The $\delta^{13}C$ values of open-vein calcites (mean = -7.3‰, variance = 1.6‰, and n = 21) were compared to the $\delta^{13}C$ values of sealed-vein calcites (mean = -6.5‰, variance = 1.5‰, and n = 12) measured in this investigation. The data were found to have equal variances ($F_{calc} = 1.12 < F_{crit} = 2.65$) and to have the same mean ($t_{calc} = -1.77 < t_{crit} = 2.04$ with $\alpha = 0.05$). The lack of statistical difference between the $\delta^{13}C$ and $\delta^{18}O$ values of open-vein and sealed-vein calcite in this investigation may be an artefact of the small sample size (12 sealed-vein calcites). The pooled data set was investigated for statistically significant differences between the $\delta^{13}C$ and $\delta^{18}O$ values of open-vein and sealed-vein calcite.

B) Pooled Data

The $\delta^{13}C$ and $\delta^{18}O$ values of sealed-vein and open-vein calcite in the pooled data sets were compared to determine whether there were statistically significant differences between the means. The $\delta^{18}O$ values of open-vein calcites (mean = 19.2‰, variance = 4.8‰, and n = 90) were compared to the $\delta^{18}O$ values of sealed-vein calcites (mean = 17.2‰, variance = 3.3‰, and n = 30) in the pooled data set. The data were found to have equal variances ($F_{calc} = 1.46 < F_{crit} = 1.72$) and to have statistically ($\alpha = 0.05$) different means ($t_{calc} = 4.45 > t_{crit} = 1.98$). The $\delta^{13}C$ values of open-vein calcites (mean = -7.5‰, variance = 1.4‰, and n = 90) were compared to the $\delta^{13}C$ values of sealed-vein calcites (mean = -6.4‰, variance = 1.0‰, and n = 30) measured in this investigation. The data were found to have equal variances ($F_{calc} = 1.37 < F_{crit} = 1.72$) and to have statistically ($\alpha = 0.05$) different means ($t_{calc} = -4.56 > t_{crit} = 1.98$). There is a statistically significant difference between the $\delta^{13}C$ and $\delta^{18}O$ values of open-vein and sealed-vein calcite in the pooled data sets.

5.1.1.2 - PATTERNS OF $\delta^{18}O_{calcite}$ AND $\delta^{13}C_{calcite}$ VALUES

The $\delta^{18}O$ values of all of the fracture-infilling calcites sampled in this investigation range from 14 to 22‰. The histogram in Figure 5-1a depicts the $\delta^{18}O$ data from this investigation, separated into open-vein and sealed-vein calcite. The difference between the two groups is not statistically significant, but the sealed-vein calcite samples have a lower range of $\delta^{18}O$ values (14 to 20‰) than the open-vein calcites (15 to 22‰).

The combined data set has similar ranges of $\delta^{18}O$ values for open-vein and sealed-

vein calcites (14 to 20‰ and 14 to 23‰), and the difference between the $\delta^{18}O$ values of the two groups is statistically significant. The sealed-vein calcites from Bottomley (1988) contained three anomalously low values (-1 to +3‰) which will not be further considered in combined data sets.

The different ranges of $\delta^{18}O$ values observed for sealed-vein and open-vein calcite in the combined data set suggest precipitation from or alteration by fluids having different isotopic and physico-chemical properties. If the calcites have formed in equilibrium with these fluids, their $\delta^{18}O$ values would reflect the oxygen isotopic composition of the precipitating water source and temperature of calcite precipitation, with lower $\delta^{18}O$ values representing precipitation either at higher temperatures or from a more ^{18}O-depleted source water, or a combination of both. Hence, measurement of the $\delta^{18}O$ values of the calcite alone does not permit the resolution of which effect, temperature changes or formation from isotopically distinct source water, is controlling the observed differences in the oxygen isotopic compositions of the sealed-vein and open-vein calcites. Temperature effects are examined further in Section 5.2, making use of the fluid inclusion data.

The $\delta^{13}C$ values on calcites measured in this investigation range from -11 to -5‰. Open-vein calcite has a larger range of $\delta^{13}C$ values, from -11 to -6‰, whereas the sealed-vein calcites have a narrower range with size values (-9 to -5‰) trending towards a relatively ^{13}C-enriched end of the total range, although the difference between the groups is not statistically significant. A histogram of the $\delta^{13}C_{calcite}$ values measured in this investigation is presented in Figure 5-2a, and the combined data set is presented as Figure

5-2b. The combined data set has the same range of $\delta^{13}C$ values as measured in this investigation, however, the difference between open-vein and sealed-vein calcite values in the pooled data set is statistically significant. The difference between the mean $\delta^{13}C$ values for open-vein and sealed-vein calcite in the pooled data is indicative of different carbon sources or different precipitation conditions for the sealed-vein and open-vein fracture-infilling calcite.

The systematically lower $\delta^{13}C$ values observed in the open-vein calcites may indicate calcite precipitation during warm climate conditions. Soil zone bicarbonate is ^{13}C-depleted by biologic activity of plants (photosynthesis and respiration) to values between -23 and -15‰. The range of $\delta^{13}C$ measured is consistent with varied amounts of soil zone bicarbonate entering the fracture system and mixing with a ^{13}C-enriched carbon pool during groundwater recharge. This would most likely occur during warm climate conditions when groundwater recharge is not impeded by the overburden freezing or precipitation occurring as snow. The sealed-vein calcites have less ^{13}C-depleted values than the open-vein calcites. This is consistent with precipitation from a water isolated from the biosphere, possibly a hydrothermal formation water.

Unlike ^{18}O, ^{13}C fractionation during calcite precipitation is not very temperature dependent. The calcite phase is ^{13}C-enriched by approximately 2‰ relative to aqueous bicarbonate over the temperature range 0-100°C (Dienes et al., 1974). Thus, variation in the $\delta^{13}C$ of both open-vein and sealed-vein calcite most likely represents a change in the source of the bicarbonate. This supports the argument that the isotopic compositions of open-vein calcites have been affected by a warm climate, soil-zone ^{13}C-depleted

bicarbonate source.

The range of $\delta^{18}O$ and $\delta^{13}C$ values observed in open-vein and sealed-vein calcites in this study is consistent with the ranges observed in other investigations of fracture-infilling calcite in fractured crystalline rock groundwater flow systems. The ranges observed in this thesis are diagrammatically compared to those from other studies in Figure 5-3. An investigation of isotopic trends in fracture-infilling calcite at the Underground Research Lab (URL) of AECL in Pinawa, Manitoba found a similar range of $\delta^{18}O$ values. Jones et al. (1987) found that the $\delta^{18}O$ values measured for fracture-infilling calcite ranged between 15 and 26‰. They grouped the calcites by texture, classifying the calcite as either sucrosic or platy. They found that the sucrosic calcites tended to occur in fractures sealed to ground water flow, and had more depleted $\delta^{18}O$ values (17 to 25‰) than the platy calcites. The platy calcites tended to exist in veins open to groundwater flow, and had less depleted $\delta^{18}O$ values ranging between 18 and 26‰. A range of $\delta^{13}C$ values similar to the range measured in this investigation was also measured by Jones et al. (1987). They found that the majority of calcites had $\delta^{13}C$ values between -16 and -4‰, with one calcite having a value of -22‰. They also found a similar overlap in the $\delta^{13}C$ ranges when the calcites were considered with respect to their texture. The platy calcites (open-vein) had $\delta^{13}C$ values between -16 and -5‰, and the sucrosic calcites (sealed-vein) had $\delta^{13}C$ values between -15 and -6‰. Jones et al. (1987) attributed the $\delta^{13}C$ variation to a Rayleigh-like fractionation of the carbon reservoir during calcite precipitation. An additional study at the same site (Gascoyne et al., 1997) found a

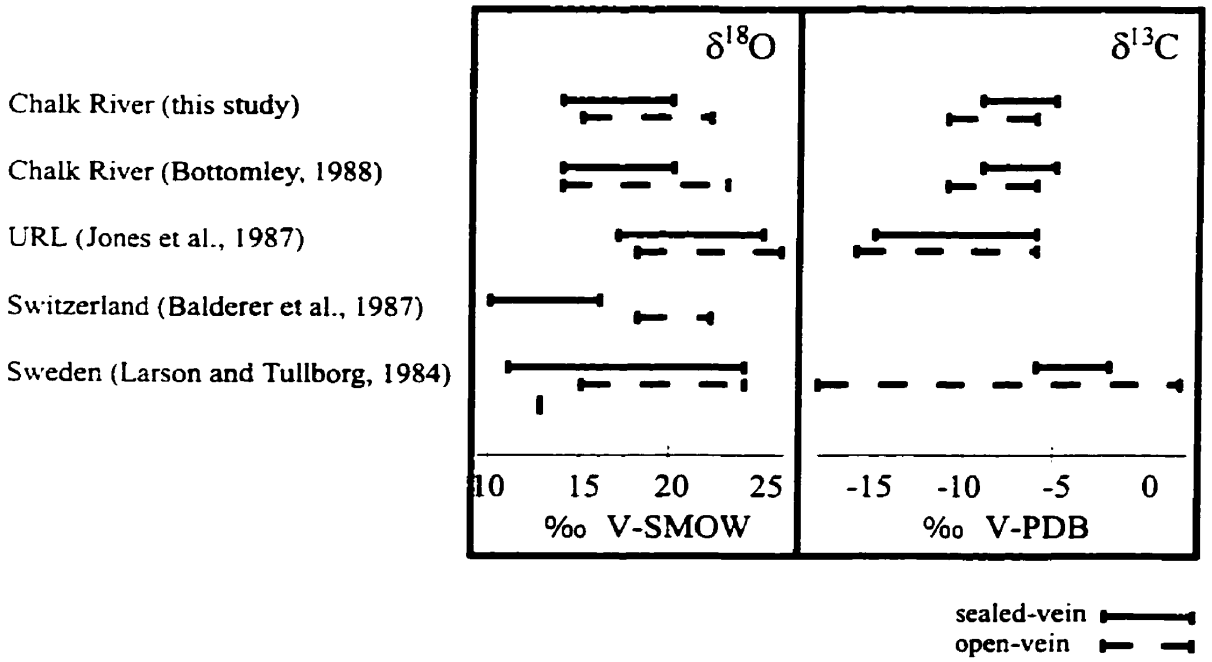

Figure 5-3 : Schematic representation of the relative ranges of $\delta^{18}O$ and $\delta^{13}C$ of sealed-vein and open-vein calcites from different shield environments.

similar range of $\delta^{18}O$ values (18 to 22‰) for fracture-filling calcites from the URL.

A study of fracture-filling calcite in Switzerland found that the measured $\delta^{18}O$ values ranged from 10 to 22‰, with those classified as sealed-vein calcite having a lower range (10 to 16‰) than open-vein calcites in the same fracture system (18 to 22‰) (Balderer et al., 1987). The Balderer et al. (1987) study measured a similar total range of $\delta^{13}C$ (-11 to +0.5‰) and found that the $\delta^{13}C_{calcite}$ in some cases was in equilibrium with the $\delta^{13}C_{bicarbonate}$. However, the water was not saturated with respect to calcite, which suggests that the isotopic equilibrium between the bicarbonate and calcite was a result of calcite dissolution, not calcite precipitation.

A study in Sweden found the total range of $\delta^{18}O$ values in calcite to be between 11 and 24‰, with sealed-vein calcite having values over the entire range, and open-vein calcite having a narrower range of values between 15 and 24‰ (Larson and Tullborg, 1984). The Larson and Tullborg (1984) study found very similar ranges of $\delta^{13}C$ values to those measured in this investigation. They found an overall range of $\delta^{13}C$ values of -18 to +2‰, with open-vein calcites spanning the entire range and sealed-vein calcite confined to the $\delta^{13}C$ range of -6 to -2‰. They made the argument that ^{13}C-depleted soil zone bicarbonate caused the variation in the $\delta^{13}C$ of the calcite.

A German study separated fracture-filling calcite into three categories, Metamorphic, Crack filling (crosscuts earlier metamorphic calcite) and Replacement (replaced primary minerals in altered areas) (Komor, 1995). The study found that Metamorphic and Crack-filling calcites had similar ranges of $\delta^{18}O$ (8 to 13‰, and 7 to

14‰ respectively) and that the Replacement calcite had a range that included higher values of $\delta^{18}O$ (10 to 18‰) (Komor, 1995). The Komor study also found there to be considerable overlap in the $\delta^{13}C$ values among Metamorphic, Crack filling and Replacement calcite. The overlap was attributed to recrystallization of calcite and water-rock interaction. The results from other geographic locations are significant as they suggest that these are not site-specific observations, but may represent similar processes which have occurred in the fracture-flow aquifers in crystalline bedrock environments globally.

5.1.2 - THEORETICAL END-MEMBERS

Several isotopically, thermally and hydrogeologically distinct fluids responsible for calcite formation on the properties of CRL have been proposed based on the geologic history of the region. The fluids are referred to as; 1) Magmatic/Metamorphic fluids; 2) "Hydrothermal" fluid (Bottomley, 1988); 3) Glacial Recharge waters; 4) Champlain Seawater; and 5) Modern-day Meteoric Recharge waters. The characteristic $\delta^{18}O$, $\delta^{13}C$, salinities and temperatures of each of these theoretical end-member fluids are summarized in Table 5-1.

Magmatic/Metamorphic Fluids

Magmatic/Metamorphic fluids are fluids which interacted with the rocks as a result of the metamorphism associated with formation of the Grenville Orogenic Front (Section 2.1.1.2). These fluids are characterized by high temperatures (600-800°C), positive $\delta^{18}O$ values and high salinity. They would tend to form calcite with a wide range of positive $\delta^{18}O$ values. Fluid inclusions in the calcites would likely have a high T_h and

TABLE 5-1 - The ranges of $\delta^{18}O$, $\delta^{13}C$, Salinity and Temperature for each of the possible end-member calcite precipitating fluids identified. The source of each value is given in parenthesis.

END-MEMBER	$\delta^{18}O$ (‰ SMOW)	$\delta^{13}C$ (‰ PDB)	SALINITY (wt % NaCl)	TEMPERATURE (°C)
Magmatic / Metamorphic	5 to 25 (Taylor, 1987)	$\delta^{13}C$= -13 to +2	7 to 30 (Kerrich, 1987)	600 to 800 (Easten and refs therein, 1992)
"Hydrothermal"	7 to 12 (Bottomley, 1988)	DIC = -8 to -7 (Bottomley, 1988)	7 to 30 (Kerrich, 1987)	~300 (used 250-350) (Bottomley, 1988)
Glacial Recharge	-28 to -18 (Seguin, 1994)	DIC =-23 to -15 *	0 **	0 to 4 **
Champlain Seawater	-12.3 to -10 (Seguin, 1994)	DIC =-23 to -15 *	0 to 3.5 (Hillaire-Marcel,1980)	0 to 4 **
Meteoric Recharge	-10 to -9 (Kotzer et al., 1998)	DIC =-23 to -15 *	0 **	0 to 10 ***

* - range of the $\delta^{13}C$ values in bicarbonate resulting from biogenic activity in the soil zone
** - approximate range of freshwater salinity and glacial meltwater temperature
*** - approximate range of surface water temperatures at CRL

high salinities (7-30 wt. % NaCl).

"Hydrothermal" Calcites

Bottomley (1988) argued that the origin of some calcites at CRL was precipitation from a "Hydrothermal" fluid. This was based on fracture mineralogy and observed trends in the $\delta^{18}O$ data. Co-precipitation of laumontite with calcite in some fractures was taken to indicate that the fracture-infilling minerals precipitated from a hot fluid, as laumontite would only co-precipitate with calcite from a CO_2 poor solution at temperatures of around 300°C (Bottomley, 1988). The parameters of the "Hydrothermal" end-member were confined by modelling the isotopic composition of calcite precipitated under variable water-rock ratios, assuming a system open with respect to oxygen, and closed with respect to carbon. Bottomley (1988) established that if the "Hydrothermal" range of $\delta^{18}O$ and $\delta^{13}C$ values of calcite were used, all the observed isotope ratios in the calcite could be modelled by calcite precipitation under variable water to rock ratios. Bottomley proposed that a meteoric water was hydrothermally reacting with the gneisses in the host pluton and precipitating calcite in the fractures under variable water to rock ratios.

Glacial Recharge

During the retreat of glaciation from the region, particularly the Laurentide ice sheet in the Wisconsin period, glacial meltwater was available for groundwater recharge (Seguin, 1994). This meltwater may have entered the fracture systems and precipitated calcite, especially immediately after isostatic rebound which had reactivated previously formed fault and fracture systems (Ates et al., 1997). Because of the low temperatures of these fluids, it is expected that calcite precipitated from glacial recharge would have

single-phase liquid fluid inclusions of low salinity. The glacial meltwater would be very ^{18}O-depleted, and there would be a large ^{18}O fractionation due to the low temperature of calcite precipitation.

Champlain Seawater

After the Wisconsin glaciation, and prior to isostatic rebound, there was an incursion of seawater which led to the formation of the Champlain Sea. During the period of time that the Champlain Sea existed, Champlain seawater may have entered the fracture system and led to calcite precipitation. Calcites precipitated from Champlain seawater would be low temperature and have fluid inclusions with salinities varying from freshwater (glacial meltwater) to seawater. The $\delta^{18}O$ of the Champlain Sea was between the $\delta^{18}O$ value of depleted glacial meltwater (-28 to -18‰) and ocean water (~0‰) (Seguin, 1994).

Modern Meteoric Recharge

The fracture-infilling calcite may have precipitated from, or re-crystallized in the presence of, modern meteoric recharge waters. Calcites precipitating from modern meteoric recharge would contain low temperature, low salinity fluid inclusions, and have $\delta^{18}O$ values of approximately 20‰, assuming the value of meteoric water is constant at approximately -10‰ at Chalk River (Kotzer et al., 1998).

Separation of Proposed End-Members

To investigate the possibilities of calcite precipitating from the five identified theoretical fluid end-members, the $\delta^{18}O$ values and temperatures of these waters (Table 5-1) are plotted on Figure 5-4, and compared with the $\delta^{18}O$ values measured on calcite

FIGURE 5-4 - Graph of $\delta^{18}O_{calcite}$ as a function of the formation temperature of the calcite. The boxes indicate the relative positions of calcite precipitating in isotopic equilibrium with the proposed end-member fluids summarized in Table 5-1. The curves represent the $\delta^{18}O$ value of a calcite which would precipitate from water of constant $\delta^{18}O$ (listed adjacent to each line) as a function of the temperature of precipitation using the oxygen isotope fractionation factor for calcite-water (O'Neil et al., 1969). The fractionation factor had been extended beyond the range established by O'Neil et al. (1969), to include the Magmatic-Metamorphic end-member. The fractionation factor was established over the range 0 to 500°C.

The histogram to the right of the plot is a reproduction of Figure 5-1a, displaying the range of $\delta^{18}O$ values measured in this investigation. The darker areas in the histogram represent sealed vein calcites, and the lighter areas represent open vein calcites. This is a modification of a figure from Bukata et al. (1997) and Bukata et al. (1998b).

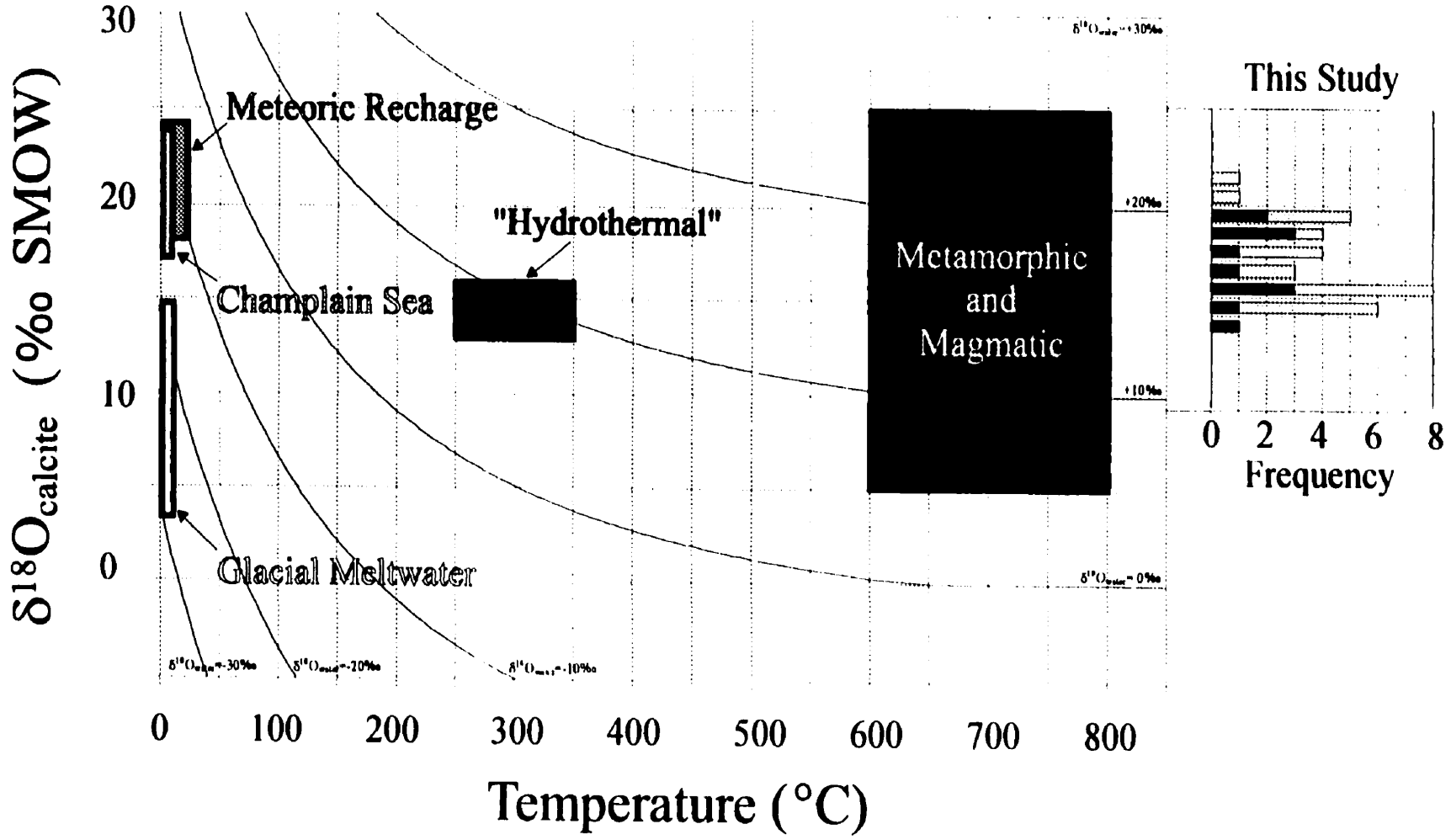
30
20
10
0
$\delta^{18}O_{calcite}$ (‰ SMOW)
Meteoric Recharge
Champlain Sea
"Hydrothermal"
Metamorphic
and
Magmatic
Glacial Meltwater
+20‰
+10‰
0‰
This Study
0 2 4 6 8
Frequency
0 100 200 300 400 500 600 700 800
Temperature (°C)

minerals from this investigation.

The range of $\delta^{18}O$ values measured on calcites in this investigation (14 to 22‰) falls within the range of $\delta^{18}O$ values for calcites which could have precipitated from all of the proposed end-members. Thus, it is impossible to use the $\delta^{18}O$ value of calcite alone to establish the nature of the calcite precipitating fluid. In order to delineate the fluid from which the calcites may have precipitated, it is necessary to establish the possible formation temperature of the calcite. This is most significant with respect to calcites which may have precipitated from a Metamorphic/Magmatic fluid, as the range of $\delta^{18}O$ values and temperatures for this fluid cover the entire range of all calcites from other end-member waters.

5.1.3 - SYSTEMATIC TRENDS

The measured $\delta^{18}O$ and $\delta^{13}C$ values in the calcite have been examined for any trends with depth and any co-variation of the isotope ratios.

Isotope Ratio Trends with Sample Depth

There are no immediately obvious trends between the $\delta^{18}O$ values of the calcites and their sampling depth. The $\delta^{18}O$ data from this investigation (Figure 5-5 a) and the combined data from this investigation and Bottomley (1988) (Figure 5-5 b) are presented as a function of depth. Bottomley (1987, 1988) and Bottomley and Veizer (1992) did not identify and discuss any possible depth trends in the data, citing the fact that the boreholes were spudded at different ground elevations and inclined at various angles, precluding any inter-comparison. In this investigation, sample depth below the surface was determined for samples from this investigation and Bottomley (1988) using the plunge

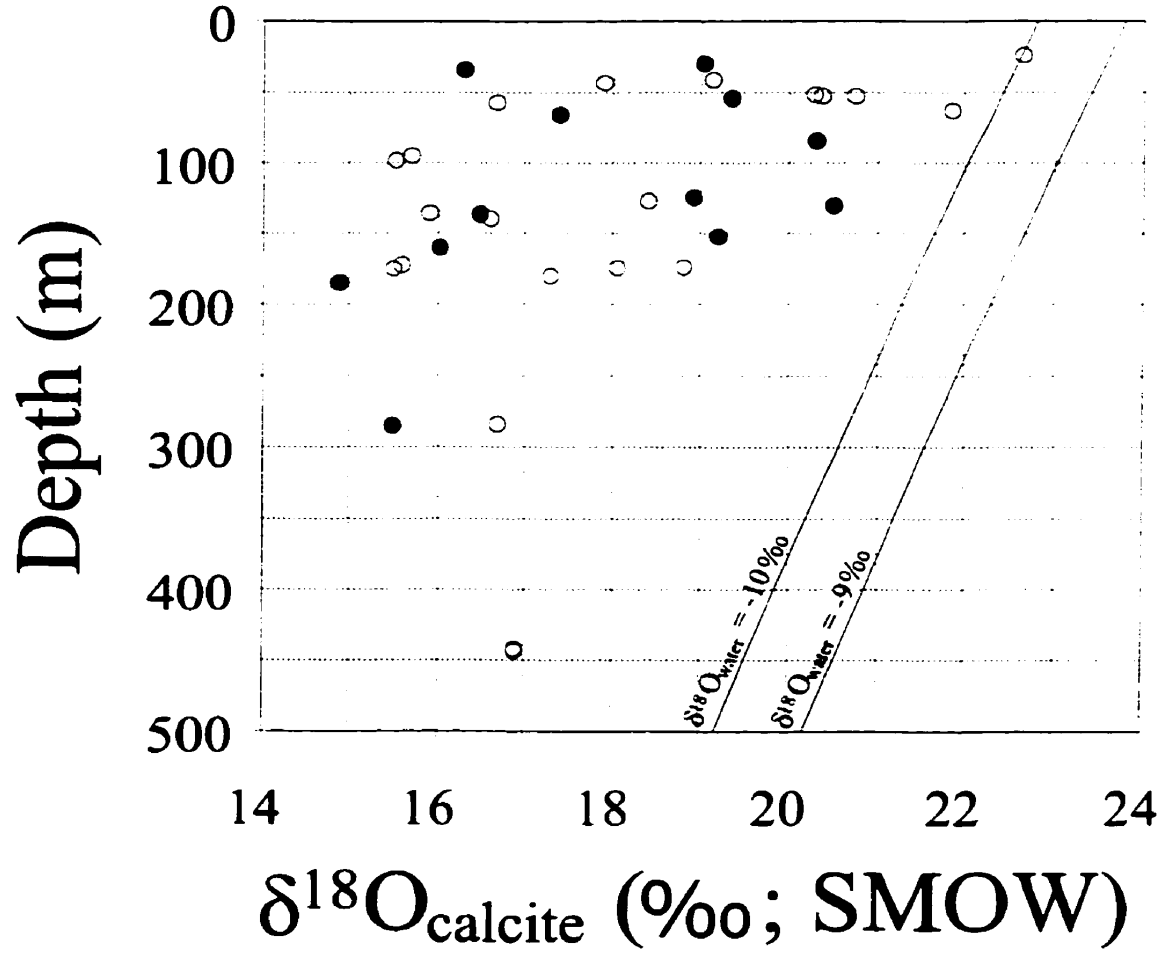

FIGURE 5-5 - a) The $\delta^{18}O$ measured for each calcite in this investigation plotted against the sample depth below surface. The sample depth was calculated using the location of the sample along the length of core and the angle at which the borehole was drilled. The empty circles represent open-vein calcites and the filled circles represent sealed-vein calcites.

The lines plotted on the graph define the ranges of $\delta^{18}O$ expected in calcite precipitating in equilibrium with modern meteoric recharge ($\delta^{18}O_{water}$ = -10 to -9‰, (Kotzer et al., 1998)), assuming a geothermal gradient of 25°C/km and using the $\delta^{18}O_{calcite\text{-}water}$ fractionation factor of O'Neil et al. (1969).

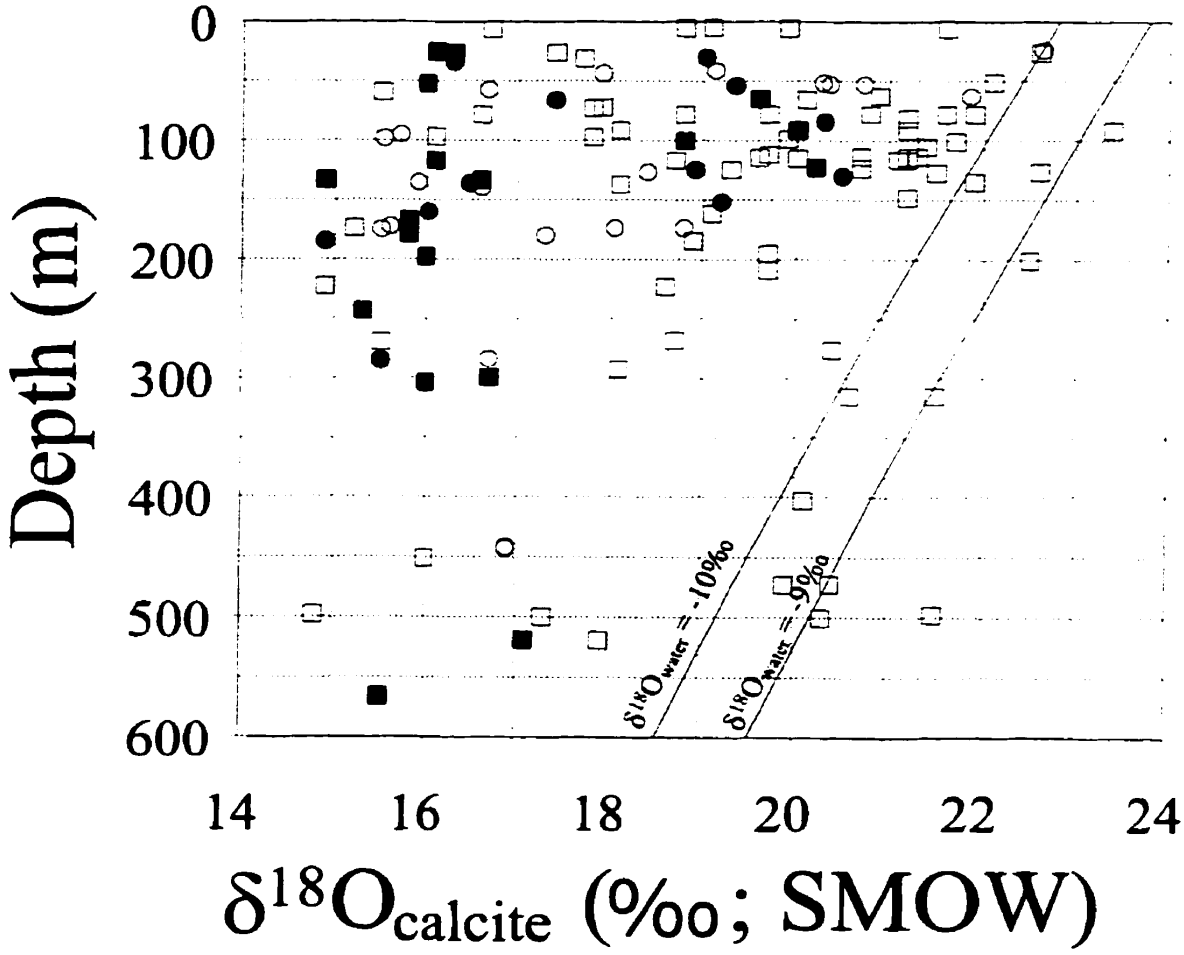

FIGURE 5-5 -b) $\delta^{18}O$ values measured in this investigation (circles) and those reported in Bottomley (1988) (squares) for fracture-infilling calcite from CRL. For both data sets, the filled symbols represent sealed-vein calcites and the empty symbols represent open-vein calcites.

As in Figure 5-4 -a), the lines define the range of $\delta^{18}O$ ratios expected in calcites precipitating in isotopic equilibrium with modern meteoric waters. The lines are plotted assuming the $\delta^{18}O_{water}$ is between -10 and -9‰, (Kotzer et al., 1998), the geothermal gradient is 25°C/km, and using the $\delta^{18}O_{calcite\text{-}water}$ fractionation factor of O'Neil et al. (1969).

angle of the borehole and the measured location of the sample along the core. The trigonometric relationship among the three variables was used to calculate the actual vertical depth below the surface of the sample. The depth below the surface was then used for sample inter-comparison despite the differences in elevation of the boreholes. Similarly, Bottomley (1987, 1988) and Bottomley and Veizer (1992) did not separate the samples into open-vein or sealed-vein prior to plotting them with depth, and therefore they did not address the apparent depth trends with respect to open-vein versus sealed-vein calcites on Figure 5-5 b.

Figures 5-5 a) and b) indicate that some of the open-vein fracture-infilling calcites have $\delta^{18}O$ values consistent with precipitation in isotopic equilibrium with modern meteoric recharge assuming a geothermal gradient of 25°C/km. However, none of the sealed-vein calcites plot within the range expected for precipitation from modern meteoric recharge. This suggests that the sealed-vein calcite has precipitated under conditions quite different from conditions that currently exist in the fracture system.

The sealed-vein calcites in Figure 5-5 b) have a narrower range of $\delta^{18}O$ values and seem to have more isotopically depleted values than the open-vein calcites at all depths. The open-vein calcite spanned a wider range of $\delta^{18}O$ values, including the entire range observed in the sealed-vein calcites, and the range of values expected for calcites precipitating in isotopic equilibrium with modern meteoric recharge. One possibility is that the sealed-vein calcites may have been re-crystallized with varying amounts of modern meteoric recharge to form open-vein calcite. This is consistent with the calcite precipitation from time-integrated water-rock ratios, as argued by Bottomley (1987, 1988)

and Bottomley and Veizer (1992). The absence of sealed-vein calcite in equilibrium with modern recharge further supports the argument that the sealed-vein calcite may have formed previously, and is being altered by modern recharge. ^{14}C ages on the DIC in groundwater presently occupying the fractures range from modern to 12.7 ka (Lee et al., 1998), and thus any calcite currently precipitating in the fractures would contain "modern" bicarbonate. These ages are consistent with pristine post-glacial recharge and post-glacial recharge which contains dissolved carbonate minerals.

Other studies on carbon and oxygen isotope systematics in fracture-infilling calcites have also looked for trends in the $\delta^{18}O$ value with depth. In some studies, such as Komor (1995) and Gascoyne et al. (1997), no relationship with depth has been observed. Jones et al. (1987) found that both $\delta^{18}O$ and $\delta^{13}C$ values span large ranges at shallow depth, and narrower ranges at greater depth. They argued that this observation is consistent with calcite formation as a result of mixing between surface waters and a deep-seated fluid. Balderer et al. (1987), and Larson and Tullborg (1984) found that some of the calcites may have precipitated in isotopic equilibrium with modern recharge at temperatures consistent with the geothermal gradient. Hall et al. (1995) found a systematic trend in $\delta^{18}O$ with depth for calcites around Yucca Mountain, and have attributed it to a model of groundwater movement causing high (170-180°C/km) geothermal gradients. Regardless of site-specific interpretation, systematic trends of $\delta^{18}O$ values in calcite with depth have been observed in some, but not all investigations.

There are no clear depth related trends observed in the carbon isotopic compositions for calcites from CRL, although Figures 5-6 a) and b) indicate that the

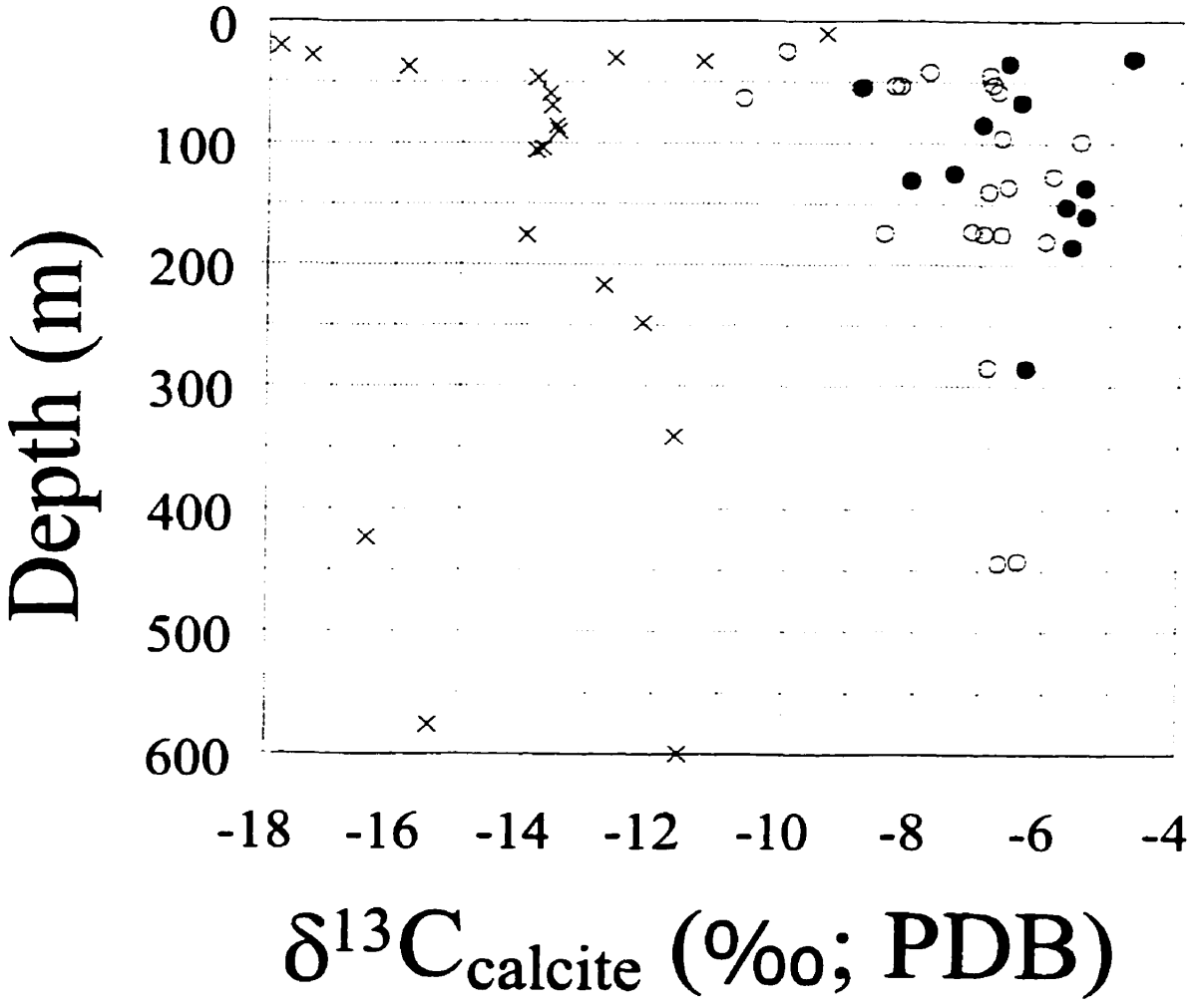

FIGURE 5-6 -a) $\delta^{13}C$ plotted against sample depth for the calcites sampled at CRL in this investigation. The filled circles represent sealed-vein calcites and the empty circles represent open-vein calcites.

The 'X' represent the $\delta^{13}C$ values of calcite which would precipitate in equilibrium with the HCO_3^- sampled at that specific depth from boreholes at CRL. The $\delta^{13}C_{calcite}$ was determined using the calcite-bicarbonate fractionation factor of Deines et al. (1974), and assuming a geothermal gradient of 25°C/km. The $\delta^{13}C_{bicarbonate}$ values were taken from Gascoyne and Kotzer (1997), Bottomley (1984) and Milton (1985).

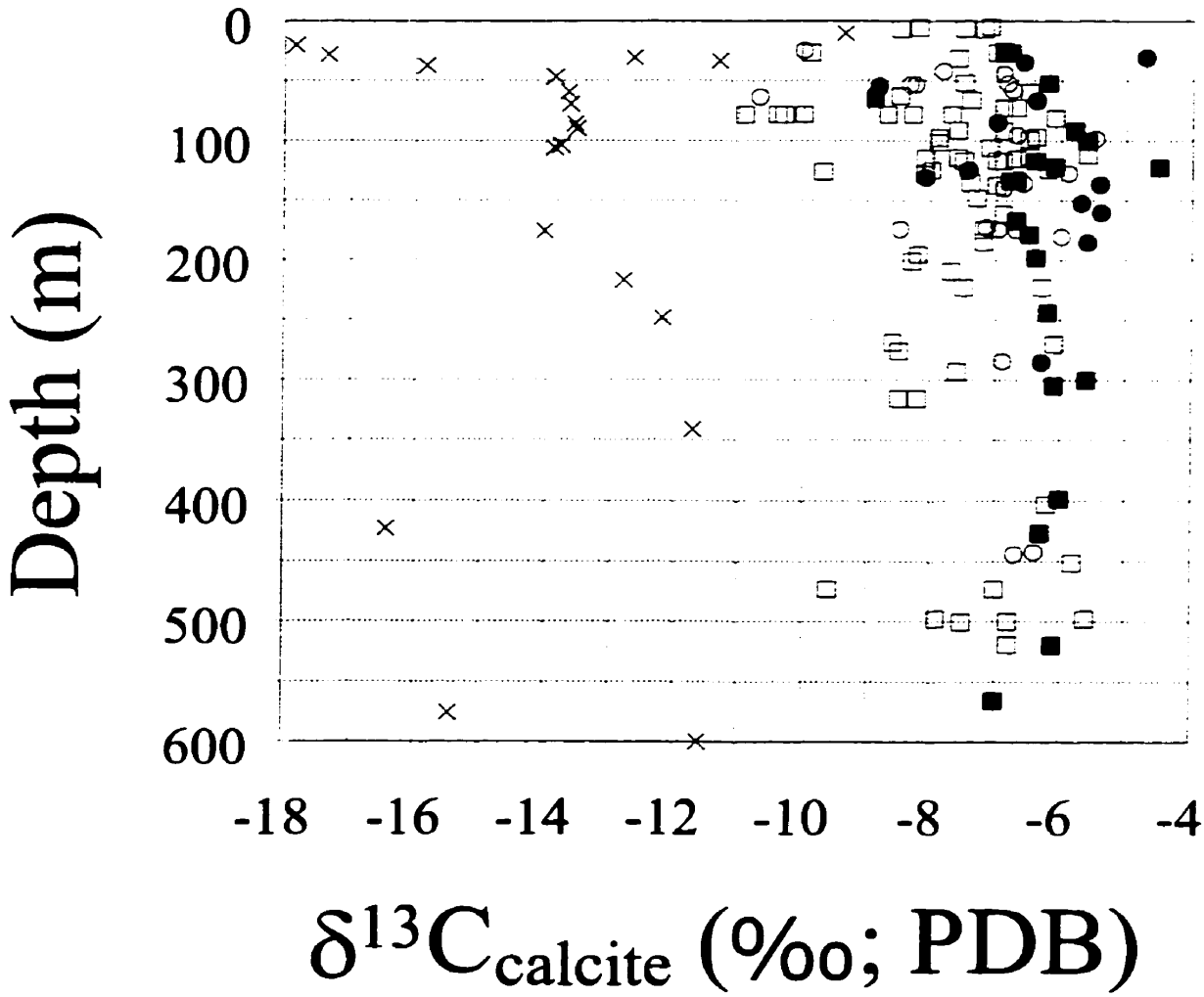

FIGURE 5-6 -b) $\delta^{13}C$ plotted against sample depth for the calcites sampled at CRL in this investigation (circles) and from Bottomley (1988)(squares). The filled symbols represent sealed-vein calcites and the empty symbols represent open-vein calcites.

The 'X' represent the $\delta^{13}C$ values of calcite precipitated in equilibrium with the HCO_3^- sampled at that specific depth from boreholes at CRL. The $\delta^{13}C_{calcite}$ was determined using the calcite-bicarbonate fractionation factor of Deines et al. (1974), and assuming a geothermal gradient of 25°C/km. The $\delta^{13}C_{bicarbonate}$ values are taken from Gascoyne and Kotzer (1997), Bottomley (1984) and Milton (1985).

open-vein calcites tend to have a wider range of values including more ^{13}C-depleted values at all depths. This is consistent with calcite precipitation or post depositional alteration of open-vein calcite with biologically ^{13}C-depleted bicarbonate. The shallow vein calcites have a more dispersed range of $\delta^{13}C$ values, including more ^{13}C-depleted values. These observations are consistent with the $\delta^{18}O$ data, and support the argument that modern precipitation or alteration of previously deposited calcite is occurring, and is occurring to a greater extent in the shallow sub-surface.

Figures 5-6 -a) and -b) also indicate that with the exception of a few shallow open-vein calcites, the majority of the calcite is not precipitating in isotopic equilibrium with the $\delta^{13}C$ of the bicarbonate currently present in the groundwater. All the calcites have more ^{13}C-enriched values than predicted for calcites precipitating in isotopic equilibrium with modern meteoric recharge. The same pattern of sealed-vein calcite isotopic values plotting further from equilibrium with modern recharge observed with respect to $\delta^{18}O$ (Figures 5-5 -a) and -b)) is also observed with respect to $\delta^{13}C$ (Figures 5-6 -a) and -b)). This supports the argument that the sealed-vein and open-vein calcites precipitated under geochemically different conditions, with the open-vein calcite most likely precipitating from relatively modern meteoric recharge or representing recrystallization of previously deposited calcite in the presence of lower temperature meteoric fluids.

The near-surface open-vein calcite (<150 m) is closer to being in isotopic equilibrium with modern meteoric recharge than the sealed-vein calcite sampled from all depths. This pattern is consistent with sealed-vein calcite deposition in a hydrothermal

environment, followed by greater chemical and isotopic alteration of calcite by recrystallization in the more hydrologically active near-surface fracture-flow system to form open-vein fracture-infilling calcite. These observed isotopic disequilibria are more pronounced with depth. While this may be an artefact of sampling bias (fewer deep-seated calcites present and sampled), it may also represent the saturation of groundwater with respect to calcite occurring at shallow recharge depths, and a lack of chemical disequilibrium substantial enough to dissolve or precipitate calcite in deep fractures. The ground water at CRL has a low bicarbonate concentration (70 to 350 ppm, Lee et al., 1998 and references therein); as a result, calcite precipitation and recrystallization in the shallow bedrock fractures exert greater control on the $\delta^{13}C$ value of the DIC than does the input of soil zone ^{13}C-depleted bicarbonate. Greater DIC interaction with fracture carbonates causes the precipitation of calcite having ^{13}C-enriched $\delta^{13}C$ values relative to soil zone bicarbonate at all depths in the hydrogeologic system.

The trends of $\delta^{13}C$ values with depth observed in this investigation have been observed in other investigations, and are most often attributed to crystallization of carbonate minerals in the presence of groundwaters carrying a soil-zone ^{13}C-depleted bicarbonate. Bottomley (1987, 1988) and Bottomley and Veizer (1992) noted that none of the calcites measured were in isotopic equilibrium with modern meteoric recharge for both ^{13}C and ^{18}O at CRL. They concluded that a process more complicated than simple calcite precipitation from modern meteoric recharge was occurring. Bottomley and Veizer (1992) noted that the same depth trend observed in the CRL calcites was occurring at the East Bull Lake sampling site (elsewhere on the Canadian Shield), and attributed it

to the impact of ^{13}C-depleted soil zone bicarbonate precipitating calcite under conditions of variable water to rock ratios. Komor (1995) observed a similar depth trend in calcite precipitating to depths of 700 m, but found that at depths greater than 700 m, the trend did not exist. Balderer et al. (1987) observed that the $\delta^{13}C$ values roughly trended with depth for calcite precipitation in isotopic equilibrium with bicarbonate, and that the observed trend possibly reflected the geothermal gradient. However, Balderer et al. (1987) noted that there was considerable scatter observed in the data.

Relationship Between Sample $\delta^{13}C$ and $\delta^{18}O$ values

There may be a very weak linear relationship between $\delta^{13}C$ and $\delta^{18}O$ ($r^2 = 0.47$ this study, and $r^2 = 0.12$ in the combined data set), as indicated in Figures 5-7 a) and b). However, there is too much scatter in the data (low r^2 values) to conclude that the true relationship between the two isotopes is linear. It is more probable that the relationship between $\delta^{13}C$ and $\delta^{18}O$ follows the curved path of progressive recrystallization under time-integrated increasing water to rock ratios as proposed by Bottomley (1987, 1988) and Bottomley and Veizer (1992), wherein the source of the oxygen is the fluids and the sources of the carbon are the rocks, minerals and soils. The trend in Figure 5-7b suggests progressive recrystallization of sealed-vein "hydrothermal" calcite with modern fluids, either Champlain Seawater or Modern Meteoric Recharge.

The sealed-vein calcites measured in this investigation, as well as those from Bottomley (1988), span a narrower range of $\delta^{13}C$ and $\delta^{18}O$ values than the open-vein calcites, and tend to cluster toward the "hydrothermal" end-member on Figure 5-7 b). The open-vein calcites have isotopic values which span from the "hydrothermal" end-

FIGURE 5-7 -a) i) $\delta^{13}C$ plotted against $\delta^{18}O$ for all the calcites sampled in this investigation. The figure also shows the regions where calcite precipitating in equilibrium with "Hydrothermal" fluids, Champlain Seawater and Modern Meteoric Recharge waters would plot. The boundaries of these regions are defined in Table 5-1. The sealed-vein calcites are represented as filled circles and the open-vein calcites are represented as empty circles.
ii) The same data plotted on a narrower range of $\delta^{13}C$ and $\delta^{18}O$ values to show the dispersion in the data. The line is the regression line through the data points. The equation of the linear regression is, $\delta^{13}C = -0.43*\delta^{18}O + 0.81$. The r^2 value of the regression is 0.47, and therefore the relationship is weak.

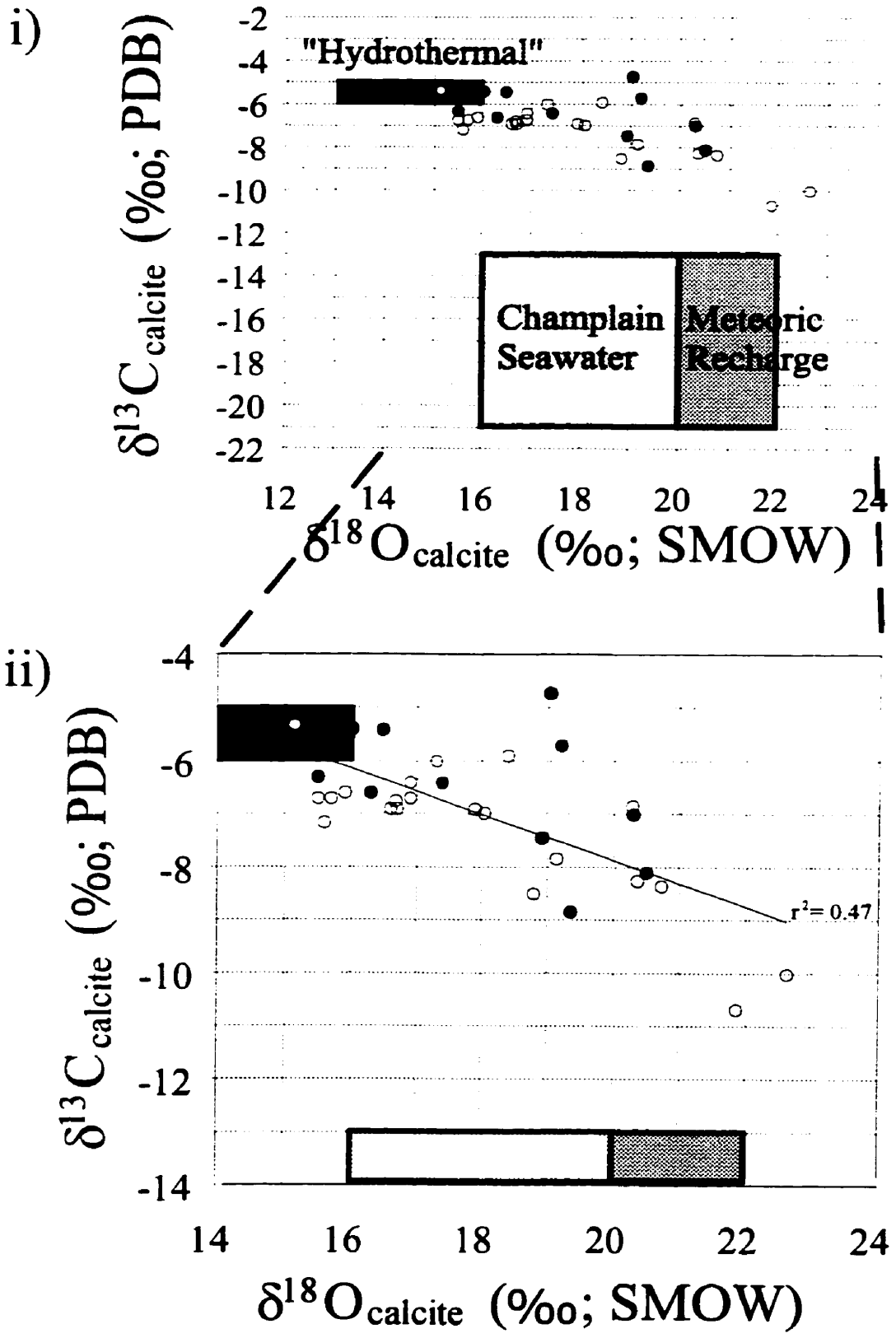
i)
"Hydrothermal"
Champlain Seawater
Meteoric Recharge
δ13Ccalcite (‰; PDB)
δ18Ocalcite (‰; SMOW)
ii)
r2= 0.47
δ13Ccalcite (‰; PDB)
δ18Ocalcite (‰; SMOW)

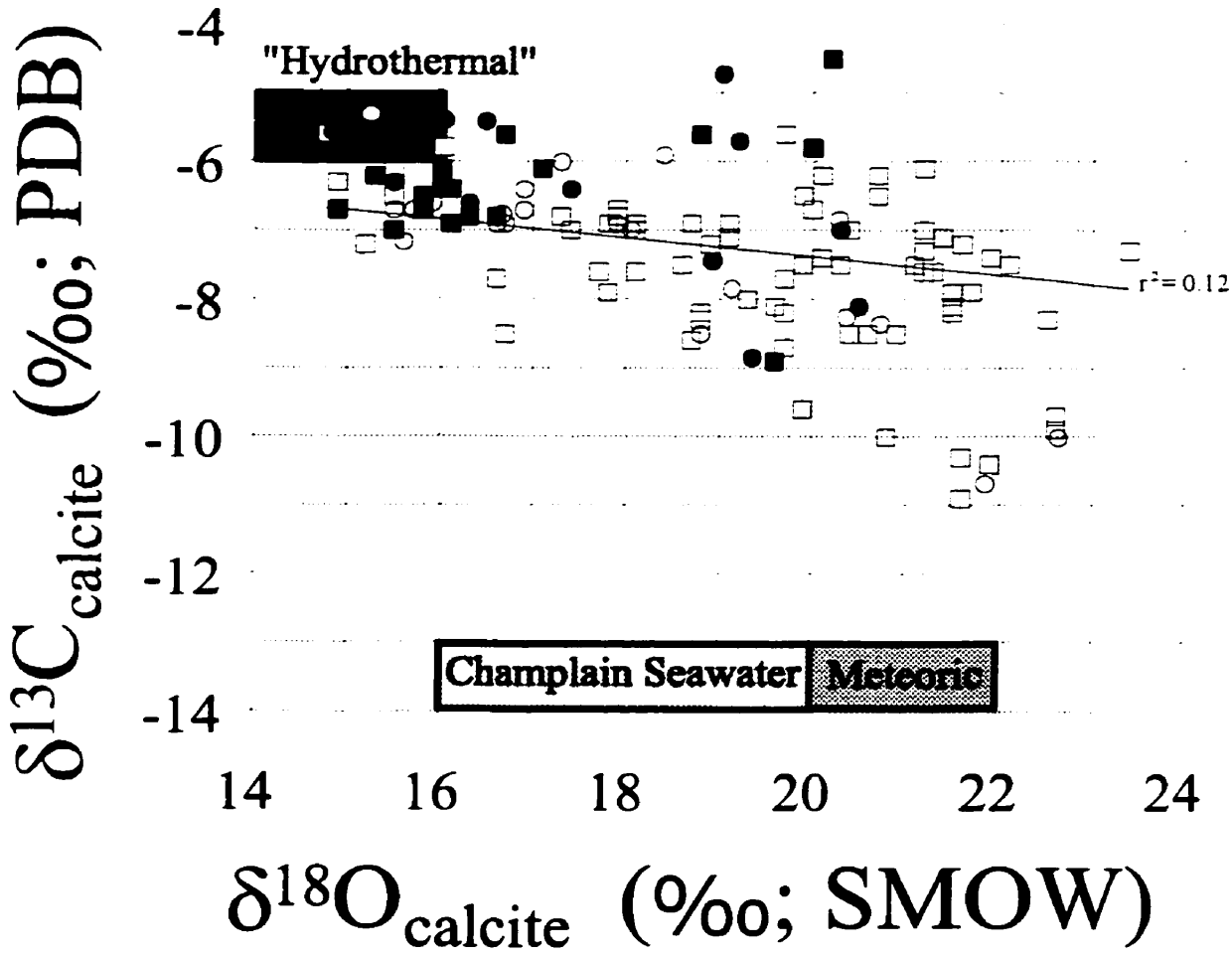

FIGURE 5-7 -b) $\delta^{13}C$ plotted against $\delta^{18}O$ for calcites sampled at CRL in this investigation (circles) and by Bottomley (1988) (squares). The sealed-vein calcites are represented by the filled symbols, and the open-vein calcites are represented by the empty symbols. The figure also shows the regions where calcite precipitating in equilibrium with "Hydrothermal" fluids, Champlain Seawater and Modern Meteoric Recharge waters would plot. The boundaries of the regions are defined in Table 5-1.

The data is plotted on a narrow range of $\delta^{13}C$ and $\delta^{18}O$ values to show the dispersion in the data, and as a result, the relative sizes of the end-member ranges are not accurate. The dashed line represents the regression line through the data points ($\delta^{13}C = -0.14*\delta^{18}O - 4.68$). The r^2 value of the regression is 0.12, and therefore the true relationship is not linear.

member to values approaching the modern meteoric recharge end-member. Many of the $\delta^{18}O$ values of the open-vein calcites fall within the range of the Meteoric Recharge end-member, but the $\delta^{13}C$ values only approach the Meteoric/Champlain Seawater end-members. As previously discussed, this is most likely due to the low bicarbonate concentrations of the groundwater at CRL leading to recycling of DIC during recrystallization of calcite with a less ^{13}C-depleted value. This will result in the $\delta^{13}C$ value of the DIC becoming a weighted average reflecting the degree of mixing between soil zone CO_2 and previously precipitated calcite. The observed pattern of sealed-vein calcite clustering towards the "hydrothermal" end-member and open-vein calcites trending toward the modern end-members suggests either progressive recrystallization of hydrothermal calcite with modern meteoric recharge or the sealed-vein calcites are generally older and have not been recrystallized by subsequent fluids, as they occupy fractures that have not been hydrologically active. Further, the larger shift in $\delta^{18}O$ values than in $\delta^{13}C$ values suggests that the calcites are exhibiting open system behaviour with respect to ^{18}O and closed to semi-open system behaviour with respect to ^{13}C.

The trend between $\delta^{13}C$ and $\delta^{18}O$ observed in this investigation is consistent with that observed by Bottomley (1987, 1988) and by Bottomley and Veizer (1992). Bottomley (1987) argued that this trend could be produced by one of three processes; 1) mixing of hydrothermal and cool waters at the time of calcite precipitation; 2) low temperature recrystallization of a relatively ^{18}O-depleted calcite under variable water rock ratios; or 3) episodic calcite precipitation from meteoric waters on reactivated fractures previously lined with hydrothermal calcite. Given the low r^2 values for the relationship

between $\delta^{13}C$ and $\delta^{18}O$, the first possibility is unlikely. If calcite precipitation were occurring as a result of end-member water mixing there would be a stronger linear relationship between $\delta^{13}C$ and $\delta^{18}O$, consistent with a two component mixing model. The third process proposed by Bottomley (1987) is not entirely inconsistent with the second, and may account for the semi-closed system behaviour exhibited by the ^{13}C in this investigation and in Bottomley (1987, 1988), and Bottomley and Veizer (1992). Bottomley and Veizer (1992) concluded that the trend was probably caused by time integrated recrystallization of calcite from a system with variable water to rock ratios (10^1 to 10^5), for example open with respect to ^{18}O and semi-closed with respect to ^{13}C.

Bottomley and Veizer (1992) observed similar trends in calcites taken at East Bull Lake and White Lake, both located on the Canadian Shield. The samples from the White Lake pluton exhibited a trend which supported a model of calcite precipitation during fluid mixing between hydrothermal fluids and fluids having carbon and oxygen isotope compositions reflecting interactions with sedimentary rocks, as opposed to CRL and East Bull Lake that appear to have undergone recrystallization with fluids which have interacted with their crystalline host rocks.

Jones et al. (1987) observed a strong linear relationship ($r = 0.91$) between the $\delta^{13}C$ and $\delta^{18}O$ from calcites taken at Whiteshell. They attributed the relationship to calcite precipitation during cooling or during mixing of two distinct end-members. They argued that the isotopic composition of the carbon source may have changed over time or that a Rayleigh-like distillation process may have occurred with respect to bicarbonate during calcite precipitation. Jones et al. (1987) tend to favour a mixing model, as the

temperatures required to explain the measured $\delta^{18}O$ values in some of the calcites were unreasonable (< 0°C).

A reinterpretation of the $\delta^{18}O$ and $\delta^{13}C$ values in calcite deposits around Yucca Mountain, Nevada was undertaken by Hill et al. (1995). They observed a similar pattern in the $\delta^{18}O$ and $\delta^{13}C$ to that observed in this investigation. However, rather than trending between two end-members, the calcite-vein deposits formed two distinct clusters. The authors identified the calcites as precipitating from distinct geochemical environments, a hydrothermal and a modern recharge water. Adjacent to, and overlapping with the hydrothermal calcites, plotted a series of calcite-opal samples from the surface. The authors interpreted this isotopic composition as indicating precipitation from an upwelling modern hydrothermal water, rather than the previous interpretation of a descending meteoric fluid given by Szabo and Kyser (1990).

Summary of the Stable Isotope Trends of Carbon and Oxygen in Calcites

The isotopic evidence suggests a hydrothermal origin for the calcite, followed by alteration with modern meteoric recharge. At the same site, Bottomley (1987) found that some of the sealed-vein calcite had co-precipitated with laumontite. This suggested a formation temperature of just below 300°C. Similar mineral associations have been observed in fracture-infilling calcite from other locations (Larson and Tullborg, 1984). Laumontite and prehnite, both high temperature minerals, co-precipitated with the Swedish fracture-filling calcite measured by Larson and Tullborg (1984). They concluded that this indicated the presence of a residual hydrothermal calcite in the fractures. Observed co-precipitation of high temperature minerals has been used to

constrain a hydrothermal origin of calcite in samples from CRL and elsewhere.

Bottomley (1988) and Bottomley and Veizer (1992) compared the Rare Earth Element (REE) pattern measured in the fracture-infilling calcite with the host gneisses at CRL and concluded that the host rock was the source of the REE's in the calcites. This genetic link between the calcite and the host gneiss suggests that they formed under similar conditions and further suggests an initial hydrothermal origin for the calcites. Some of the calcites identified as hydrothermal by Bottomley (1987) are associated with vein silicates. However, these calcites have $\delta^{18}O$ values which may indicate deposition or alteration by a "low temperature" end-member. This suggests that the calcites, although initially deposited under hydrothermal conditions may have been altered by interaction with a low temperature, ^{18}O-depleted recharge water.

Micro-scale isotopic variations observed across fracture-infilling calcite would indicate that multiple precipitation-recrystallization events had occurred during calcite deposition. Only one sample taken in this thesis was thick enough (~1 cm) to allow for multiple 20-30 mg samples to be taken for isotopic analysis, and there was no observed isotopic shift along the growth axis of the calcite. The sample was taken at a depth of 193m from borehole RH1, and had a range in $\delta^{18}O$ values of only 0.2‰ (14.7 to 14.9‰), and a range in $\delta^{13}C$ values of 0.1‰ (-5.7 to -5.8‰) along the cross section. Both isotopic values were within the precision of the measurement technique used. Bottomley and Veizer (1992) found a perpendicular variation in two petrographically distinct growth generations on a sample taken from a depth of 574.3 m in borehole CR9 at CRL. The calcite nearest the wall rock was older and had a $\delta^{18}O$ of 14.8 ‰, and $\delta^{13}C$

of -5.6 ‰. The younger generation of calcite had $\delta^{18}O$ of 21.5 ‰ and $\delta^{13}C$ of -7.9‰. In addition to being "older" and "younger" on the basis of stratigraphy, radiocarbon analysis indicated that the older calcite had a lower ^{14}C activity than the younger calcite, 0.799 (+/- 0.036) and 1.582 (+/-0.056) pmc, respectively (Bottomley and Veizer, 1992).

Bottomley and Veizer (1992) also observed an isotopic variation along one of the fracture surfaces. A sample from CR12, which is a borehole located approximately 600 m west of CR9, at 77 m depth had a 6‰ variation in $\delta^{18}O$ (16.6 to 22.6‰) and a 3.2‰ $\delta^{13}C$ variation (-7.7 to -10.9‰) over a span on 25 cm along the fracture. This indicated a preferential flowpath/re-activation zone in the fracture, or variations in conditions for crystallization. A similar, although less pronounced isotopic variation was observed in a calcite examined in this investigation. A sample from a depth of 181 m in borehole RH3 was sampled at several points along the fracture to test for isotopic homogeneity. Ranges in $\delta^{18}O$ values of 0.9‰ (15.0 to 15.9‰), and in $\delta^{13}C$ values of 0.4‰ (-5.7 to -6.3‰) were observed in the sample. The isotopic variation observed along the fracture surface in this investigation and in Bottomley and Veizer (1992) is attributed to preferential groundwater flowpaths and regions of calcite precipitation or recrystallization in the fracture system.

Micro-scale isotopic heterogeneity and evidence for multiple calcite precipitation events have also been observed in calcites from elsewhere on the Canadian Shield (Jones et al., 1987), in Sweden (Larson and Tullborg, 1984) and in Germany (Komor, 1995). Jones et al. (1987) found that individual fracture-infilling calcite samples had isotopic and mineralogical textures which showed evidence of multiple precipitation events. They

analysed two such samples and found a 1‰ variation in the oxygen and a 3‰ shift in the carbon isotopic compositions in the first sample, and a 2‰ $\delta^{18}O$ and 1.6‰ $\delta^{13}C$ shift in values from the second sample. These intra-sample trends were consistent with the linear inter-sample trend observed for the rest of the data set. The study on fracture-infilling calcite in Sweden noted that small-scale isotopic variation in the calcite was consistent with the calcite petrography (Larson and Tullborg, 1984). Komor (1995) used cathodoluminescence to identify multiple growth events in the calcites from Germany. It was found that the distinct growth regions in samples which contained both metamorphic and crack-filling calcite had similar $\delta^{13}C$, but had $\delta^{18}O$ variations up to 1.5‰. In all studies, including the present one, intra-sample isotopic variation has been observed and is taken to be indicative of multiple precipitation events at either different temperatures, or from crystallization of calcite from a fluid composed of different amounts of two or more isotopically and thermally distinct end-members in a mixing model.

5.2 - FLUID INCLUSION MICRO-THERMOMETRY

The homogenization temperature and the melting temperature of fluid inclusions from the calcites were used to determine the minimum formation temperature and salinity of the fluid responsible for formation of the calcite. The T_h and the T_m of fluid inclusions from the prepared thin sections were used to characterize the geochemical conditions under which the fracture-infilling calcite precipitated. The range of measured T_h and calculated salinity is interpreted with respect to the cooling history of the region in an attempt to constrain the timing of the calcite precipitation in the fracture systems at CRL. Figures 5-8 and 5-9 are photo-microscopic images of fluid inclusions examined in this

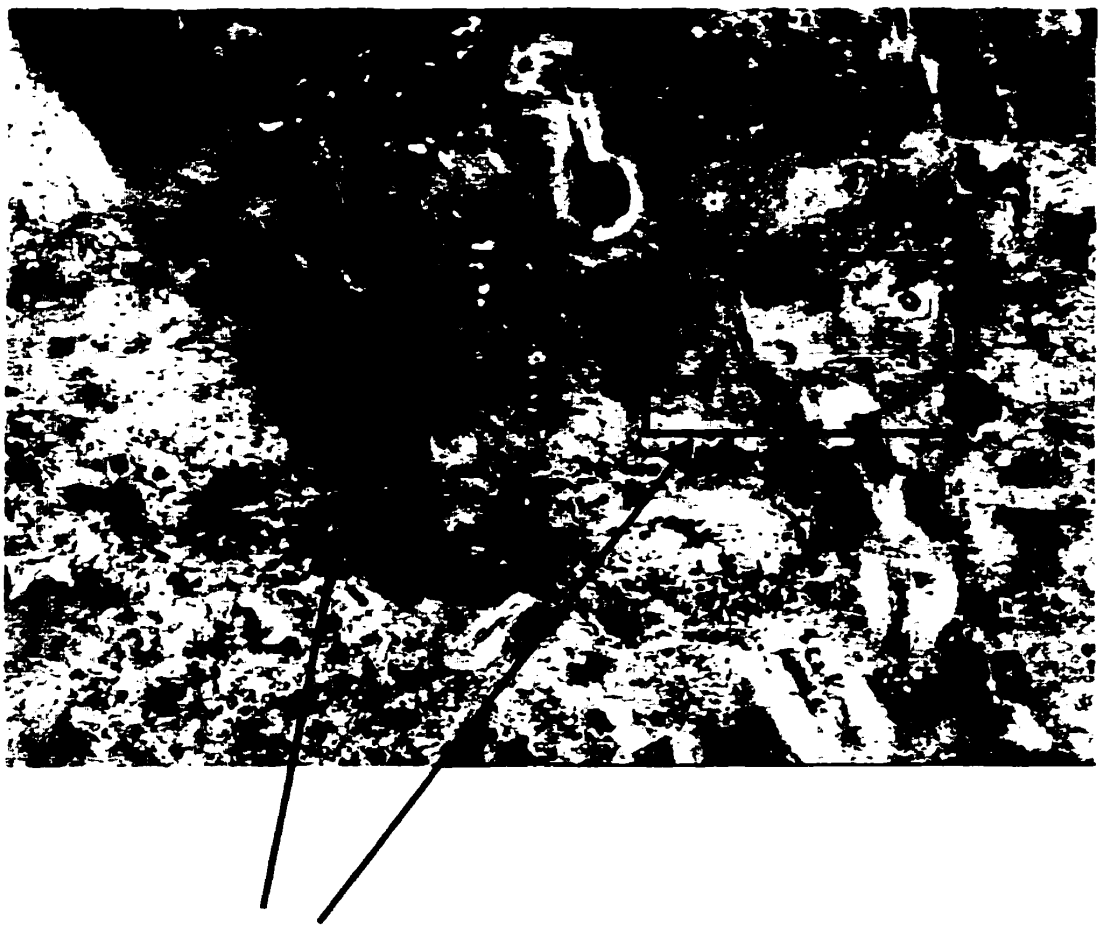

FIGURE 5-8 - Computer captured image (200X magnification) of a thin section of calcite RH3-65.3. The growth band is indicated on the figure. The area in the box is shown in Figure 5-9 under higher magnification.

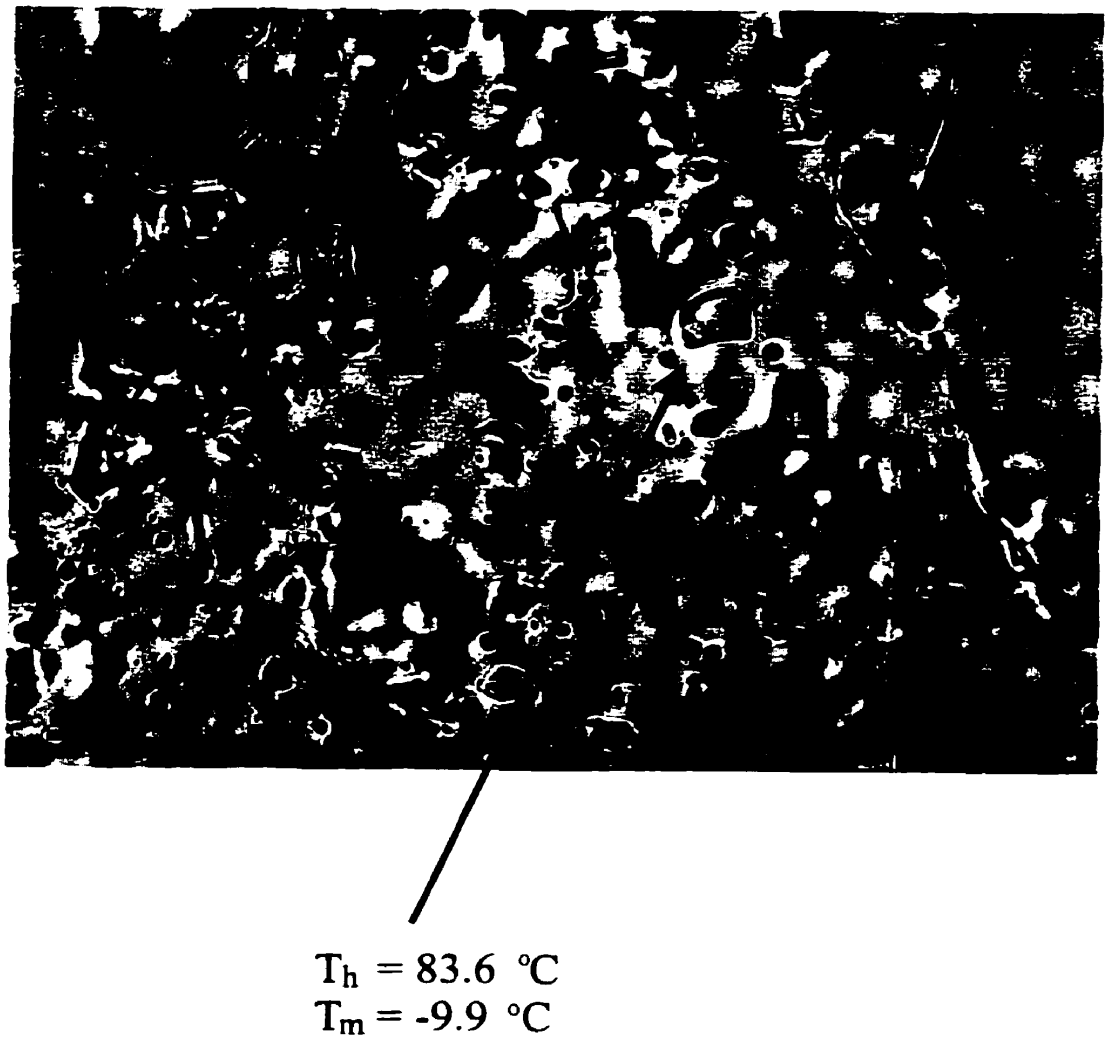

FIGURE 5-9 - High magnification (600X) computer captured image of a primary fluid inclusion in a thin section from RH3-65.3. The T_h and T_m of the fluid inclusion in °C, are listed.

investigation. Figure 5-8 is under moderate magnification (200X) and depicts a fluid inclusion sample from RH3-65.3 relative to the growth band. Figure 5-9 is an image of sample RH3-65.3 under high magnification (600X) wherein the fluid inclusion is more visible. The T_h and T_m values measured for the fluid inclusion are listed on Figure 5-9.

Range of Measured T_h and Calculated Salinities

The homogenization temperatures measured in the fracture-infilling calcites sampled indicate that the majority of the fluid inclusions formed at temperatures below 100°C, with most forming between 70-90°C. There were a couple of fluid inclusions which had T_h less than 50°C, suggesting a formation from fluid at temperatures possibly similar to modern-day. Vapour bubbles may not nucleate in fluid inclusions formed at less than 50°C due to internal pressure, thus for any low temperature fluid inclusion, it may only be said that the T_h was less than 50°C (Goldstein and Reynolds, 1994). A small number of fluid inclusions had T_h greater than 100°C, and three samples had T_h greater than 200°C. A histogram displaying the range of measured T_h is presented in Figure 5-10 -a). The range of T_h measured in the calcite suggests initial fracture-infilling calcite formation from one of two environments; 1) precipitation from hydrothermal-metamorphic formation waters during regional cooling, with the majority of fluid inclusions forming when the temperature was 70-90°C; or 2) calcite precipitation at a depth which corresponds to 70-90°C under the normal geothermal gradient (~25°C/km), followed by uplift to the final sample depth by surface erosion.

The salinity of the fluid inclusions was calculated using the T_m and equation 1-7 (Figure 5-10 b). The data indicate that the majority of fluid inclusions formed from a low

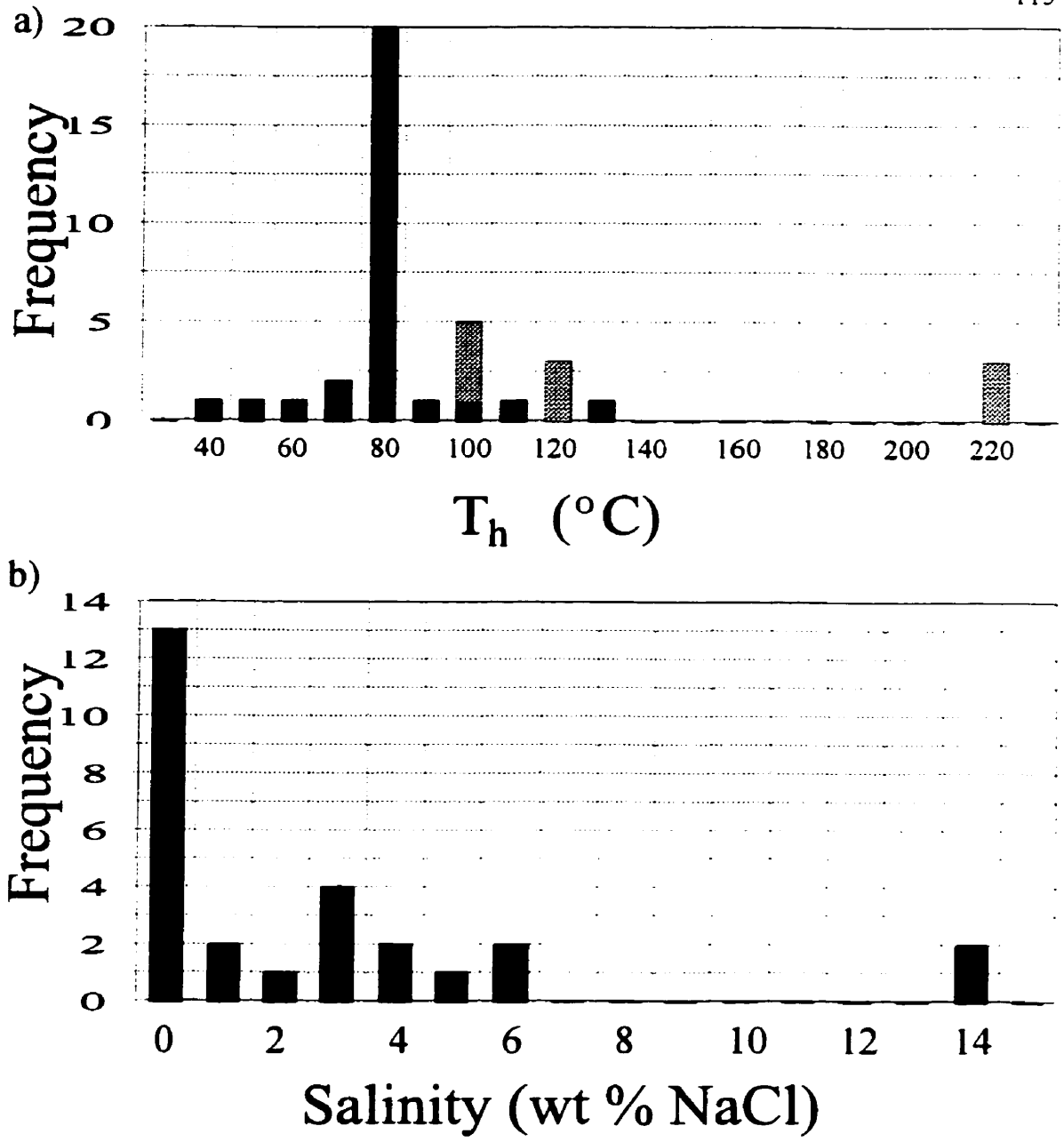

FIGURE 5-10 - a) Histogram of T_h measured in the fluid inclusions sampled in this investigation. The lighter areas represent fluid inclusions which were not heated all the way to T_h (see text). The majority of fluid inclusions had T_h between 70-90°C, most had T_h<140°C, and only a few had T_h>200°C.
b) Histogram of the salinity (as wt. % NaCl) for the fluid inclusions as determined by melting point depression (T_m). Most of the fluid inclusions had salinity levels of <6 wt. % NaCl, with 13 having less than 1 wt. % NaCl and 12 between 1 and 6 wt. % NaCl. Only two fluid inclusions had calculated salinity of >10 wt. % NaCl.

salinity (0-1 wt. % NaCl) water. This is consistent with calcite precipitation from meteoric water during plutonic cooling, or recrystallization of hydrothermal calcite by a low salinity water. Several other fluid inclusions formed from water with a salinity between 1 and 6 wt. % NaCl, consistent with both the Champlain Sea (0-4 wt. % NaCl) (Seguin, 1994 and references therein), and fresh water mixing with a high salinity Magmatic/Metamorphic water or "Canadian Shield Brine." In addition, there were a couple of fluid inclusions that formed from higher salinity (>10 wt. % NaCl) water. Kerrich (1987a and b) reported a range of 7 to 30 wt. % NaCl for metamorphic waters from the Canadian Shield. The higher salinity fluid inclusions measured fall within that range, and suggest that these fluid inclusions and their host calcites may have formed from a residual metamorphic fluid, or during regional metamorphism and are at least several hundred million years old.

The range of salinities measured in the fluid inclusions, low (0-1 wt. % NaCl), intermediate (1-6 wt. % NaCl) and high (>10 wt. % NaCl), are consistent with initial calcite precipitation during cooling from a high salinity (7-30 wt. % NaCl) metamorphic fluid at high temperature, and recrystallization with lower salinity, lower temperature, groundwaters (possibly Champlain seawaters or Meteoric recharge waters).

Geologic Significance of Measured T_h

The T_h range measured in the fluid inclusions suggests that the calcites may have formed as a result of several different hydrogeologic processes. 1) The calcites may have formed from cooler, regional metamorphic waters; 2) from a mixed meteoric-metamorphic fluid formed as a result of an ingress of meteoric waters along deep-seated

fractures during cooling; or, 3) from a much younger, mixed water source having temperatures dictated by the geothermal gradient. The calcite may have also precipitated from upwelling deep seated hot fluids such as the hydrothermal fluids proposed by Bottomley (1988). Each of these possible scenarios will be considered with respect to the regional geology of the Chalk River area.

There are two important considerations in the interpretation of the fluid inclusion data. First, the fluid inclusions themselves represent micro-samples within individual calcites and primary fluid inclusions reflect the geochemical conditions that existed for the specific growth band in the calcite. Second, fluid inclusions provide specific information about the physico-chemical condition of the hydrogeologic system at the time of calcite formation. They cannot unequivocally eliminate all possible mechanisms for the generation of those geochemical conditions.

Fluid Inclusion Formation During Regional Metamorphism and Cooling

If it is assumed that the rocks hosting the fracture systems have only been affected by cooling, and that this cooling has the same characteristics as that of the Grenville Orogen, then the range of T_h values suggests that the majority of the calcites having fluid inclusion temperatures of 70-90°C formed between 600-800 Ma. This can be shown from the established cooling history of the Central Gneiss Belt (CGB) for the Grenville Orogeny presented as Figure 5-11. Given that the cooling curve does not indicate any post-peak Ottawan metamorphic thermal events in the CGB, the temperatures of homogenization from the fluid inclusions suggest the calcites could have formed from regional metamorphic waters present during post-metamorphic cooling at approximately

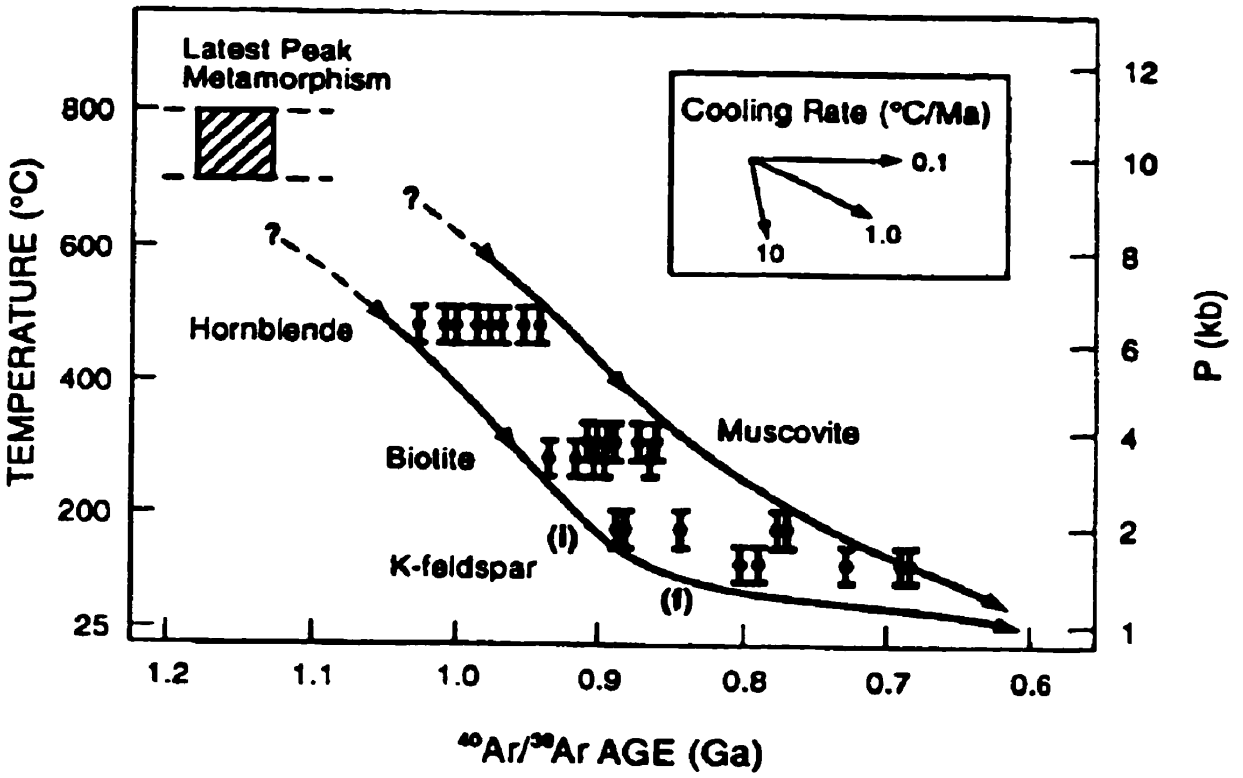

FIGURE 5-11) The cooling curve of the Grenville orogeny taken from Reynolds (1992). The T_h range measured in this thesis (70-90°C) suggests that the majority of the fluid inclusions formed between 600-800 Ma. The group of fluid inclusions with T_h>200°C formed over 900 Ma, while the fluid inclusions with T_h<50°C formed recently (0-100 Ma), assuming that the fracture system has only undergone cooling since formation.

600-800 Ma (Figure 5-11).

Calcites Formed at Normal Geothermal Gradient Temperatures and Later Emplaced by Erosion

It is possible that the calcites formed after peak-metamorphic times at depths in the rock where a normal geothermal gradient would be consistent with the homogenization temperatures, and have been brought to shallower depths by erosion at the surface. Assuming a geothermal gradient of 25°C/km, temperatures of 70-90°C would occur at depths of 2.8 to 3.6 km.

The geologic history of the Grenville Province presented by Easten (1992) indicates that tens of km of rock were uplifted and eroded over a 400 million-year time period, which was largely completed by 800 Ma and that the region has been a peneplain for the last 500 Ma. Erosional uplift of the fracture system by 2.6-3.6 km over the last 500 Ma is possible and this scenario cannot be eliminated outright. Such a mechanism may be used to explain the presence of the bulk of the fluid inclusions with a T_h between 70-90°C in the calcites. However, it cannot explain the coexistence of fluid inclusions with significantly higher T_h in the same depth interval. If the 70-90°C fluid inclusions are the result of erosional uplift, then the higher temperature fluid inclusions at the same depth must be hydrothermal in origin. Whether the bulk of the calcites with fluid inclusions (T_h= 70-90°C) were formed under the geothermal gradient or represent formation during post-metamorphic cooling, the existence of fluid inclusions with higher T_h in the same samples as fluid inclusions with T_h <50°C, indicates that multiple precipitation events under different thermal regimes are recorded in the calcites.

The possibility that the calcites with 70-90°C fluid inclusions were formed at temperatures dictated by an average continental geothermal gradient and were subsequently uplifted by erosion cannot be definitively excluded. Therefore, the age determined using the cooling history of the Grenville Province (600-800 Ma) must be taken as the maximum possible age for the crystallization of these calcites. Assuming that the rate of erosional uplift is not greater than the rate of uplift for the orogeny (0.07-0.14 km/Ma; Cosca, 1989), the minimum age can be estimated as 18 Ma. Therefore, whether the origin of the calcites containing fluid inclusions with T_h values of 70-90°C is due to the geothermal gradient or regional metamorphism, an age of formation between 18-600 Ma can be estimated using the cooling history and the uplift rate of the metamorphic terrain.

Recent Calcite Formation From Upwelling Water

A final possible mechanism for the formation of calcite having fluid inclusions with T_h between 70-90°C is an upwelling deep seated hydrothermal fluid. The formation of 70-90°C fluid inclusions would require water from a depth of 2.6-3.6 km rapidly moving to depths of 30-160 m adiabatically and precipitating calcite. This mechanism would explain the range of T_h observed in the fluid inclusions but it is not a geologically reasonable scenario in the region around CRL. There are presently no geothermal springs in the area, nor are there any travertine/tufa deposits to indicate geothermal spring activity in the geologic history of the area.

The salinity and homogenization temperature ranges measured in this investigation are consistent with temperature and salinity ranges in fluid inclusions from

fracture calcites sampled from other geologically similar terrains. Larson and Tullborg (1984) observed a wide range of T_h, from less than 50°C to 175°C, in two-phase (liquid and vapour) fluid inclusions in calcite with variable but low salinity. Szabo and Kyser (1990) noted that there were no fluid inclusions in the calcite samples they examined, and noted that this was consistent with low temperature calcite formation. The fluid inclusion information measured in this investigation appears to contradict the stable isotope evidence. Calcite samples with bulk stable isotope values consistent with a low temperature formation from meteoric recharge have fluid inclusions with T_h between 70-90°C. However, these two seemingly contradictory observations are consistent with multiple precipitation events and the bulk of the calcite forming at low temperatures. The low temperature precipitation of calcite on top of an altered hydrothermal calcite would preserve the hydrothermal fluid inclusions, form few low temperature fluid inclusions and give the calcite isotopic ratios which reflect a weighted average isotopic composition of the waters from which the calcites formed.

The most extensive investigation of fluid inclusions in fracture filling calcite was undertaken by Blyth et al. (1998). They examined the fracture-filling calcite from a site in Olkiluoto, Finland. Using a combination of fluid inclusions and stable isotopes they identified four possible calcite precipitating fluids in the fracture system. While there is considerable overlap in the ranges of $\delta^{13}C$, $\delta^{18}O$, T_h and salinity among the four groups, each group of calcites can be determined to precipitate from a hydrogeologically reasonable fluid by combinations of the four parameters.

Fluid inclusion data is most meaningful when used to complement additional

geochemical analysis and when considered within a reasonable geologic framework for the study site. Hall et al. (1995) suggest that the range of T_h observed (40-100°C) in fluid inclusions from calcites in the vicinity of Yucca Mountain may be formed from an upwelling deep seated hydrothermal fluid. While such a formation scenario is possible, it is not the most likely one given the stable isotope and U/Th data in the calcites. It is important to consider fluid inclusion data as representing a micro-sample of the formation temperature and salinity of the fluid responsible for formation of that section of the mineral. Primary fluid inclusions record the conditions of formation of that part of the mineral proximal to the fluid inclusion. It is important to consider the observations within the framework of additional complementary geochemical petrographic and geologic information.

5.3 - URANIUM SERIES ANALYSIS

Uranium series ages and U-Th geochemistry of the calcites indicate that they formed episodically under variable geochemical conditions.

Bulk Calcite Precipitation Ages

The $^{230}Th/^{234}U$ ages were calculated for twelve calcites, seven from open-veins, and five from sealed-veins. The ages are listed in Table 5-2, including the ^{232}Th corrected ages for three samples with low $^{230}Th/^{232}Th$ activity ratios. The ages were calculated according to the method given in Appendix II. Approximately 1 g of calcite was necessary to perform U-series analysis, thus only bulk calcite sample analysis was possible. If multiple growth generations were present, they would have been homogenized, and the age determined would represent a weighted average for the entire

TABLE 5-2) Summary of the $^{234}U/^{230}Th$ ages calculated for the samples from this investigation, including the ^{232}Th corrected ages for the samples with a $^{230}Th/^{232}Th$ activity ratio <15.

a) Open vein calcites

SAMPLE	$^{234}U/^{230}Th$ Age (Uncorrected)		^{232}Th Corrected	
	Age (ka)	Error (ka) (1-σ)	Age (ka)	Error (ka) (1-σ)
E1-26.5	334.9	- 98.9 + undefined	-	-
RH3-43	249.8	- 28.5 + 38.8	192.3	- 12.1 + 13.5
RH3-65.3	0	+ 2.2	-	-
RH3-65.3 (re-count)	0	+ 9	-	-
RH3-102.2	> 350	-	-	-
CR9-167.5	> 350	-	-	-
CR9-172.5	130.3	- 6.1 + 6.4	107.5	- 5.1 + 5.3
CR9-547.7	84.9	- 23.2 +28.3	-	-

b) Sealed vein calcite.

SAMPLE	$^{234}U/^{230}Th$ Age (Uncorrected)		^{232}Th Corrected	
	Age (ka)	Error (ka) (1-σ)	Age (ka)	Error (ka) (1-σ)
E1-150.5	165.1	-25.1 +31.1	121.8	-18.5 +21.5
E1-176.5	>350	-	-	-
RH1-193.2	>350	-	-	-
RH3-181	U too low	-	-	-
CR18-30	75.2	-42.1 +61.3	-	-

sample. The weighted average would be affected by both the U-series age of each precipitation event, and the absolute concentration of U and Th in each generation. It is important to consider the calculated ages as "bulk-deposition" ages, not absolute ages of a single precipitation event.

Milton (1985, 1987) and Milton and Brown (1987) suggested that, since α-recoil effects remove ^{234}U, the ages calculated should be considered to represent the residence time of U in the calcite. Such a distinction is important to make if the calcite is micro-sampled in an attempt to date an individual event, or if it is assumed that the calcite represents a single precipitation event. As α-recoil is a surface process and the sample was bulk sampled, any ^{234}U loss at the surface would only contribute to the uncertainty in interpretation caused by the homogenization of earlier growth generations. As a result, the interpretation of the calculated age has considerably more uncertainty than the analytical technique itself.

The ages calculated for the calcites range from <9 ka to >350 ka, the upper limit of U/Th dating. Only three calcites had measurable amounts of ^{232}Th requiring detrital Th corrections, and the magnitude of the correction was <30% of the uncorrected age. The range of ages calculated for fracture-infilling calcites in this investigation is consistent with those determined on calcites from similar fracture systems at CRL and documented in Milton (1985) and proposed in Bottomley (1987) and Bottomley and Veizer (1992). Milton (1985) performed U-series dating on four fracture-infilling calcites from CRL and found ages of 47.3 (+/- 35), 152 (+/- 119), 41.7 (+/- 13), and 124.7 (+/- 30) ka, with evidence of calcite recrystallization in each of the samples. Bottomley (1987) and

Bottomley and Veizer (1992) state that U-series age data indicate multiple precipitation/recrystallization events in the calcites. They determined the model $^{87}Sr/^{86}Sr$ age of the host gneisses to be 1.3 Ga and argue that, based on the $^{87}Sr/^{86}Sr$ ratios in the calcites, the "hydrothermal" calcites must be at least 400 Ma, most likely 700-800 Ma. These ages are consistent with the $^{230}Th/^{234}U$ age of >350 ka measured in four of the calcites in this investigation (Table 5-2). The U-series ages and the approximate time of formation of the calcites based on comparisons of their fluid inclusion homogenization temperatures (this study) and the cooling history of the region are consistent with both the U-series ages measured previously (Milton, 1985) and the $^{87}Sr/^{86}Sr$ model ages of the "Hydrothermal" calcite (Bottomley, 1987; and Bottomley and Veizer, 1992).

ICP-MS/α-Spectrometry Intercomparison

The concentration of U and Th in the fracture-infilling calcites was determined by both α-spectrometry and ICP-MS. Figures 5-12 a) and b) are plots of the U and Th concentrations measured by ICP-MS versus the concentrations determined by α-spectrometry. The measurements plot close to the 1:1 line for both U and Th, suggesting that the concentrations determined by each technique are in agreement.

However, the same sample (CR9-172.5) is an outlier on both the U and the Th plot (Figures 5-12 a) and b) respectively). α-spectrometry determined a higher U concentration and a lower Th concentration in the sample than was measured by ICP-MS. This may be an artefact of natural variation within the calcite, as separate samples were taken for ICP-MS and α-spectrometry rather than using a split of the same sample. It is possible that the sample taken for ICP-MS contained detrital contamination which caused

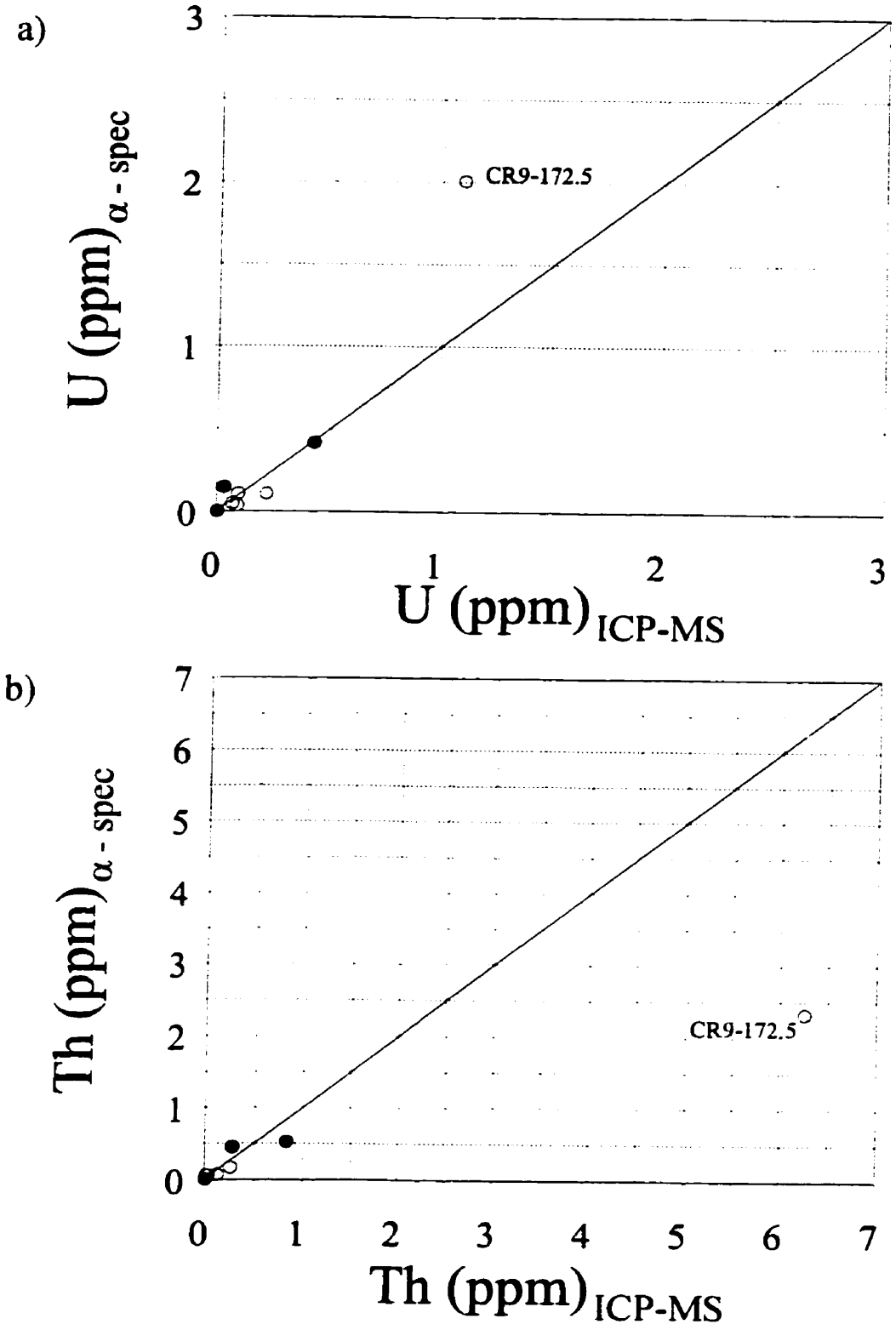

FIGURE 5-12) Concentration of U (**a**) and Th (**b**) measured in the calcites by ICP-MS versus the concentration measured by α-spectrometry. Empty circles represent open-vein calcites and filled circles represent sealed-vein calcites. The line is a 1:1 relationship.

one anomalous result. Unfortunately, CR9-172.5 had both the highest U and Th concentration of all the samples analysed. Thus, it is impossible to rule out the possibility that the techniques disagree at higher U and Th concentrations. Regardless, it seems that the U and Th concentrations measured by ICP-MS and α-spectrometry are in good agreement.

U/Th Trends with Sample Depth

Calcites precipitating from a water recharging into fractures in a homogeneous hydrologic system would be expected to have U-ages which display a temporal trend from youngest at the surface, to oldest at depth. Likewise, if the open-vein fractures are an indication of the hydraulic conductivities of the system to an ingress of younger groundwaters, the ages of the open-vein calcites would be expected to be younger than the ages of sealed-vein calcites. However, Figure 5-13 indicates that there is no systematic trend in the U-ages either as a function of sample depth or whether they presently appear as open-vein or sealed-vein systems.

Several factors, including a relatively small sample size, might explain the absence of a trend between calcite age and sample depth. The fractures sampled may not be hydrologically interconnected. Thus, "open-vein" calcites may only be open on the scale of centimetres to metres, and not located in presently hydrologically active fracture systems. Alternately, the "sealed-vein" calcites may be in hydrologically isolated fractures or may be fractures which have recently been sealed to groundwater flow. Further, unless there is clear evidence from the fluid inclusion data, there is no way to discern if a calcite is located in a fracture which is actively precipitating or dissolving

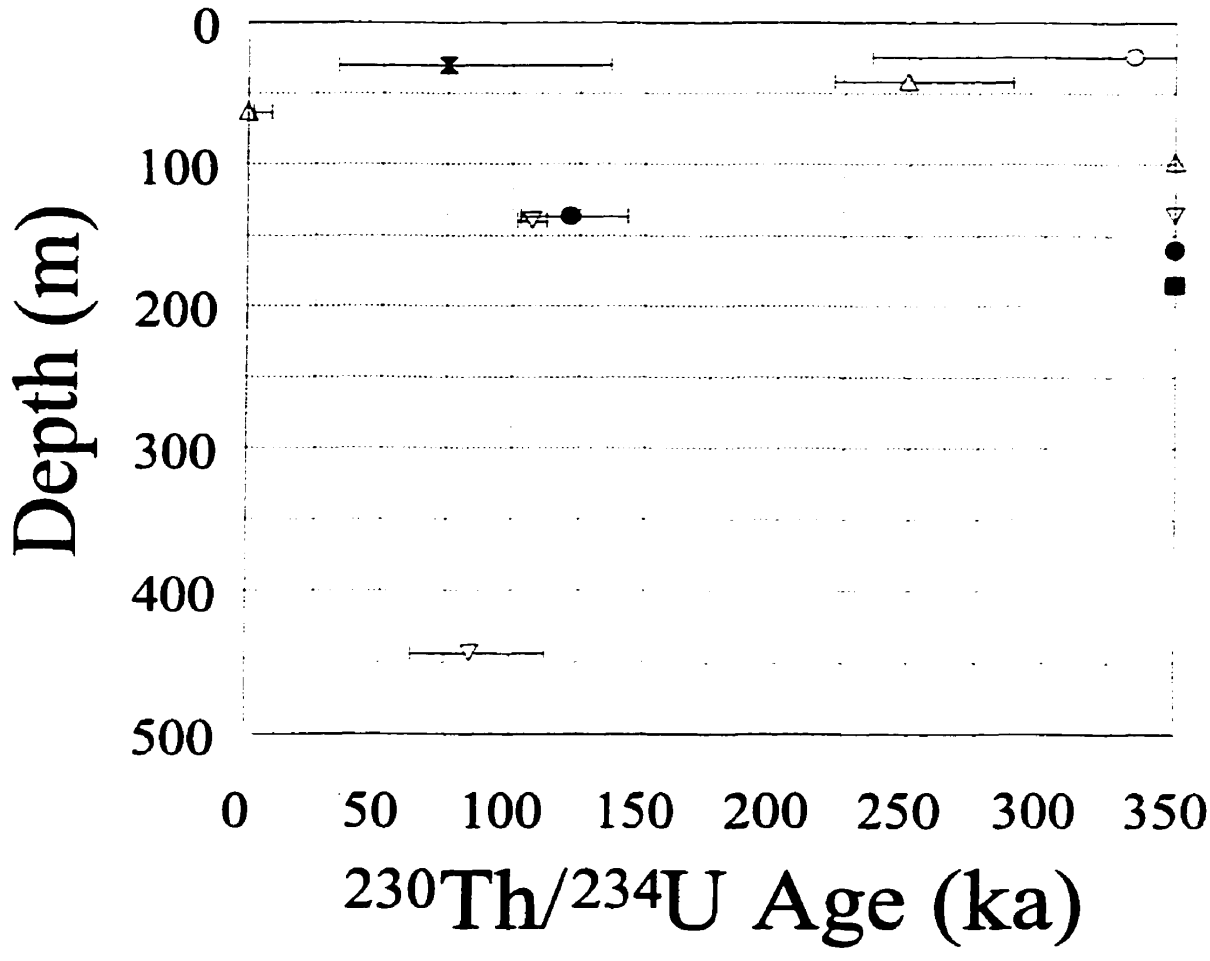

FIGURE 5-13) Plot of the $^{230}Th/^{234}U$ age as a function of sample depth. The samples from borehole E1 are circles, RH1 are squares, RH3 are upward pointing triangles, CR9 are downward pointing triangles and CR18 is an hourglass. The filled symbols represent sealed vein calcites and the empty symbols represent open vein calcites. The bars represent the analytical error associated with the calculated age. The samples which plot with an age of 350 ka and no error, actually have ages of >350 ka.

calcite, nor is the long term stability of present conditions clear. Thus an open-vein calcite in a vein actively precipitating calcite would generate a relatively young age, while an open-vein calcite in a fracture actively dissolving calcite would generate an age indicative of the timing of an earlier calcite deposition period. The U-age is also based on the analysis of a bulk calcite sample, thus if multiple precipitation events occurred in the calcite, they would be homogenized and the generation containing the highest initial U concentration would exert the most influence on the calculated age of the sample. For these reasons, it is important to interpret the U-ages as representing an average age of bulk calcite precipitation or at least be able to constrain which of these calcites have U/Th systematics resulting in a non-interpretable "mixed age."

In addition to a lack of a depth trend with respect to all the calcites, Figure 5-13 also shows that there is no depth trend among samples from the same borehole. This indicates that the fractures from the same borehole are not necessarily hydrologically connected, a phenomenon which is quite common for fracture-controlled hydrogeologic systems in fractured granitic terrains. The lack of a clear U-age depth trend in the fracture-infilling calcites suggests that there are preferential groundwater flowpaths, and that not all of the fractures participate in active groundwater flow. The U-ages also indicate that the calcites have precipitated episodically throughout the hydrogeologic history of the region.

In an examination of secondary calcite from drill cores around Yucca Mountain, Szabo and Kyser (1990) found that despite a ^{18}O-depleted trend in the calcites with depth which suggested calcite precipitation from meteoric recharge at temperatures consistent

with the current geothermal gradient, there was no such trend in the U-ages for the calcites. Szabo and Kyser concluded that this suggested that the U-ages were recording episodic periods of calcite precipitation from meteoric recharge. A similar process may be occurring at CRL.

Comparisons of the concentrations of U and calculated U-ages on the calcites in this thesis found no relationship. This may be the result of bulk sampling of the calcites which effectively homogenizes the U concentrations in the samples, or it may indicate that calcite precipitation has occurred from genetically distinct waters. Gascoyne et al. (1997) found that fracture-infilling calcites from the URL plotted into two groups, those with Pleistocene ages (<130 ka) and U concentration less than 5 ppm, and U rich (>10 ppm) calcites with ages >350 ka. Such a pattern clearly indicates calcite precipitation from two geochemically distinct groundwaters during the hydrogeologic history of the region. A similar pattern was not observed in the samples from CRL analysed in this investigation, but a lack of a pattern is not inconsistent with episodic precipitation and recrystallization.

The U and Th concentrations measured in the calcites have been compared with their sampling depth (Figures 5-14, 5-15). As can be seen, there is no systematic relationship between U and Th concentration and sample depth. There are also no systematic differences between open-vein and sealed-vein calcite with regard to U and Th concentration. The ranges of U (0-2.5 ppm) and Th (0-6.5 ppm) concentrations measured in the calcite samples fall between the concentrations found in a metamorphic gneiss and the concentrations in surficial and ocean waters (Table 1-1). This suggests that the origin

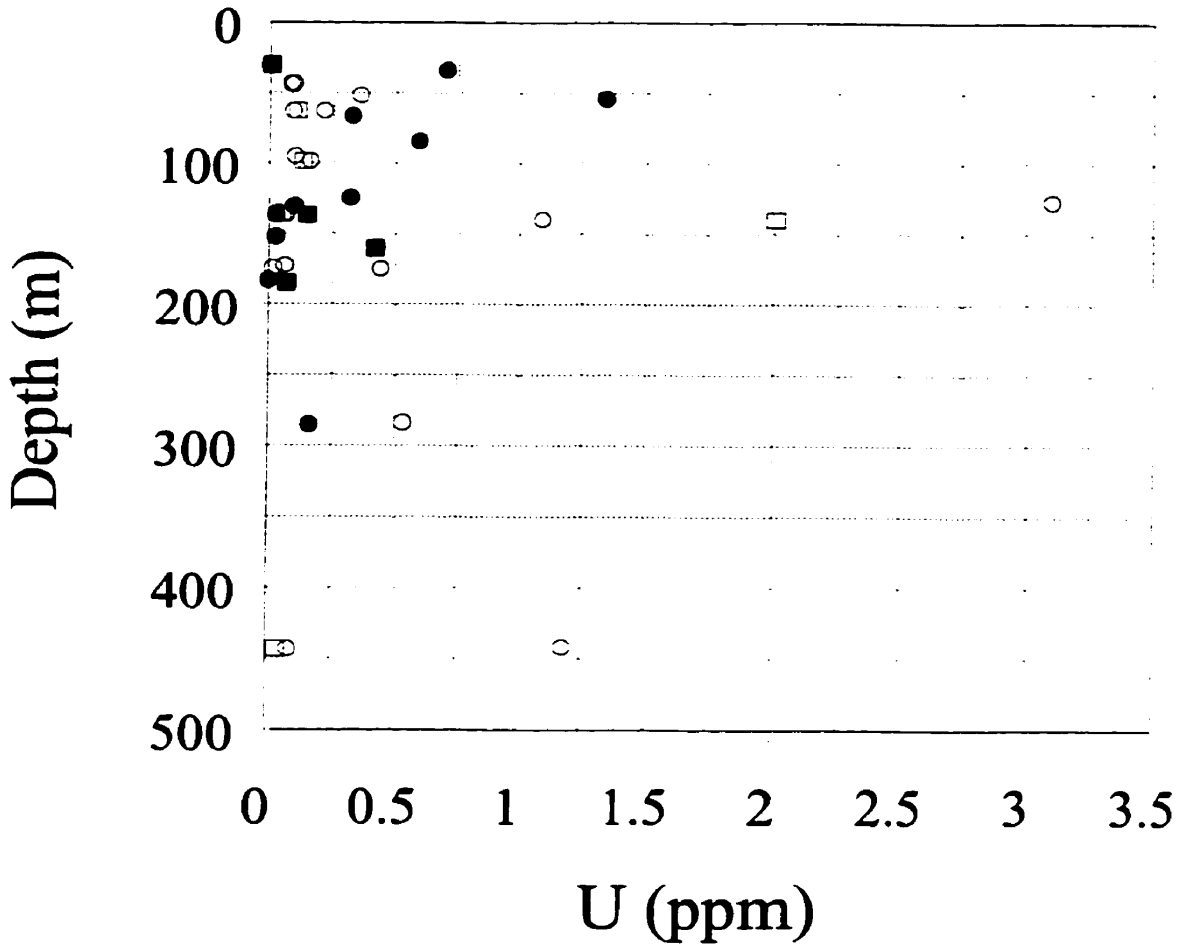

FIGURE 5-14) The U concentration (ppm) of the fracture-infilling calcite sampled in this investigation plotted against the depth of the sample. The circles represent samples measured by ICP-MS and the squares are samples measured by α-spectrometry. For both the samples measured by ICP-MS and α-spectrometry, the filled symbols represent sealed vein calcites and the empty symbols represent open vein calcites.

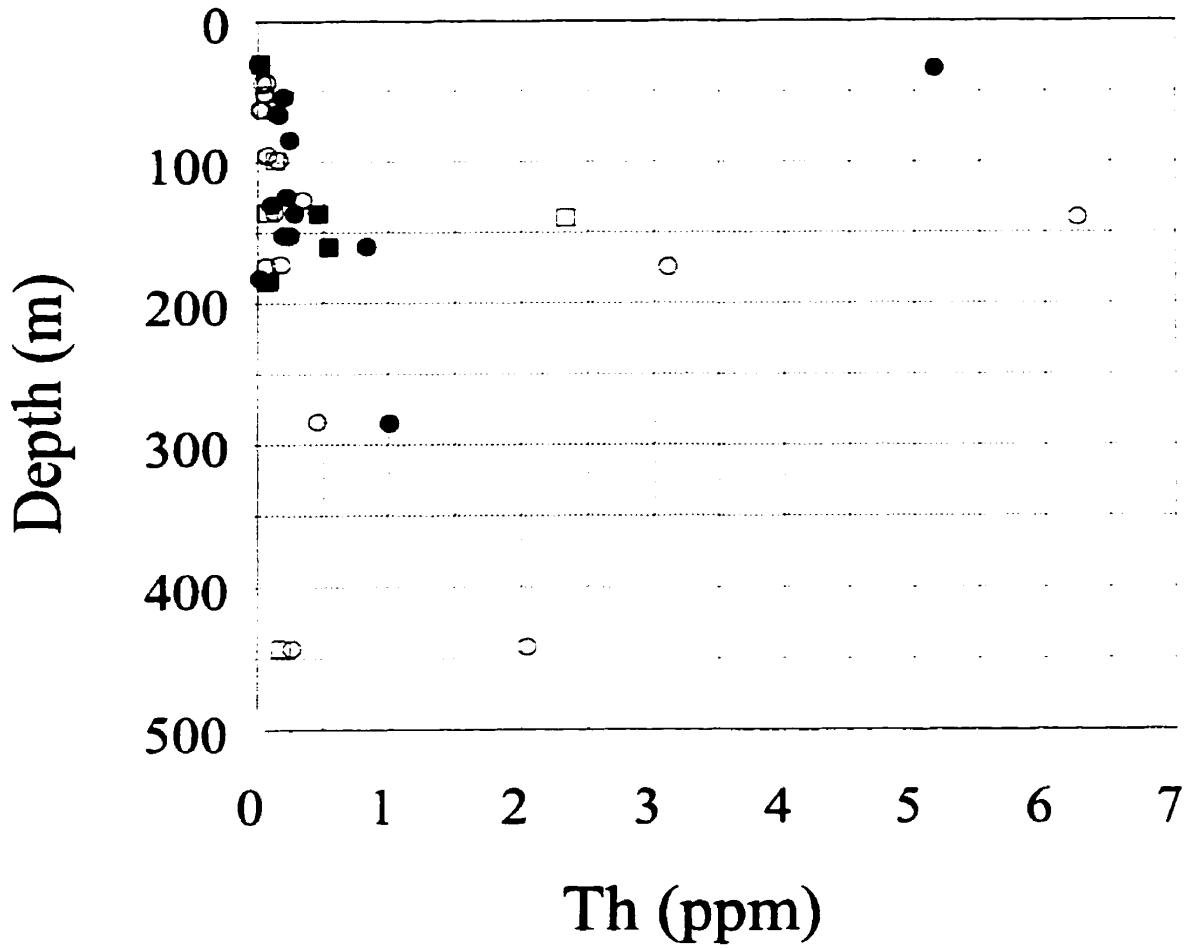

FIGURE 5-15) The Th concentration (ppm) of the fracture-infilling calcites sampled in this investigation plotted against the depth of the sample. The circles represent samples measured by ICP-MS and the squares are samples measured by α-spectrometry. For both the samples measured by ICP-MS and α-spectrometry, the filled symbols represent sealed vein calcites and the empty symbols represent open vein calcites.

of the U and Th is largely being overprinted by the rocks themselves. Figures 5-14 and 5-15 also display a wider range of concentrations in the near surface than at depths greater than 150 m. Although this may be a sampling artefact, it may also indicate that U and Th are being differentially released by weathering of the overburden according to redox conditions and subsequently incorporated by calcite during precipitation from meteoric recharge.

U/Th Geochemistry

The solubilities of U and Th are redox sensitive. U is more soluble under oxidizing conditions and Th is more soluble in reducing environments. The U and Th concentrations measured in the calcites were plotted against one another on Figure 5-16 to determine if the calcite precipitated from an oxidizing or a reducing environment. Calcite precipitated from an oxidizing environment would be expected to have a higher U than Th concentration due to the different solubility of the actinides. The opposite would be true for calcite precipitated from a reducing fluid. The data suggest that the fracture-infilling calcite at CRL has precipitated from both oxidizing and reducing environments. However, there is no clear relationship between open-vein and sealed-vein calcite precipitation and estimated redox conditions of the precipitating fluid. The U and Th concentrations in the calcite support a model of episodic calcite precipitation under variable geochemical conditions.

5.4 - INTEGRATION OF STABLE ISOTOPE, FLUID INCLUSION AND U-SERIES ANALYSIS

One of the strengths of performing stable isotope, fluid inclusion and U/Th

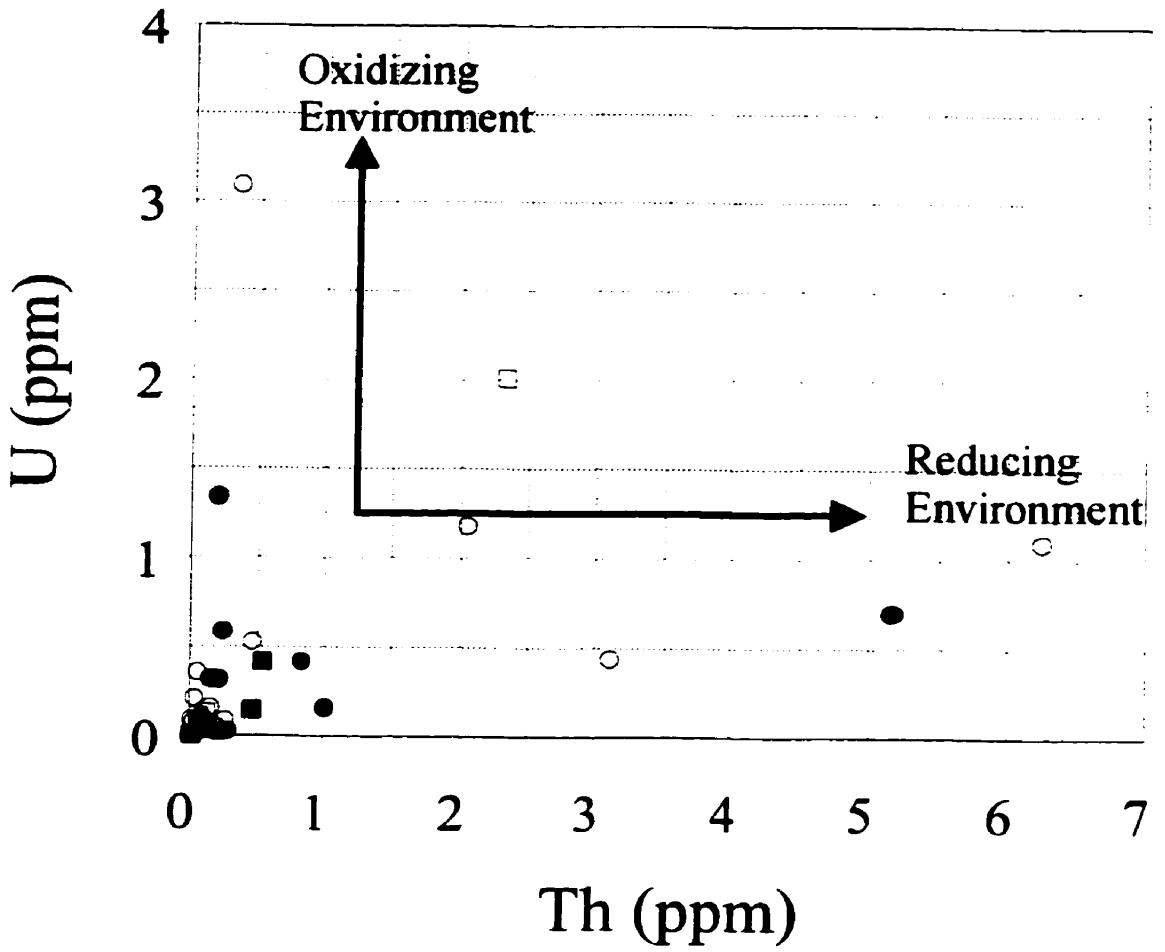

FIGURE 5-16) The concentration of Th (ppm) plotted against the U concentration (ppm) measured in each of the calcites sampled in this investigation. The squares represent samples measured by α-spectrometry and the circles represent samples measured by ICP-MS. Empty symbols represent open vein calcites and filled symbols represent sealed vein calcites.

analysis on the same sample is that it allows conclusions to be based upon an integration of all the analyses. This permits the physico-chemical properties and timing of the fluid precipitating calcites to be constrained to a greater degree than with any individual analysis.

Groundwater Salinity

The temperature of final melting (T_m) of the fluid inclusions was used to determine the salinity of the calcite precipitating fluid. The salinity was plotted against the minimum formation temperature of the fluid inclusion (T_h) in Figure 5-17. The U-series ages for the samples were added to determine if the fluid inclusions recorded a temporal change in salinity during formation. The analysis shows that calcites with fluid inclusions having homogenization temperatures of between 70-90°C formed from fluids having salinities ranging from freshwater (0 wt. % NaCl) to brackish fluids (<10 wt. % NaCl). Even within the same sample there is evidence of calcite recrystallization or formation from waters having a range of salinities. These observations are consistent with calcite precipitation from geochemically and thermally distinct fluids. Calcite precipitation from high salinity metamorphic waters (7-30 wt. % NaCl, Kerrich, 1987a and b) diluted by low salinity meteoric recharge to form calcites containing fluid inclusions with salinities proportionate to the contribution of each end-member would explain these observations.

The U-series ages listed on Figure 5-17 appear to be discordant with the ages of fluid inclusion formation based on their T_h and the cooling curve of the pluton (Figure 5-11). In all cases, with the possible exception of calcites with U-series ages >350 ka, the

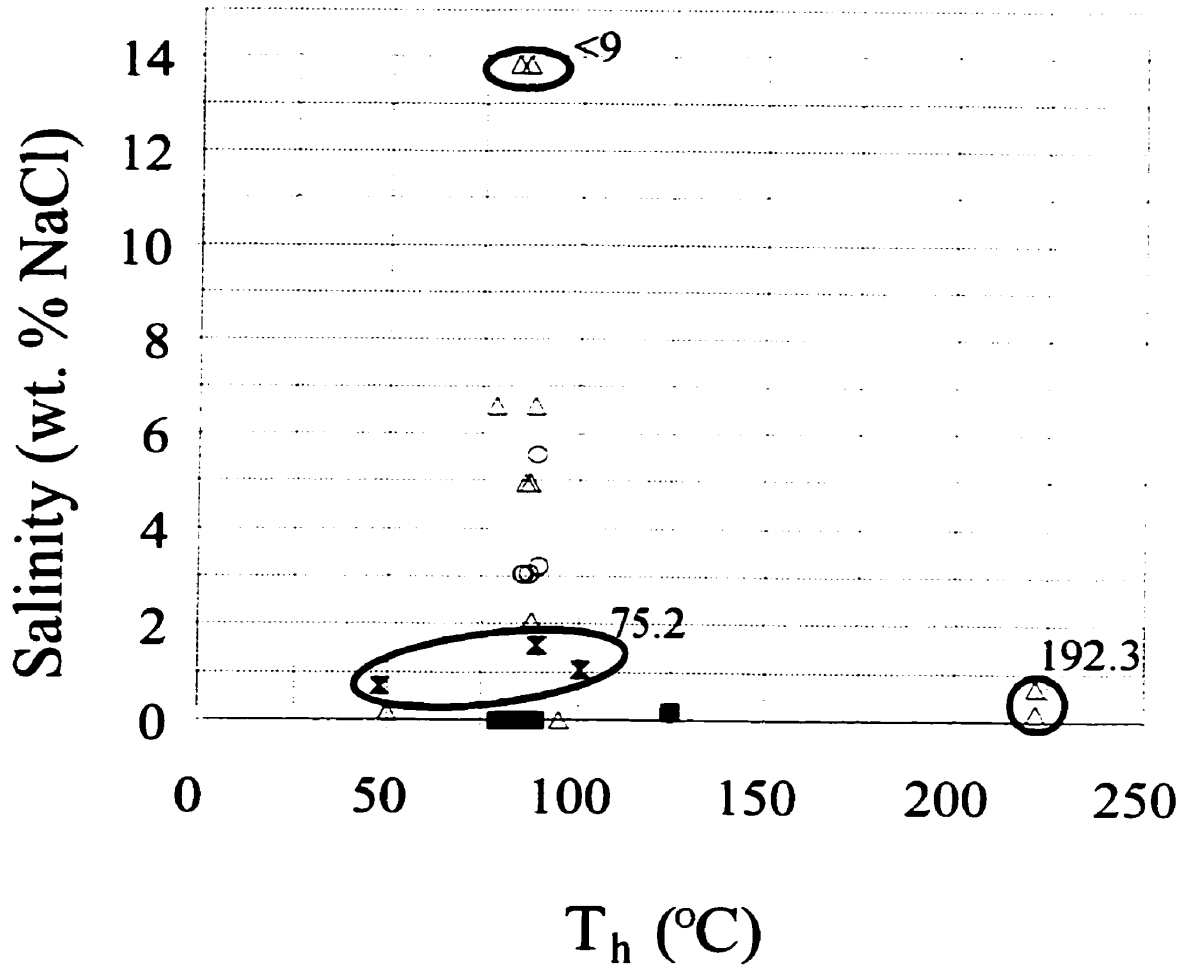

FIGURE 5-17) Plot of all the fluid inclusion data for which a T_m and a T_h were determined. The salinity as calculated using the T_m is plotted against the T_h measured in the same inclusion. Fluid inclusions from E1 are circles, RH1 are squares, RH3 are upward pointing triangles, and CR18 is an hourglass. Sealed vein calcites are represented as filled symbols and open vein calcite are empty symbols. Calcites which have been U-series dated are circled and the calculated age (in ka) is listed above the data set.

U-series ages are much younger than the estimated ages based on fluid inclusion thermometry would suggest. This is due to the effect of bulk sampling for U, compared with micro-sampling individual fluid inclusions. Fluid inclusions are more likely to occur in high temperature calcite and thus any calcite precipitated hydrothermally may contain more fluid inclusions than the calcite formed at low temperatures of <50°C. The fluid inclusions were located and identified petrographically by scanning the thin section for growth bands from the host rock surface of the fracture towards the centre of the fracture. This may have skewed the results by characterizing more hydrothermal than low temperature fluid inclusions. The calcite crystals grew from the wall towards the centre of the fracture initially, and calcite recrystallization has made growth bands from the late stages of calcite formation difficult to identify. Two-phase (liquid/vapour) fluid inclusions with constant liquid to vapour ratios were more frequently observed and were easier to characterize petrographically in calcite which has been partially recrystallized and thus may be over-represented in the data.

The fluid inclusion data indicates that the calcites formed from multiple thermally and chemically distinct fluid events. The absence of large numbers of fluid inclusions with T_h representative of the present thermal regime in the fracture system suggests that no calcite was observed to have precipitated under Pleistocene conditions, that is, the present regional climate and the regional geology for the last million years. The presence of high temperature fluid inclusions in samples with U-series ages of <350 ka is consistent with their being remnants of an unaltered "hydrothermal" precipitation event. As such, they are further evidence of multiple calcite precipitation events in the fracture

system. The range of salinity recorded in the calcites indicates that during cooling the rocks were affected by fluids of variable salinity which ranged from highly saline, older metamorphic fluids to younger low salinity waters.

Calcite precipitation from water with different salinity is evident when the $\delta^{18}O_{calcite}$ is plotted against fluid inclusion salinity (Figure 5-18). High salinity fluid inclusions (>10 wt. % NaCl) plot within the range of values expected for the magmatic/metamorphic calcite end-member, and several of the low salinity fluid inclusions plot within the range of values expected for the Champlain Seawater end-member. It is important to note that the Champlain Sea was formed because of a westward progression of the Atlantic Ocean which was diluted by glacial meltwater and local meteoric precipitation shortly after the end of Wisconsin glaciation. As a result, it has a $\delta^{18}O$ and salinity range which represents a mixing of these end-members. The same range of $\delta^{18}O$ values as that of the Champlain Sea would be created by mixing magmatic/metamorphic (5 to 25‰), meteoric recharge (~10‰) and glacial meltwaters (-28 to -18‰). Therefore, the samples which plot within the Champlain Seawater end-member may in fact represent fluid inclusions which formed in calcite precipitating from hydrothermal fluids mixing with an ^{18}O-depleted meteoric recharge during cooling. Unfortunately only one sample which plotted in the Champlain Sea end-member underwent U-series dating. It had an age of <9 ka which does not preclude bulk precipitation from either the Meteoric Recharge or the Champlain Seawater end-member.

Although most of the calcites plot within or nearest the Champlain Seawater end-member (Figure 5-18), it is impossible to eliminate calcite precipitation from a mixture of

FIGURE 5-18) $\delta^{18}O_{calcite}$ plotted against the salinity of the calcite precipitating fluid determined by the T_m of fluid inclusions. The figure also includes the position of calcite precipitated in equilibrium with the potential calcite precipitating fluids identified in Section 5.1 and summarized in Table 5-1. A legend of the symbols used is given below. The empty symbols represent open vein calcites and the filled symbols represent sealed vein calcites. The same symbol is used for each fluid inclusion from the same sample. **a)** Plot showing the range of values observed relative to the size and location of the potential end-members fluids. **b)** Same data plotted on a narrower range of $\delta^{18}O$ and salinity. Allows for observation of dispersion within the data relative to the location of the end members. The U-ages (in ka) of those calcites dated are presented adjacent to the data.

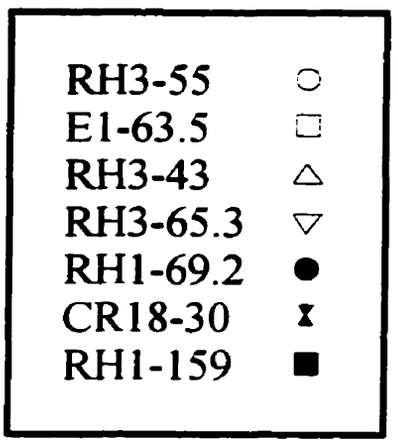

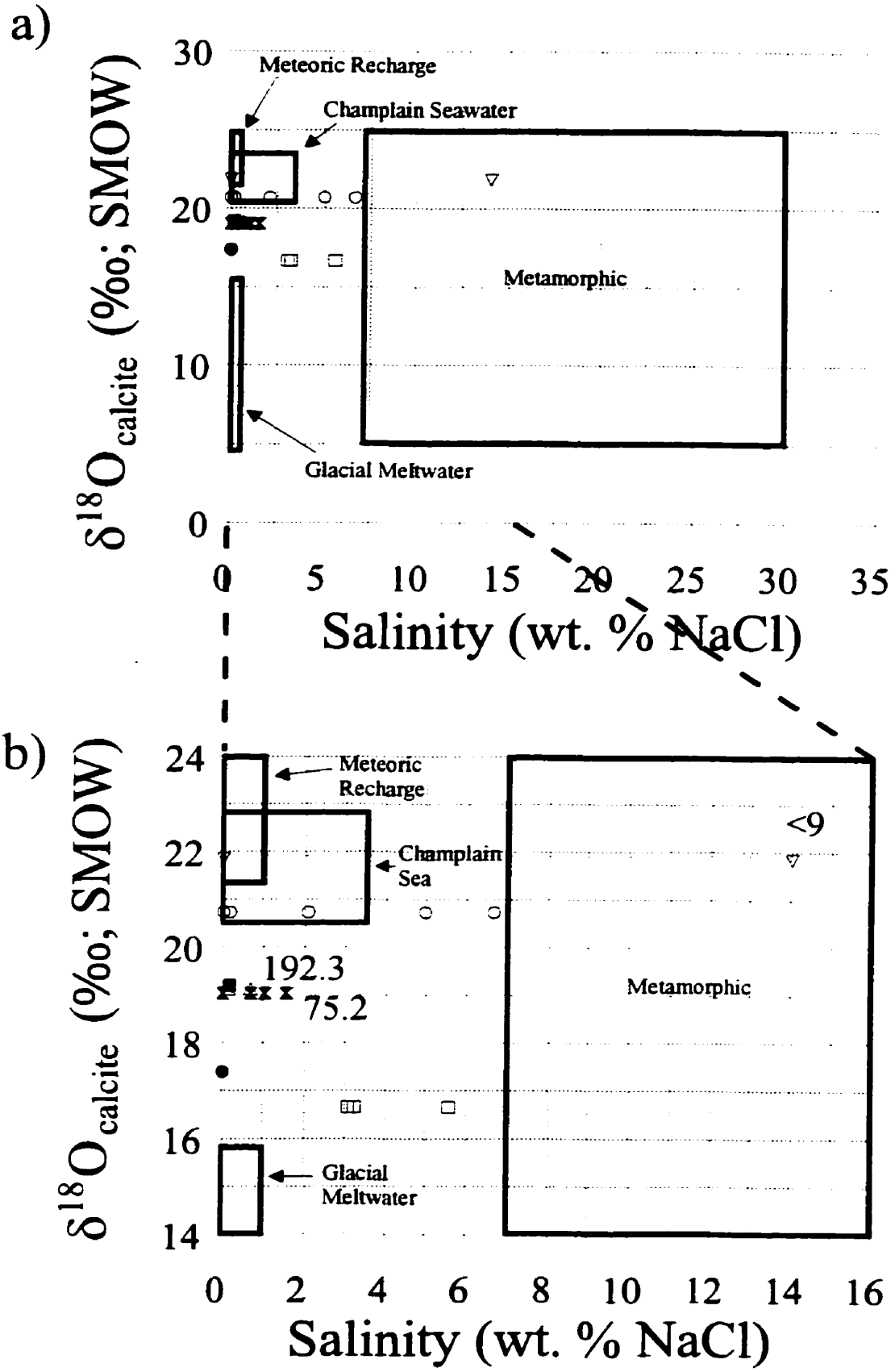
a)
30
20
10
0
Meteoric Recharge
Champlain Seawater
Metamorphic
Glacial Meltwater
$\delta^{18}O_{calcite}$ (‰; SMOW)
0 5 10 15 20 25 30 35
Salinity (wt. % NaCl)
b)
24
22
20
18
16
14
Meteoric Recharge
Champlain Sea
<9
192.3
75.2
Metamorphic
Glacial Meltwater
$\delta^{18}O_{calcite}$ (‰; SMOW)
0 2 4 6 8 10 12 14 16
Salinity (wt. % NaCl)

all the end-members as an origin of the calcite. The most recently precipitated areas of the calcite formed at low temperatures and had an absence of fluid inclusions. Therefore, the fluid inclusion salinity data can be interpreted as reflecting early shifts in the geochemical characteristics of the precipitating fluid, and the stable isotope data can be seen to reflect later shifts in the geochemical composition (origin) of the precipitating fluid. The range of fluid inclusion salinity and the shift in the stable isotope ratios of the fracture-infilling calcites shown in Figures 5-18 a) and b) indicate that the calcites in the fractures sampled at CRL likely formed from a Magmatic/Metamorphic fluid and, since then, have undergone multiple precipitation/recrystallization with fluids which may be associated with Glacial Recharge, Champlain Seawater and Meteoric Recharge events.

The evolution of calcite precipitation from a saline ^{18}O-enriched fluid to a low salinity ^{18}O-depleted fluid can be seen by comparing the fluid inclusion salinity, the $\delta^{18}O_{water}$ calculated using the measured $\delta^{18}O_{calcite}$, and the crystallization temperature determined from fluid inclusion T_h values (Figure 5-19). None of the data plots within any of the suggested end-member fluid fields, but instead plots between the Magmatic/Metamorphic and the Meteoric Recharge fields (Figure 5-19). This is consistent with initial calcite precipitation from Magmatic/Metamorphic fluid with subsequent alteration by a ^{18}O-depleted low salinity fluid. The fact that the data trends toward the meteoric recharge region does not preclude calcite recrystallization by any earlier fluids such as Champlain Seawater or Glacial Meltwater Recharge, which plot beyond the Meteoric Recharge field on Figure 5-19. Partial recrystallization of a Magmatic/Metamorphic calcite by Meteoric Recharge, Champlain Seawater or Glacial

FIGURE 5-19) Fluid inclusion salinity calculated using the T_m and equation given in Chapter 1 is plotted against the $\delta^{18}O_{water}$ calculated using the $\delta^{18}O_{calcite}$, fluid inclusion T_h and the fractionation factor of O'Neil et al (1969). The samples from open vein calcites are represented as empty symbols and the sealed vein calcites are represented as filled symbols. When multiple fluid inclusions were sampled from the same calcite, the same symbol was used to plot each data point from the same calcite. The symbol legend is given below. The U-series ages for all samples are listed above the data points. **a)** The graph axes are large enough to plot the entire field of values for each of the end members (information in Table 5-1) as well as all the data from this investigation. **b)** A narrower range of $\delta^{18}O_{water}$ and salinity to allow for the examination of any trends in the data.

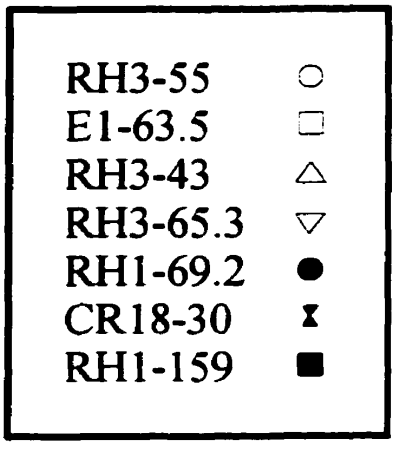

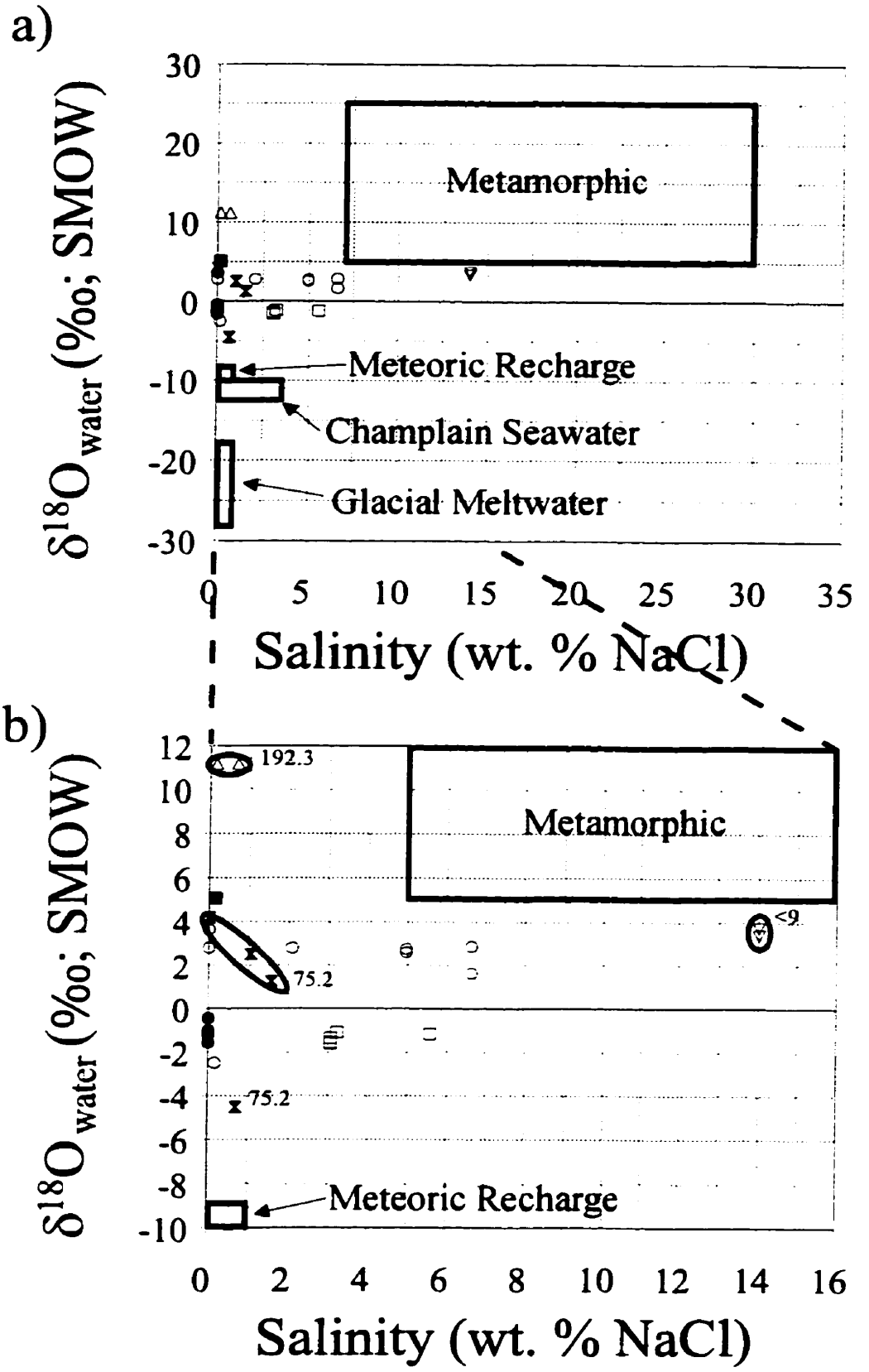
a)
$\delta^{18}O_{water}$ (‰; SMOW)
30
20
10
0
-10
-20
-30
Metamorphic
Meteoric Recharge
Champlain Seawater
Glacial Meltwater
0
5
10
15
20
25
30
35
Salinity (wt. % NaCl)
b)
$\delta^{18}O_{water}$ (‰; SMOW)
12
10
8
6
4
2
0
-2
-4
-6
-8
-10
192.3
Metamorphic
<9
75.2
75.2
Meteoric Recharge
0
2
4
6
8
10
12
14
16
Salinity (wt. % NaCl)

Recharge may result in the range of values observed in the calcites.

There are no trends in the fluid inclusion data when the samples are categorized as from an open-vein or a sealed-vein calcite. This may be due to the relatively small sample set or it may reflect multiple calcite precipitation events, and calcite precipitation under changing geochemical conditions. The presence of different salinity values in fluid inclusions taken from the same calcite indicates the geochemistry of the fluid was changing during calcite precipitation. It is also possible that any temporal trend may have been obscured by sample homogenization during bulk calcite sampling for U and stable isotopes. These effects and the very small sample size may account for the lack of U and Th relationship with sample categorization in Figure 5-19.

Bulk sampling of calcite had two effects on the data, both of which are seen on Figure 5-19. The first is the generation of U-series ages which appear to be discordant with the locations of the samples relative to the end-member fields, and the second is that the $\delta^{18}O_{water}$ values approach but do not plot within any of the end-member fields. Two examples of this are RH3-65.3 and RH3-43, both of which are open-vein calcites. RH3-65.3 has a U-series age of <9 ka and plots near the magmatic/metamorphic end-member and RH3-43 has a U-series age of 192.3 ka and a $\delta^{18}O_{water}$ value of +11‰. Both the ages and the calculated $\delta^{18}O_{water}$ are inconsistent with the geologic history of the region. These discordances occur because the fluid inclusions represent the geochemical conditions during a discrete moment in the calcite precipitation, whereas the bulk samples represent the weighted average for the entire calcite precipitation history. The U-age determined for the fracture-infilling calcites is directly affected by the concentrations of U and Th in

the calcite precipitating fluid, although both have ages within the Quaternary period. The value of a micro-sample will be discordant with the determined U-age if that micro-sample does not represent the calcite precipitation event exerting the most influence on the U-series age. This is especially true for fluid inclusion data, as crystals formed at lower temperatures are more ordered and less prone to imperfections, thus less likely to contain fluid inclusions. Thus, the fluid inclusion measurements in the earlier generations of calcite which formed under Magmatic/Metamorphic conditions appear discordant with the U and stable isotope data if the bulk of calcite precipitation occurred later. This is most likely the case for all the age discordance observed on Figures 5-17, 5-18 and 5-19. The U-ages therefore cannot be compared directly with the fluid inclusion data, as the fluid inclusion data is subjective and affected by the suitability of the fluid inclusion selected for micro-thermometric analyses. In this study, the fluid inclusions seem to mainly reflect periods of calcite precipitation from older, higher temperature fluids.

Similarly, the $\delta^{18}O_{water}$ plotted for each sample will only approach the fields for each of the end-members without ever plotting within the end-member, because the Magmatic/Metamorphic temperatures are over-represented by the fluid inclusion T_h. This over-representation most likely occurred for two reasons: 1) greater tendency for formation of fluid inclusions at higher temperatures; and 2) fluid inclusions formed at temperatures less than 50°C are single-phase at room temperature, and therefore yield indeterminate T_h. As a result, the data plot between the end-member responsible for the formation of the fluid inclusion (Magmatic/Metamorphic) and the end-member with the

greatest influence on the $\delta^{18}O_{calcite}$ (Meteoric, Champlain Seawater or Glacial Recharge). This effect is compounded because isotopic fractionation is higher at lower temperatures. Thus, the use of a higher temperature for calcite formation than that at which the bulk of the calcite precipitated results in higher $\delta^{18}O_{water}$ values being calculated. The data presented in Figures 5-18 and 5-19 indicate that the calcites were initially precipitated in magmatic/metamorphic fluids at high temperatures followed by subsequent precipitation and alteration by low salinity ^{18}O-depleted fluids.

Isotopic Evolution of Calcite Precipitating Fluids

The $\delta^{18}O_{calcite}$ was plotted against fluid inclusion T_h (Figure 5-20). The location of the data relative to the end-member fields suggests that the calcite was initially formed from a "Hydrothermal" fluid and has subsequently been altered by increasingly ^{18}O-depleted waters during cooling, consistent with the data discussed above. In this case, there is a trend apparent in the calcite when the samples are considered as open-vein or sealed-vein calcite. The sealed-vein calcites tend to have lower $\delta^{18}O$ values and have fluid inclusions which cover a wider range of temperatures. However, there is considerable scatter in the data and any observed trend may be an artefact of the relatively small sample size. Figure 5-20 b) suggests that the range of data may be the result of end-member fluid mixing, calcite precipitation from an end-member during cooling, or a combination of end-member mixing and cooling. The ranges of $\delta^{18}O$ and T_h values suggest that the fluid inclusions initially formed from the magmatic/metamorphic fluid during regional metamorphism and initial regional cooling, and then formed from mixtures of the magmatic/metamorphic fluids and a ^{18}O-depleted fluid during the

FIGURE 5-20) a) The same plot as Figure 5-3 except with the T_h from fluid inclusions plotted against the measured $\delta^{18}O_{calcite}$ for each sample. The curves were plotted using the $\delta^{18}O_{calcite\text{-}water}$ fractionation factor of O'Neil et al. (1969) and the $\delta^{18}O_{water}$ value given above each curve. The sources for the values defining each end member field are given in Table 5-1. The calcite sample represented by each symbol is given in the legend below. The empty symbols represent open vein calcites and the filled symbols represent sealed vein calcites. The arrows extending from the data points indicate that heating was stopped prior to T_h to prevent decrepitation of other fluid inclusions in the sample.
b) The same plot with a narrower range of $\delta^{18}O_{calcite}$ than a). The numbers to the right of the symbols represent the U-series age in ka. The pattern observed suggests precipitation from a "Hydrothermal" fluid followed by recrystallization with increasingly $\delta^{18}O$ depleted waters at lower temperatures. The arrow labelled "cooling" represents the direction of a $\delta^{18}O_{calcite}$ trend which would be observed if a constant $\delta^{18}O_{water}$ were precipitating calcite during cooling, and the line labelled "mixing" represents the direction of a $\delta^{18}O_{calcite}$ trend which would be observed if two or more distinct $\delta^{18}O_{water}$ end members were mixing during cooling.

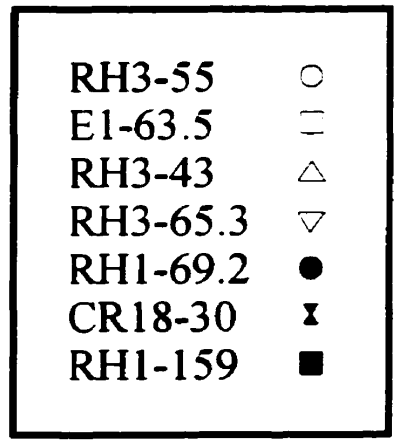

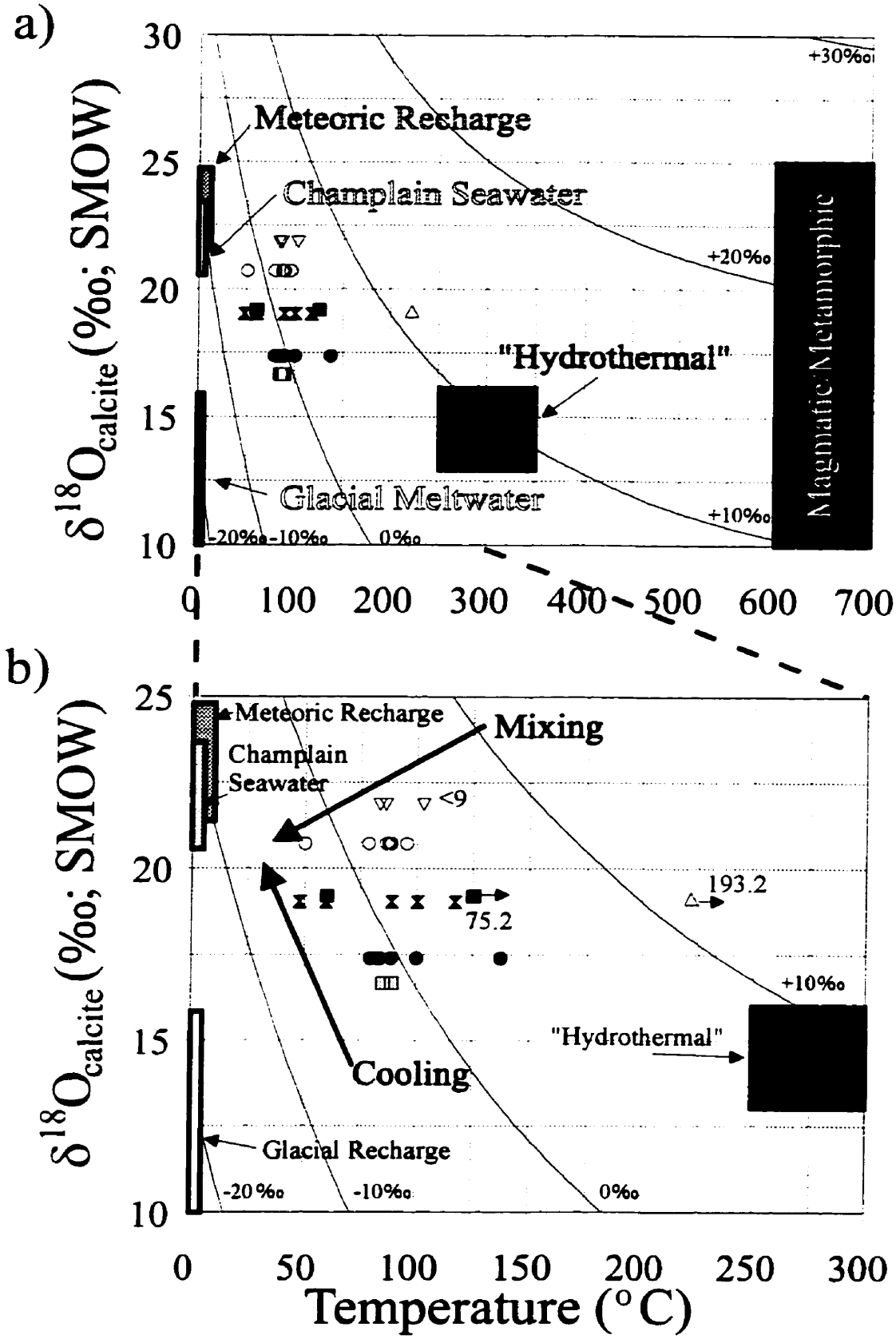
a)
Meteoric Recharge
Champlain Seawater
"Hydrothermal"
Glacial Meltwater
Magmatic Metamorphic
+30‰
+20‰
+10‰
-20‰
-10‰
0‰
δ18Ocalcite (‰; SMOW)
30
25
20
15
10
0
100
200
300
400
500
600
700
b)
Meteoric Recharge
Champlain Seawater
Mixing
Cooling
<9
193.2
75.2
+10‰
"Hydrothermal"
Glacial Recharge
-20‰
-10‰
0‰
δ18Ocalcite (‰; SMOW)
25
20
15
10
0
50
100
150
200
250
300
Temperature (°C)

remainder of the history of the region. However, the nature of bulk sampling for $\delta^{18}O_{calcite}$ versus micro-sampling for T_h may shift the position of the data points on Figure 5-20. If the fluid inclusions are present in an earlier generation of precipitated calcite and the bulk isotope ratio is more representative of a later calcite precipitating fluid, as was suggested by Figures 5-18, and 5-19, the stable isotope composition of the calcite precipitated from the precursor of the fluid inclusions may be different from the bulk measurement.

Bottomley (1988) noted that an outer growth layer had a 6.7‰ higher $\delta^{18}O$ than an inner growth layer on a calcite from CRL. If the fluid inclusions plotted on Figure 5-20 are present in earlier growth layers which may have lower $\delta^{18}O$ values than the bulk sample, then the earlier generation of calcite may have also precipitated from a less ^{18}O-enriched fluid than is indicated by Figure 5-20. Unfortunately, the relative contribution of individual calcite precipitation events is unknown. If the fluid inclusions are present in a zone of the calcite with a less enriched $\delta^{18}O$ value than the bulk value, the evolution of $\delta^{18}O_{water}$ would have to follow the cooling curve as indicated on Figure 5-20 b) to under 50°C and then follow a mixing curve with a slope proportionate to the relative contributions of each end-member. Whether the fluid inclusions are assumed to represent an earlier layer, a record of cooling, or to be representative of the bulk calcite, the most likely mixing end-members are Meteoric Recharge and "Hydrothermal" fluids if a two component mixing model is assumed. However, this does not preclude a contribution by Glacial Recharge or Champlain Seawater. Given the relative volumes of each end-member, it is reasonable to assume that the bulk $\delta^{18}O$ observed in the calcite was most affected by Meteoric Recharge.

The U-ages presented on Figure 5-20 b) support the argument that the fluid inclusions represent older generations of calcite. According to Figure 5-11, the regional temperature has been below 50°C for the last 400-600 Ma, and assuming a geothermal gradient of 25°C/km, all of the samples examined in this investigation would have been formed at temperatures well below 50°C for the last 350 ka. If the calcite age is affected by the sampling of earlier generations, the calculated age would be older than the actual age. As all the sample ages on Figure 5-20 are < 350 ka, it can be concluded that the bulk of the calcite precipitation is occurring at temperatures below 50°C. Thus, the bulk of the calcite precipitated from "younger" ^{18}O-depleted fluids, and the fluid inclusion T_h represents older generations. RH3-65.3 is an excellent example of such a record of multiple calcite precipitation events. It has fluid inclusions with T_h between 80-110°C which suggests an age of 700-800 Ma, a U-series age of less than 9 ka, and a stable isotope composition consistent with precipitation from modern meteoric recharge. The U and $\delta^{18}O$ data is consistent with formation from a meteoric recharge alone, and the T_h is evidence for recrystallization of an original Magmatic/Metamorphic calcite. RH3-65.3 is an example of near complete recrystallization with modern meteoric recharge while the other samples represent varying degrees of recrystallization and multi-component fluid mixing.

The fluid inclusion T_h, the $\delta^{18}O_{calcite}$, and the calcite-water fractionation factor of O'Neil et al. (1969) were used to back calculate the $\delta^{18}O$ of the calcite precipitating fluid (Figure 5-21). The measured data plot on a curve between the "Hydrothermal" and the Meteoric Recharge end-member regions. This is consistent with recrystallization of a

metamorphic calcite by ^{18}O-depleted waters. The strong linear appearance of the data is an artefact of the data manipulation. A single $\delta^{18}O_{calcite}$ measurement, and multiple fluid inclusion measurements, were made in the same sample. Each fluid inclusion T_h measured then used the same $\delta^{18}O_{calcite}$ to calculate the $\delta^{18}O_{water}$. Therefore, they all plot along the curve defined by the fractionation factor. Despite this, the data does plot between the $\delta^{18}O_{water}$ field for Magmatic/Metamorphic fluids and the ^{18}O-depleted end-member groups, once again suggesting progressive recrystallization.

The same relationship between U-series age, T_h and stable isotopes observed in Figure 5-20 is observed in Figure 5-21. The fluid inclusion T_h is interpreted as representing a residual "Hydrothermal" calcite event which has been subjected to subsequent calcite recrystallization, while the isotope and age data represent weighted averages of all precipitation events in the calcite. If it is assumed that the bulk of the calcite precipitated/recrystallized at 5°C (approximating the temperature of each low temperature end-member), the samples on Figure 5-21 b) would have precipitated from fluids with $\delta^{18}O$ between -16 and -12‰, assuming the "hydrothermal" component of each sample had a negligible impact on the $\delta^{18}O_{calcite}$. The less ^{18}O-enriched values Bottomley (1988) observed in the earlier precipitated calcite would translate to a slightly less depleted range of $\delta^{18}O_{water}$. Regardless, the modelled range of $\delta^{18}O_{water}$ at 5°C is consistent with the range of $\delta^{18}O_{water}$ for the Meteoric Recharge and Champlain Seawater end-members. This range also does not eliminate the possible contribution of Glacial Recharge to the secondary calcite precipitating fluids.

Figure 5-21 displays the same apparent pattern among $\delta^{18}O$, U-series age, and

FIGURE 5-21) $\delta^{18}O_{water}$ of the calcite precipitating fluid as calculated using the measured $\delta^{18}O_{calcite}$, fluid inclusion T_h and the calcite-water fractionation factor of O'Neil et al. (1969). Open vein calcites are represented by empty symbols and sealed vein calcites are represented by filled symbols. The symbol legend is given below. The symbols with arrows connected represent fluid inclusions which were not heated to T_h, heating was stopped to preserve other fluid inclusions on the same slide. The potential end member regions presented in Table 5-1 are also plotted on the figure.
a) Fluid inclusion data plotted on axes with a wide enough range to permit the entire area of each end member to be plotted. This allows the dispersion of the data relative to the location and size of each end member to be seen.
b) Same plot on a narrower range of $\delta^{18}O$ and T. The numbers to the right of the data are the U-series ages for the bulk sample (in ka) as determined by α-spectrometry.

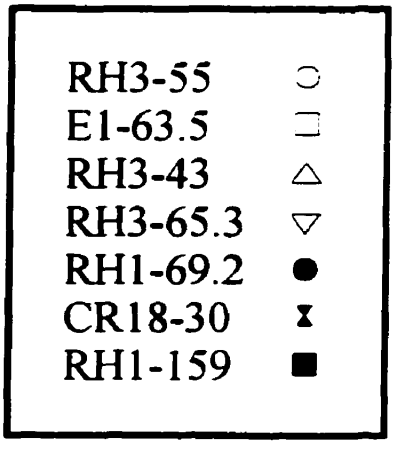

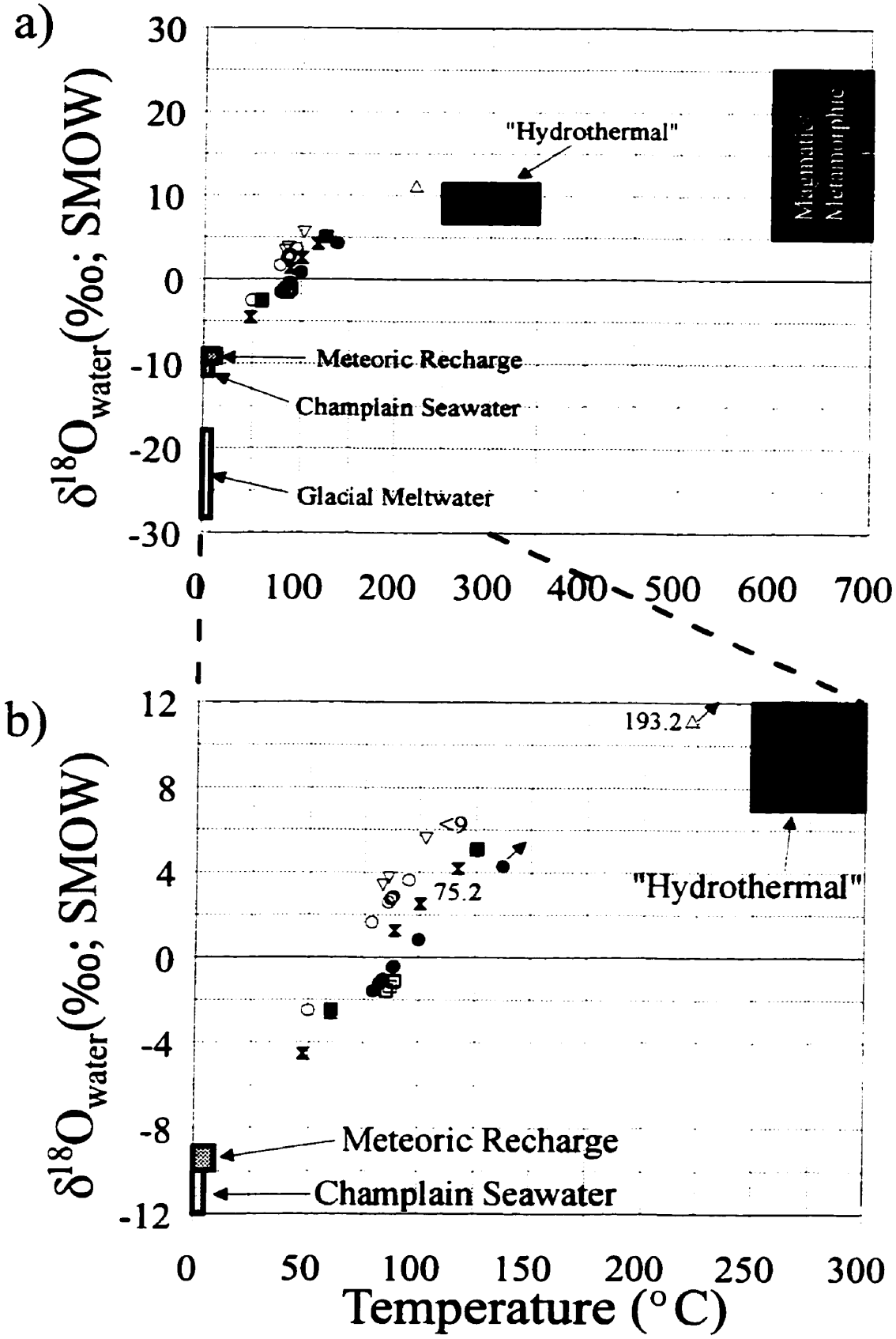
a)
30
20
10
0
-10
-20
-30
$\delta^{18}O_{water}$(‰; SMOW)
"Hydrothermal"
Magmatic / Metamorphic
Meteoric Recharge
Champlain Seawater
Glacial Meltwater
0
100
200
300
400
500
600
700
b)
12
8
4
0
-4
-8
-12
$\delta^{18}O_{water}$(‰; SMOW)
193.2
<9
75.2
"Hydrothermal"
Meteoric Recharge
Champlain Seawater
0
50
100
150
200
250
300
Temperature (°C)

open-vein versus sealed-vein fractures as seen in Figure 5-20. The open-vein calcites tend to have higher calculated $\delta^{18}O_{water}$ and younger ages than the sealed-vein calcites, although it is impossible to make any conclusions with respect to age as there were only three samples which underwent U-series, stable isotope and fluid inclusion analysis. Figure 5-21 suggests that the calcites have been altered by progressively ^{18}O-depleted waters since a "Hydrothermal" formation, and that even "young" calcites contain a residual hydrothermal component.

Co-Evolution of Calcite $\delta^{13}C$ and $\delta^{18}O$ Values?

The $\delta^{13}C$ and $\delta^{18}O$ values were examined with respect to the calculated $^{230}Th/^{234}U$ ages to determine if there was a temporal evolution in the isotopic composition of fracture-infilling calcites from CRL. Figure 5-22 is a reproduction of the plot of $\delta^{13}C$ against $\delta^{18}O$ (Figure 5-7), except that only the samples which were U-series dated have been plotted. In addition to the trend of progressive recrystallization of older calcites formed from higher temperature fluids with lower temperature waters seen in the stable isotopes, there is also a pattern in the U-series ages of the calcites. All four of the calcites which have $^{230}Th/^{234}U$ ages >350 ka, plot within or near the "Hydrothermal" end-member in Figure 5-22. U-series ages of >350 ka for all the samples in the "Hydrothermal" end-member are consistent with the stable isotope evidence of an early crystallization from a higher temperature fluid. Unfortunately it is not possible to establish the exact age for these calcites, although due to their higher formation temperatures as established by micro-thermometry on fluid inclusions, it is assumed that they are hundreds of millions of years old.

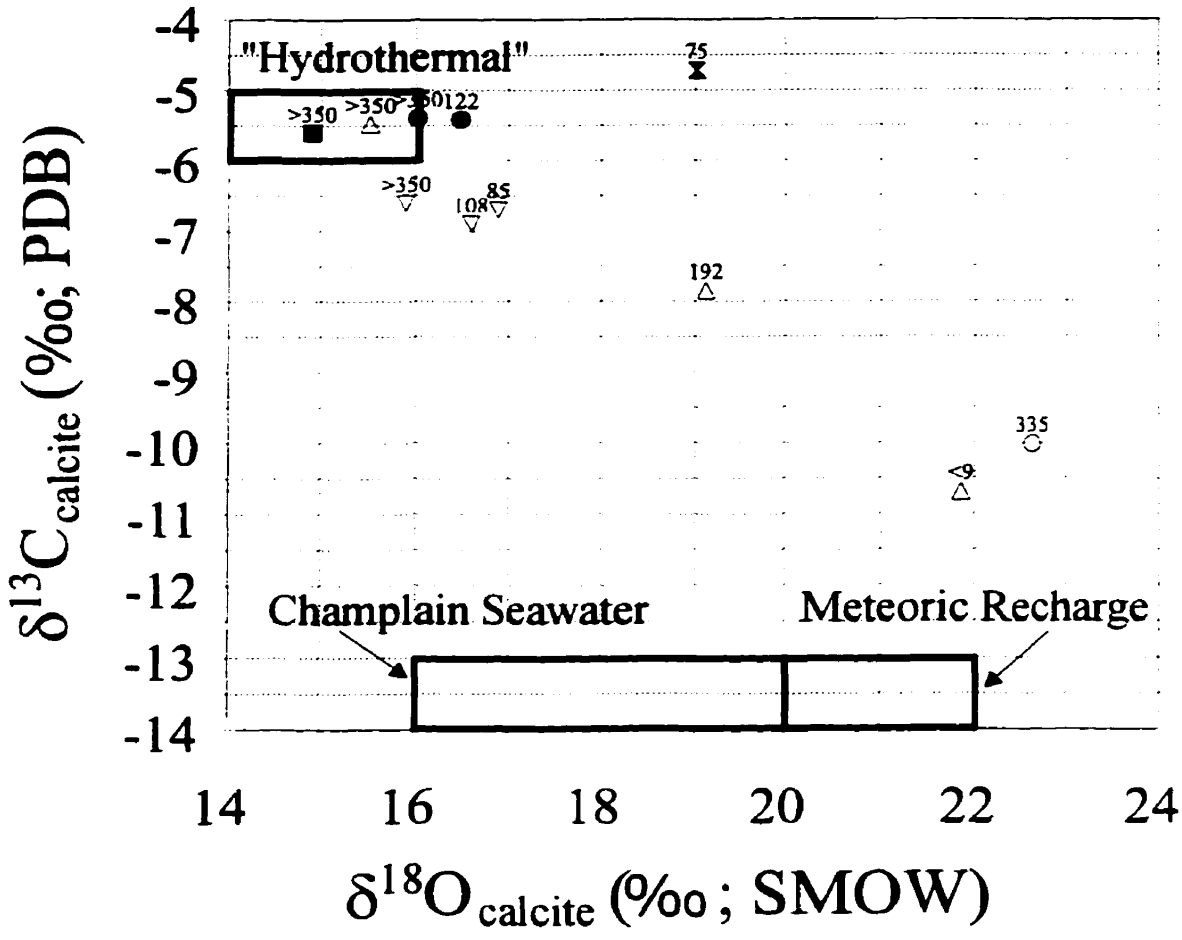

FIGURE 5-22) Plot of the $\delta^{18}O$ against $\delta^{13}C$ measured in the calcites from this investigation. The samples are plotted according to the borehole they were sampled from and whether they were characterized as open or sealed to groundwater flow. Calcites from borehole E1 are circles, RH1 are squares, RH3 are upward pointing triangles, CR9 are downward pointing triangles and CR18 are hourglasses. The open vein calcites are represented as empty symbols and the sealed vein calcites are represented as filled symbols. The U-series ages (in ka) determined by α-spectrometry for the samples are listed above the data points. Part of the "Hydrothermal", Champlain Seawater and Meteoric Recharge end member fields as characterized in Table 5-1 are also plotted. This figure is a modification of a figure from Bukata et al. (1998b).

The distribution of calcites with ages >350 ka relative to the end-members was examined statistically to determine if it occurred by chance alone. If a binomial distribution is assumed and the probability that each calcite have an age >350 ka is set at 50% (very conservative given the length of geologic time), the null hypothesis that 7 of 8 calcites which plot outside the hydrothermal end-member have ages <350 ka due to chance had to be rejected at the 95% confidence level. It was not possible to reject the null hypothesis that all 3 calcites which plotted within the "Hydrothermal" end-member have ages >350 ka due to chance, given the small data set. These observations are consistent with calcite precipitation or recrystallization under isotopic conditions occurring during mixing of two or more end-members or calcite recrystallization from the late Pleistocene to present.

In the data set, there is no clear trend of progressive recrystallization in the isotopic composition of the fracture-infilling calcites if the age of the calcite is taken as an indicator of "progressive" precipitation or recrystallization, outside of the statistical test previously performed. This is because the calcites were sampled from numerous locations on the properties of CRL which contain fractures which have transported fluids that may or may not be hydrologically and temporally connected. The U-series ages plotted with the stable isotope data on Figure 5-22 further support a model of precipitation or recrystallization events recorded in the calcites from ^{13}C-depleted and ^{18}O-depleted waters. It is important to note that a better relationship is found between the stable isotope and U-series data than between either the isotope or U-series and the fluid inclusion data (Figures 5-20 and 5-21). This is most likely because both the U-series and

stable isotope data are based on bulk samples of the calcite and the fluid inclusion data represent micro-samples. Comparing two pieces of data which represent weighted averages will place them between two end-members on a mixing line, while comparing a weighted average to an exact value representing one of the end-members will skew the data. Figure 5-22 indicates initial calcite formation under "Hydrothermal" conditions followed by subsequent calcite precipitation from low temperature ^{13}C-depleted and ^{18}O-depleted waters.

Is Calcite Precipitation Correlated With Interglacial Periods?

An investigation by Ates et al. (1997) into the effect of continental glaciation by a Laurentide-size ice sheet on the safe storage of radioactive waste in the Canadian Shield found that faulting and fracturing of the host rock would occur along the perimeter of the ice sheet during both glacial loading and unloading. The U-series ages measured in fracture-infilling calcite in this investigation and from previous investigations on the Canadian Shield were examined to test for a correlation with periods of continental glaciation (Figure 5-23). All but one of the ages measured in the present investigation fall within interglacial periods, and the one exception occurs at the end of the glacial period and has an error range which straddles the glacial termination. The timing of calcite precipitation in fractures therefore appears to be linked with interglacial periods.

The observations from this investigation are consistent with the timing of fracture-infilling calcite precipitation from previous investigations at CRL (Milton, 1985), and elsewhere on the Canadian Shield (Gascoyne et al., 1997; and Szabo, 1997), shown in Figure 5-23 b). Fracture-infilling calcite precipitation on the Canadian Shield has

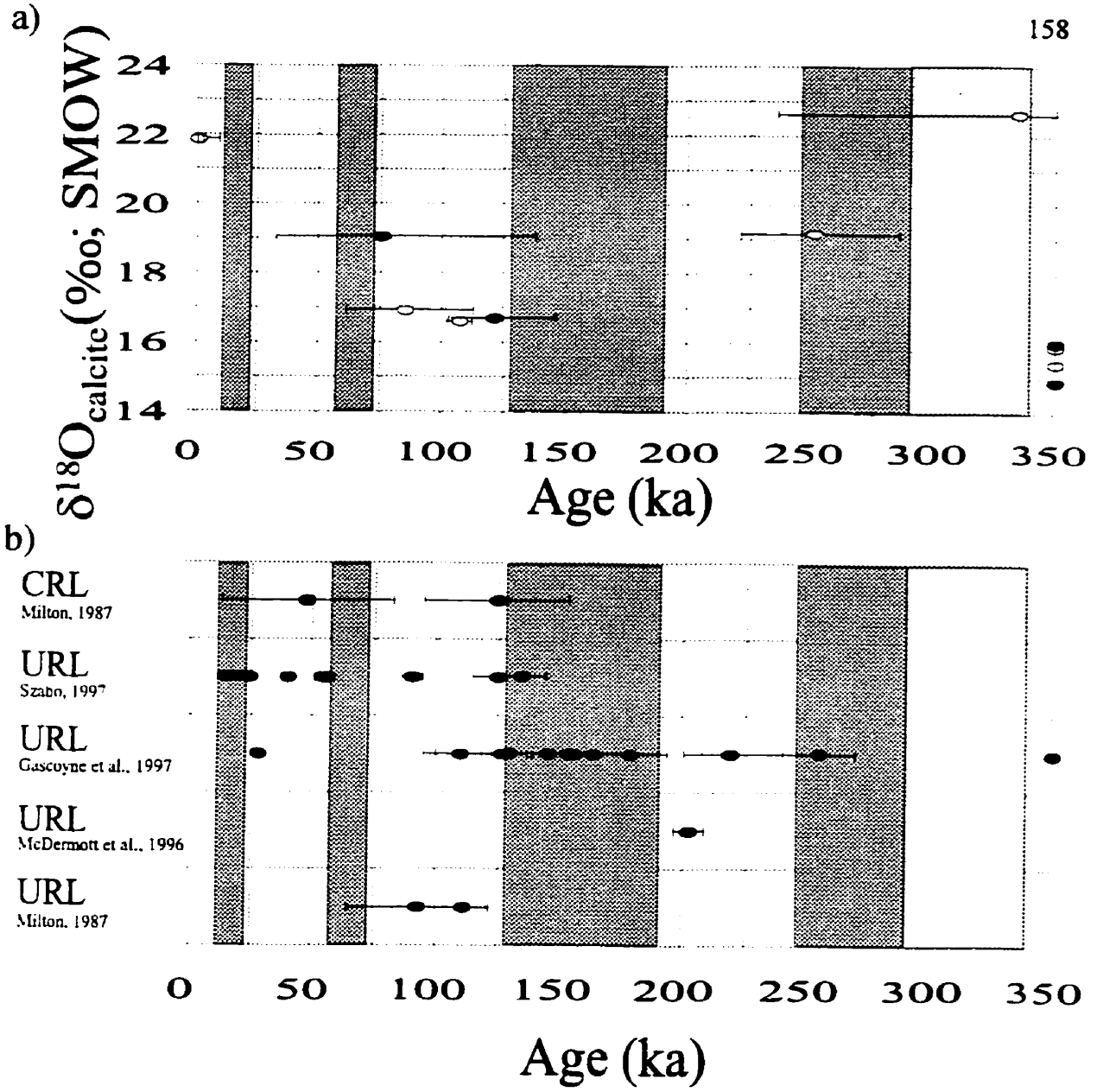

FIGURE 5-23) Plot of U-series age for the fracture-infilling calcites from this investigation against a) $\delta^{18}O$. Plot b) shows U-series ages for fracture-infilling calcites from previous investigations on the Canadian Shield, at Chalk River (CRL) and the Underground Research Laboratories (URL) in Pinawa, Manitoba. The darkest regions on the figures are the glacial periods as determined by Martinson et al. (1987), and the lighter shaded region extends the glacial onset of isotope stage IX to beyond 300,000 years using the date from Winograd (1992). In a), the empty circles represent open vein calcites and the filled circles represent sealed vein calcites. The symbols in b) do not distinguish between open and sealed vein calcite. The bars indicate the analytical error associated with each age calculation.

primarily occurred during interglacial periods. These observations are entirely consistent with those of McDermott et al. (1995) who determined that fracture calcite precipitation in shield environments (primarily the Fennoscandian Shield) clustered around the end of interglacial periods. McDermott et al. (1995) concluded that this indicated a change in the fracture-flow system linked to glaciation. This is likely the case in the fracture system examined in this investigation as well.

Whether the ages of the calcites in this investigation could fall during interglacial periods by chance was examined. Assuming an equal probability of fracture-infilling calcite precipitation per unit time during both glacial and interglacial periods, and assuming that the U-series ages and the glacial-interglacial transition dates are fixed (without associated error), the occurrence of calcite precipitation was tested for randomness using a binomial distribution test at a 95% confidence level. The null hypothesis that the timing of calcite precipitation during interglacial periods occurred by chance had to be rejected for both my data set and the combined data set. In addition, the null hypotheses that; 1) my data contained a higher proportion of calcites with ages >350 ka than the collected data set; and 2) that my data had a higher proportion of calcites with interglacial ages than the collected data set had to be rejected at the 95% confidence level.

Figure 5-23 a) examines the U-ages of the calcite with respect to the $\delta^{18}O$ value of the calcite. There does not appear to be any pattern in the $\delta^{18}O$ of the calcite with respect to whether the calcites are open-vein or sealed-vein. However, there may be a relationship in the $\delta^{18}O$ values with regard to their proximity to the onset of glacial retreat. The $\delta^{18}O$ in calcites formed closest to the onset of interglacial periods appear to

have more ^{18}O-depleted values. While this may be an artefact of small sample size, it may also reflect addition of a glacial meltwater component to calcite precipitating fluid. However, there is no systematic variation in the $\delta^{13}C$ (not plotted) which would help support this, and it is difficult to characterize the isotopic composition of DIC from a post-glacial component. Arguably a post-glacial DIC would be less ^{13}C-depleted than once an interglacial period had begun in earnest.

Figure 5-23 indicates that the youngest calcite (RH3-65.3) with an age of <9 ka has the most depleted $\delta^{13}C$ and most enriched $\delta^{18}O$ of all the samples. These observations are consistent with post-Wisconsin recharge conditions. In this investigation, it appears that fracture-infilling calcites precipitated immediately after the onset of interglacial periods record $\delta^{18}O$ values consistent with incorporation of a glacial meltwater component into the precipitating fluid. However, there are not enough data to definitively conclude that the calcite records a glacial meltwater component. The precipitation of fracture-infilling calcite on the Canadian Shield appears to be restricted to interglacial periods.

6 - SUMMARY AND CONCLUSIONS

$\delta^{13}C$, $\delta^{18}O$, U-series ages and fluid inclusion T_h and salinity of the fracture-infilling calcite from borehole samples at CRL provide a record of the palaeohydrology of the region. The $\delta^{18}O$ and $\delta^{13}C$ of the calcite provide information about the source of water and DIC involved in precipitation of the calcite. The U-series ages indicate the timing of calcite precipitation, and the fluid inclusions give an indication of the salinity and minimum temperature of the fluid responsible for the formation of the fluid inclusions. Together, these analyses provide an indication of the geochemistry of the waters responsible for fracture-infilling calcite precipitation at CRL.

Calcite occurring in fractures characterized by visual inspection as open to groundwater flow tended to have more ^{18}O-enriched and more ^{13}C-depleted values than calcite occurring in fractures sealed to groundwater flow. The ranges of $\delta^{18}O$ values measured in both open-vein and sealed-vein calcites overlap the ranges of all fluids identified as possibly precipitating calcite in the fractures. The $\delta^{13}C$ values fall between a "Hydrothermal" calcite and a calcite precipitated from soil zone ^{13}C-depleted bicarbonate.

There are slight trends in the $\delta^{13}C$ and $\delta^{18}O$ values of the calcites with sample depth. The $\delta^{18}O$ values loosely trend from open-vein calcites in the shallow bedrock (<150 m), which are in isotopic equilibrium with modern meteoric recharge, to less enriched sealed-vein calcite at depth. In the shallow bedrock, the $\delta^{13}C$ of some fracture-infilling calcite is in isotopic equilibrium with the DIC, but none of the $\delta^{13}C$ values in calcites from depths greater than 100 m are in isotopic equilibrium with the DIC. Also, none of the fracture-infilling calcites sampled were in isotopic equilibrium with both the

$\delta^{18}O$ and $\delta^{13}C$ of the groundwater presently in the fractures. This suggests that a scenario more complex than calcite precipitation from modern recharge is occurring in the fractures. The trend observed between the $\delta^{18}O$ and $\delta^{13}C$ of the fracture-infilling calcite suggests that the calcites were initially formed from a "Hydrothermal" fluid and have been subsequently re-crystallized by modern recharge. The isotopic variation in the calcites suggests that the system has been open with respect to ^{18}O, and semi-open to closed with respect to ^{13}C.

The majority of fluid inclusions sampled were formed from fluids with salinity less than 6 wt. % NaCl and at temperatures between 70 and 90°C. This suggests that the fluid inclusions formed in calcite precipitated during post-metamorphic regional cooling. The timing of fluid inclusion formation based on T_h is 600-800 Ma. The range of salinity measured is consistent with either mixing of high salinity (7 to 30 wt. % NaCl) metamorphic fluid with a lower salinity fluid, or fluid inclusion formation during multiple calcite precipitation events from geochemically distinct fluids. The T_h and salinity data suggest that the fluid inclusions were formed during post-metamorphic cooling from a diluted metamorphic fluid.

A method was developed for U/Th extraction and separation using the EiChrom UTEVA resin prior to analysis by α-spectrometry. The extraction and separation were rapid, requiring less than one day to perform, and gave excellent U/Th separation and recovery. Greater than 70% U and greater than 80% Th recovery was obtained on standards. The average U recovery was adversely affected by an anomalously low (34%) recovery from one sample. An age of 44.7 (+/-4.2) ka was calculated for a well-

characterized speleothem which agrees within 1-σ with all published ages for the same speleothem, including the most precise 47.58 +/-1.17(1-σ) ka determined by TIMS (Li et al., 1989). The developed technique was used to calculate ages of <9 ka to >350 ka for the fracture-infilling calcites analysed. The U and Th concentrations in the calcite determined using the column method agree well with the concentrations measured by ICP-MS and provide further validation of the technique.

There is no correlation between sample U/Th concentration or U-series age and sample depth. This indicates that calcite precipitation and recrystallization has occurred in the fractures. A trend observed between the U and Th concentrations in the calcites indicates that calcite precipitation has occurred under both oxidizing and reducing conditions. Overall, the U and Th data suggest episodic calcite precipitation from geochemically distinct fluids.

The U-series ages and the stable isotope data appear to be discordant with the fluid inclusion data. This is a result of the fluid inclusion micro-sampling. Fluid inclusions reflect the geochemistry of the fluid involved in precipitation of that zone of calcite which included the fluid inclusion formation. Most of the calcites examined in this investigation formed during multiple precipitation events. Thus a calcite with a U-series age <350 ka and fluid inclusions which are 600-800 Ma old could only have formed under multiple precipitation events spanning from the time of fluid inclusion formation to less than the U-series age determined for the calcite.

Fluid inclusion T_h used to interpret the stable isotope ratios resulted in slightly skewed data. The data did not plot within any of the end-member regions, but instead

plotted on a mixing line between the end-members responsible for the formation of the fluid inclusions, and the end-member exerting the most influence on the stable isotope ratio measured in the bulk calcite. The stable isotope, fluid inclusion and U-series data suggest initial calcite formation during regional metamorphism and cooling, followed by calcite precipitation and recrystallization from low temperature fluids, most likely meteoric recharge.

Co-variation of the $\delta^{13}C$ and $\delta^{18}O$ indicates a trend from "Hydrothermal" calcite to calcite formed from Meteoric Recharge. The calcites in isotopic equilibrium with the "Hydrothermal" end member all have ages >350 ka, and all but one of the calcites trending between the two end members have ages less than 350 ka, with the youngest calcites plotting nearest to the Meteoric Recharge end member. The U-series ages of calcites in the fractures of crystalline rock suggest that precipitation is restricted to interglacial periods, and the calcites precipitated nearest to the glacial-interglacial transitions have the lowest $\delta^{18}O$ values. This apparent trend in $\delta^{18}O$ composition is consistent with a glacial meltwater component of the recharge leading to calcite precipitation immediately following glacial retreat.

The stable isotope, fluid inclusion and U/Th analysis of the fracture-infilling calcites at CRL suggests that the calcites initially formed during post-metamorphic cooling and have been subsequently altered by low temperature recharge. The sealed-vein calcite is more likely to reflect a "Hydrothermal" origin and the open-vein calcite is more likely to reflect recrystallization or subsequent calcite precipitation from a low temperature, low salinity fluid. The stable isotope, fluid inclusion and U/Th analysis of

fracture-infilling calcite provides powerful information about the geochemical environment of calcite precipitation. This information is useful in constructing the regional palaeohydrogeology.

REFERENCES

Adriaens, A.G., Fassett, J.D., Kelly, W.R., Simons, D.S. and Adams, F.C., 1992. Determination of Uranium and Thorium Concentrations in Soils: Comparison of Isotope Dilution-Secondary Ion Mass Spectrometry and Isotope Dilution-Thermal Ionization Mass Spectrometry. Analytical Chemistry, 64: 2945-2950.

Anderson, S.L., 1990. Reply (to Comment by Cosca, Sutter and Essene); American Journal of Science. v 240: 205-207.

Anderson, W.T., Mullins, H.T. and Ito, E., 1997. Stable isotope record from Seneca Lake, New York: Evidence for a cold paleoclimate following the Younger Dryas. Geology, 25(2): 135-138.

Apostolidis, C., Molinet, R., Richir, P., Ougier, M. and Mayer, K., 1998. Development and validation of a simple, rapid and robust method for the chemical separation of uranium and plutonium. Radiochimica Acta, 83(1): 21-25.

Ates, Y., Bruneau, D. and Ridgway, W.R., 1997. Continental glaciation and its potential impact on a used-fuel disposal vault in the Canadian Shield. AECL-10140, COG-94-37-I, Atomic Energy of Canada Limited, Pinawa, Manitoba.

Azmy, K., Veizer, J., Bassett, M.G. and Copper, P., 1998. Oxygen and carbon isotopic composition of Silurian brachiopods: Implications for coeval seawater and glaciations. Geological Society of America Bulletin, 110(11): 1499-1512.

Baer, A.J., 1981. Two orogenies in the Grenville Belt? Nature, 290: 129-131.

Baertschi, P., 1976. Absolute ^{18}O content of Standard Mean Ocean Water. Earth and Planetary Science Research Letters, 31: 341.

Balderer, W., Fontes, J.-C., Michelot, J.-L. and Elemore, D., 1987. Isotopic Investigations of the Water-Rock System in the Deep Crystalline Rock of Northern Switzerland. In: P. Fritz and S.K. Frape (Editors), Saline water and gasses in crystalline rocks. Geological Association of Canada, pp. 175-195.

Bar-Matthews, M., Ayalon, A., Kaufman, A. and Wasserburg, G.J., 1999. The Eastern Mediterranean paleoclimate as a reflection of regional events: Soreq cave, Israel. Earth and Planetary Science Letters, 166(1-2): 85-95.

Bard, E., Hamelin, B., Fairbanks, R.G. and Zindler, A., 1990a. Calibration of the ^{14}C timescale over the past 30,000 years using mass spectrometric U-Th ages from Barbados corals. Nature, 345: 405-410.

Bard, E., Hamelin, B. and Fairbanks, R.G., 1990b. U-Th ages obtained by mass spectrometry in corals from Barbados: sea level during the past 130,000 years. Nature, 346: 456-458.

Bard, E., Hamelin, B., Arnold, M., Montaggioni, L., Cabioch, G., Faure, G., and Rougerie, F., 1996. Deglacial sea-level record from Tahiti corals and the timing of global meltwater discharge. Nature, 382: 241-244.

Blyth, A.R., Frape, S.K., Blomqvist, R. and Nissinen, P., 1998. Combining fluid inclusion studies with isotopic investigations of fracture calcite to assess the past thermal and fluid history of the Olkiluoto Research Site, Finland (Poster). In: G.S.A. (Editor), Geological Society of America Annual Meeting. Geological Society of America, Toronto, Ontario, Canada.

Bottomley, D.J., Ross, J.D. and Graham, B.W., 1984. A Borehole Methodology for Hydrogeochemical Investigations in Fractured Rock. Water Resources Research, 20(9): 1277-1300.

Bottomley, D.J., 1987. The isotope geochemistry of fracture calcites from the Chalk River area, Ontario, Canada. Applied Geochemistry, 2: 81-91.

Bottomley, D.J., 1988. The isotope geochemistry and origins of fracture calcites in the Grenville gneisses, Chalk River, Ontario. Ph. D. Thesis, University of Ottawa, Ottawa, Ontario. 264 pp.

Bottomley, D.J. and Veizer, J., 1992. The nature of groundwater flow in fractured rock: Evidence from the isotopic and chemical evolution of recrystallized fracture calcites from the Canadian Precambrian Shield. Geochimica et Cosmochimica Acta, 56: 369-388.

Brown, P.A., and Rey, N.A.C., 1983. Fractures and Faults at Chalk River, Ontario. In: M.D. Thomas and D.F. Dixon (Editors), Geophysical and Related Geoscientific Research at Chalk River, Ontario. Atomic Energy of Canada Limited, Ottawa, Ontario, pp. 39-51.

Budd, D.A. and Land, L.S., 1990. Geochemical imprint of meteoric diagenesis in Holocene ooid sands, Schooner Cays, Bahamas: Correlation of calcite cement geochemistry with extant groundwaters. Journal of Sedimentary Petrology, 60(3): 361-378.

Bukata, A.R., Kotzer, T. and Cornett, R.J., 1997. Integration of Isotopic, Mineralogic and Geologic Data to Evaluate the Fluid History of a Fractured Granite (Poster), GAC/MAC Annual Meeting, Ottawa, Ontario, pp. A-20.

Bukata, A.R., Kotzer, T. and Cornett, J., 1998a. A Technique for Extraction/Separation of U and Th from Calcite Samples Using an Ion Selective Resin. In: R. Clement and B. Burk (Editors), Proceedings of the Second Biennial International Conference on Chemical Measurement and Monitoring of the Environment, Ottawa, Canada, pp. 647-652.

Bukata, A.R., Kotzer, T. and Cornett, R.J., 1998b. Fracture-Infilling Calcite as a Proxy for the Palaeohydrogeology of a Fractured Granitic Gneiss, An Integration of Stable Isotopes, Fluid Inclusions and U-Series Dating (Talk). In: G.S.A.(Editor), Geological Society of America Annual Meeting. Geological Society of America, Toronto, Ontario, Canada, pp. A-225.

Burnett, W.C., Corbett, D.R., Schultz, M. and Fern, M., 1996. Analysis of Actinide Elements in Soils and Sediments, Proceedings 12th Annual Waste Testing and Quality Assurance Symposium. ACS/EPA, Washington, DC, pp. 77-86.

Cadieux, J.R., Jr. and Reboul, S.H., 1996. Separation and Analysis of Actinides by Extraction Chromatography Coupled with Alpha-Particle Liquid Scintillation Spectrometry. Radioactivity and Radiochemistry, 7(2): 30-34.

Carpenter, S.J., Lohmann, K.C., Holden, P., Walter, L.M., Huston, T.J., and Halliday, A., 1991. $\delta^{18}O$ values, $^{87}Sr/^{86}Sr$ and Sr/Mg ratios of Late Devonian abiotic marine calcite: Implications for the composition of ancient seawater. Geochimica et Cosmochimica Acta, 55: 1991-2010.

Catto, N.R., Patterson, R.J. and Gorman, W.A., 1981. Late Quaternary marine sediments at Chalk River, Ontario. Canadian Journal of Earth Science, 18: 1261-1267.

Catto, N.R., Patterson, R.J. and Gorman, W.A., 1982. The late Quaternary geology of the Chalk River region, Ontario and Quebec. Canadian Journal of Earth Science, 19: 1218-1231.

Chappell, J., Omura, A., Esat, T., McCulloch, M., Pandolfi, J., Ota, Y., and Pillans, B., 1996. Reconciliation of late Quaternary sea levels derived from coral terraces at Huon Peninsula with deep sea oxygen isotope records. Earth and Planetary Science Letters, 141: 227-236.

Clark, I.D., Khoury, H.N., Salameh, E., Fritz, P., Goksu, Y., Wieser, A., Causse, C., and Fontes, J.-C., 1991. Travertines in Central Jordan: Implications for palaeohydrology and dating. In: I.A.E.A. (Editor), Isotope Techniques in Water Resources Development. International Atomic Energy Agency, Vienna, pp. 551-565.

Clauer, N., Frape, S.K. and Fritz, B., 1989. Calcite veins of the Stripa granite (Sweden) as records of the origin of the groundwaters and their interactions with the granitic body. Geochimica et Cosmochimica Acta, 53: 1777-1781.

Coplen, T.B., Winograd, I.J., Landwehr, J.M. and Riggs, A.C., 1994. 500,000-Year Stable Carbon Isotopic Record from Devils Hole, Nevada. Science, 263: 361-365.

Cosca, M.A., 1989. Cooling and inferred uplift/erosion history of the Grenville Orogen, Ontario: Constraints from $^{40}Ar/^{39}Ar$ thermochronology; unpublished PhD Thesis, University of Michigan, Ann Arbor, Michigan, 223 pages.

Craig, H., 1957. Isotopic standards for carbon and oxygen and correction factors for mass-spectrometric analysis of carbon dioxide. Geochimica et Cosmochimica Acta, 12: 133-149.

Croudace, I., Warwick, P., Taylor, R. and Dee, S., 1998. Rapid procedure for plutonium and uranium determination in soils using a borate fusion followed by ion-exchange and extraction chromatography. Analytica Chimica Acta, 371: 217-225.

Crowley, T.J., 1994. Potential reconciliation of Devils Hole and deep-sea Pleistocene chronologies. Paleoceanography, 9(1): 1-5.

Culshaw, N.G., Corrigan, D., Jamieson, R.A., Ketchum, J., Wallace, P., and Wodicka, N., 1991. Traverse of the Central Gneiss Belt, Grenville Province, Georgian Bay: Geological Association of Canada, Toronto'91, Guidebook, Field Trip B.3, 40 pages.

Davison, C.C., Gascoyne, M., Kozak, E.T., Sikorsky, R.I. and Tomsons, D., 1995. Geology, geophysics and hydrogeology of boreholes RH-1, RH-2, and RH-3 drilled at the Chalk River Laboratories Property near Deep River, Ontario. Prepared for the Siting Task Force, for Low-Level Waste Management, STF Tech. Bib. No. 358.

Deines, P., Langmuir, D., and Harmon, R.S., 1974. Stable carbon isotope ratios and the existence of a gas phase in the evolution of carbonate ground waters. Geochimica et Cosmochimica Acta, 38: 1147-1164.

Demeny, A., Gatter, I. and Kazmer, M., 1997. The genesis of Mesozoic red calcite dikes of the Transdanubian range (Hungary): Fluid inclusion thermometry and stable isotope compositions. Geologica Carpathica, 48(5): 315-323.

Dicken, A.P., 1997. Radiogenic Isotope Geology. Cambridge University Press, Cambridge, 490 pp.

Dugal, J.J.B. and Kamineni, D.C., 1983. Lithology, Fracture Intensity, and Fracture Filling of Drill Core from Chalk River Research Area, Ontario. In: M.D. Thomas and D.F. Dixon (Editors), Geophysical and Related Geoscientific Research at Chalk River, Ontario. Atomic Energy of Canada Limited, Ottawa, Ontario, pp. 53-74.

Easten, R.M., 1992. The Grenville Province and the Proterozoic History of Central and Southern Ontario. In: R.M. Easten (Editor), Geology of Ontario. Ontario Geological Survey, pp. 714-902.

Edwards, R.L., Chen, J.H. and Wasserburg, G.J., 1986/87. ^{238}U-^{234}U-^{230}Th-^{232}Th systematics and the precise measurement of time over the past 500,000 years. Earth and Planetary Science Letters, 81: 175-192.

EiChrom Industries, 1994. Uranium and Thorium in Soil (Single Column). Analytical Procedures: 9.

EiChrom Industries, 1997. UTEVA Resin. Eichrom Ideas, 4(2): 6.

Faure, G., 1986. Principles of Isotope Geology. John Wiley and Sons, New York, 589 pp.

Faure, G., 1991. Principles and Applications of Inorganic Geochemistry: A Comprehensive Textbook for Geology Students. MacMillan Publishing Company, New York, 626 pp.

Fontes, J.-C., Gasse, F. and Gilbert, E., 1996. Holocene environmental changes in Lake Bangong basin (Western Tibet). Part 1: Chronology and stable isotopes of carbonates of a Holocene lacustrine core. Palaeogeography, Palaeoclimatology, Palaeoecology, 120: 25-47.

Frape, S.K., Blyth, A.R., Jones, M.G., Blomqvist, R., Tullborg, E.-L., McDermott, F., and Ivanovich, M., 1992. A comparison of calcite fracture mineralogy and geochemistry for the Canadian and Fennoscandian Shields. In: Y.K. Kharaka and A.S. Maest (Editors), The Seventh International Symposium on Water-Rock Interaction. A. A. Balkema, Park City, Utah, pp. 787-792.

Fritz, P., Fontes, J.-C., Frape, S.K., Louvat, D., Michelot, J.-L., and Balderer, W., 1989. The isotope geochemistry of carbon in groundwater at Stripa. Geochimica et Cosmochimica Acta, 53: 1765-1775.

Fritz, P., Reardon, E.J., Barker, J., Brown, R.M., Cherry, J.A., Killey, R.W.D., and McNaughton, D., 1978. The carbon isotope geochemistry of a small groundwater system in northeastern Ontario. Water Resources Research, 14(6): 1059-67.

Gascoyne, M., 1977. Uranium Series Dating of Speleothem: An Investigation of Technique, Data Processing and Precision. Tech.-Memo: 77-4, McMaster University, Hamilton, Ontario.

Gascoyne, M., 1979. Pleistocene climates determined from stable isotope and geochronologic studies of speleothem. Ph. D. Thesis, McMaster University, Hamilton, Ontario, 467 pp.

Gascoyne, M., Schwarcz, H.P. and Ford, D.C., 1980. A palaeotemperature record for the mid-Wisconsin in Vancouver Island. Nature, 285: 474-476.

Gascoyne, M., Schwarcz, H.P. and Ford, D.C., 1983. Uranium-series ages of speleothem from northwest England: Correlation with Quaternary climate. Philosophical Transactions of the Royal Society of London B, 301: 143-164.

Gascoyne, M., 1992. Geochemistry of the actinides and their daughters. In: M. Ivanovich and R.S. Harmon (Editors), Uranium-series Disequilibrium: Applications to Earth, Marine, and Environmental Sciences. Clarendon Press, Oxford, pp. 34-61.

Gascoyne, M., Brown, A., Ejeckam, R.B. and Everitt, R.A., 1997. Dating fractures and fracture movement in the Lac Du Bonnet Batholith. AECL-11725, COG-96-634-I, Atomic Energy of Canada Limited, Pinawa, Manitoba.

Gascoyne, M. and Kotzer T.K., 1997. Carbon-14 dating of groundwater: Interpretation of data from the Chalk River boreholes. AECL Report, RC-1816, COG-97-010.

Genty, D. and Massault, M., 1997. Bomb ^{14}C recorded in laminated speleothems: Calculation of dead carbon proportion. Radiocarbon, 39(1): 33-48.

Goede, A., McDermott, F., Hawkesworth, C., Webb, J. and Finlayson, B., 1996. Evidence of Younger Dryas and Neoglacial cooling in a Late Quaternary palaeotemperature record from a speleothem in eastern Victoria, Australia. Journal of Quaternary Science, 11(1): 1-7.

Golder Associates, 1995. Factual results of geological and hydrogeological characterization of site E1, Chalk River Laboratories Property, Deep River, Ontario. Internal Draft prepared for the Siting Task Force by Golder Associates Ltd., Mississauga, Ontario, STF Tech. Bib. No 399.

Goldstein, R.H., 1990. Petrographic and geochemical evidence for origin of paleospeleothems, New Mexico: Implications for the application of fluid inclusions to studies of diagenesis. Journal of Sedimentary Petrology, 60(2): 282-292.

Goldstein, R.H. and Reynolds, T.J., 1994. Systematics of Fluid Inclusions in Diagenic Minerals: SEPM Short Course 31. SEPM (Society for Sedimentary Geology), Tulsa, Oklahoma, 199 pp.

Goldstein, S.J., Rodriguez, J.M. and Lujan, N., 1997. Measurement and Application of Uranium Isotopes for Human and Environmental Monitoring. Health Physics, 72(1): 10-18.

Harmon, R.S., Land, L.S., Mitterer, R.M., Garrett, P., Schwarcz, H.P., and Larson, G.J., 1981. Bermuda sea level during the last interglacial. Nature, 289: 481-483.

Harmon, R.S. and Schwarcz, H.P., 1981. Changes in ^{2}H and ^{18}O enrichment of meteoric water and Pleistocene glaciation. Nature, 290: 125-128.

Hill, C.A., Dublyansky, Y.V., Harmon, R.S. and Schluter, C.M., 1995. Overview of calcite/opal deposits at or near the proposed high-level nuclear waste site, Yucca Mountain, Nevada, USA: Pedogenic, hypogene, or both? Environmental Geology, 26: 69-88.

Hindman, F.D., 1986. Actinide Separations for α Spectrometry Using Neodymium Fluoride Coprecipitation. Analytical Chemistry, 58(6): 1238-1241.

Holmes, J.A., Street-Perrott, F.A., Ivanovich, M. and Perrott, R.A., 1995. A late Quaternary palaeolimnological record from Jamaica based on trace-element chemistry of ostracod shells. Chemical Geology, 124: 143-160.

Horwitz, E.P., Dietz, M.L., Chiarizia, R., Diamond, H., Essling, A.M. and Graczyk, D., 1992. Separation and preconcentration of uranium from acidic media by extraction chromatography. Analytica Chimica Acta, 266: 25-37.

Horwitz, E.P., 1993. New Chromatographic Materials for Determinations of Actinides, Strontium, and Technetium in Environmental, Bioassay, and Nuclear Waste Samples. W-31-109-ENG-38, U.S. Department of Energy.

Hughes, R.J. and Evans, R.D., 1996. Anomalous Results in the Determination of San Joachin Soil Reference Material (Poster), Winter Conference on Plasma Spectrochemistry, Fort Lauderdale, Florida, USA, pp. 286.

Ivanovich, M., Latham, A.G. and Ku, T.-L., 1992. Uranium-series disequilibrium applications in geochronology. In: M. Ivanovich and R.S. Harmon (Editors), Uranium-series Disequilibrium: Applications to Earth, Marine, and Environmental Sciences. Clarendon Press, Oxford, pp. 62-94.

Ivanovich, M. and Harmon, R.S. (Editors), 1992. Uranium-series Disequilibrium: Applications to Earth, Marine, and Environmental Sciences. Claredon Press, Oxford, 910 pp.

Ivanovich, M., Benitez, A.H., Chambers, A.V. and Hasler, S.E., 1994. Uranium series isotopic study of fracture infill materials from El Berrocal Site, Spain. Radiochimica Acta, 66(7): 485-494.

Jones, M.G., Frape, S.K. and McNutt, R.H., 1987. A study of the late-stage secondary fracture mineralization at the Atomic Energy of Canada Ltd. - Underground Research Laboratory site, near Pinawa, Manitoba. Unpublished report to Atomic Energy of Canada Limited: 54.

Kerrich, R., 1987a. Stable Isotope Studies of Fluids in the Crust. In: T.K. Kyser (Editor), Short Course in Stable Isotope Geochemistry of Low Temperature Fluids. Mineralogical Association of Canada, Saskatoon, pp. 258-286.

Kerrich, R., 1987b. The Stable Isotope Geochemistry of Au-Ag Vein Deposits in Metamorphic Rocks. In: T.K. Kyser (Editor), Short Course in Stable Isotope Geochemistry of Low Temperature Fluids. Mineralogical Association of Canada, Saskatoon, pp. 287-336.

Killey, R.W.D. and Devgun, J.S., 1986. Hydrogeologic studies for CRNL's proposed shallow land burial site. AECL-9345, Atomic Energy of Canada Limited, Chalk River, Ontario.

Komor, S.C., 1995. Chemistry and petrography of calcite in the KTB pilot borehole, Bavarian Oberpfalz, Germany. Chemical Geology, 124: 199-215.

Kotzer, T., Lee, D.R. and Bukata, A., 1998. Isotopic, Geochemical and Geophysical Characterization of Groundwater Flow in Fractured Crystalline Rocks (Poster), GAC/MAC Annual Meeting, Quebec City, Quebec.

Ku, T.-L. and Liang, Z.-C., 1984. The dating of impure carbonates with decay-series isotopes. Nuclear Instruments and Methods in Physics Research, 223: 563-571.

Kyser, T.K., 1987. Equilibrium Fractionation Factors for Stable Isotopes. In: T.K. Kyser (Editor), Short Course in Stable Isotope Geochemistry of Low Temperature Fluids. Mineralogical Association of Canada, Saskatoon, pp. 1-84.

Lally, A.E., 1992. Chemical Procedures. In: M. Ivanovich and R.S. Harmon (Editors), Uranium-series Disequilibrium: Applications to Earth, Marine, and Environmental Sciences. Clarendon Press, Oxford, pp. 95-126.

Larson, S.A. and Tullborg, E.-L., 1984. Stable isotopes of fissure-filling calcite from Finnsjon, Uppland, Sweden. Lithos, 17: 117-125.

Lauriol, B., Ford, D.C., Cinq-Mars, J. and Morris, W.A., 1997. The chronology of speleothem deposition in northern Yukon and its relationships to permafrost. Canadian Journal of Earth Sciences, 34: 902-911.

Lee, D., Kotzer, T., King, K., Hartwig, D. and Welch, S.J., 1998. Geochemical, isotopic and hydrologic conceptualization of groundwater flow in the bedrock of the CRL site. AECL-11930, COG-98-141-I, Atomic Energy of Canada Limited, Chalk River, Ontario.

Lemeille, E., Letolle, R., Meliere, F. and Olive, P., 1980. Isotope and other physico-chemical parameters of palaeolake carbonates: Tools for climatic reconstruction. In: I.A.E.A. (Editor), Palaeoclimates and Palaeowaters: A Collection of Environmental Isotope Studies. International Atomic Energy Agency, Vienna, pp. 135-150.

Li, W.-X.,Lundberg, J., Dicken, A.P., Ford, D.C., Schwarcz, H.P., McNutt, R., and Williams, D., 1989. High-precision mass-spectrometric uranium-series dating of cave deposits and implications for palaeoclimate studies. Nature, 339: 534-536.

Li, H.-C., Ku, T.-L., Stott, L.D. and Anderson, R.F., 1997. Stable isotope studies on Mono Lake (California). 1. $\delta^{18}O$ in lake sediments as proxy for climatic change during the last 150 years. Limnology and Oceanography, 42(2): 230-238.

Lindblom, S., 1987. Evidence of fracturing and fluid movements in granite from Finnsjon, Sweden, derived from inclusions in fracture-filling calcite and prehnite. Chemical Geology, 61: 241-251.

Ludwig, K.R., Simmons, K.R., Szabo, B.J., Winograd, I.J., Landwehr, J.M., Riggs, A.C., and Hoffman, R.J., 1992. Mass-Spectrometric ^{230}Th-^{234}U-^{238}U Dating of the Devils Hole Calcite Vein. Science, 258: 284-287.

Lumbers, S.B., and Vertolli, V.M., 1991. Proterozoic plutonism within the Central Gneiss Belt and Grenville Front Tectonic Zone, Grenville Province, Ontario: in Program with Abstracts, Geological Association of Canada-Mineralogical Association of Canada-Society of Economic Geologists, v 16, p. A77.

Lundegard, P.D., 1994. Mixing zone origin of ^{13}C-depleted calcite cement: Oseberg Formation sandstones (Middle Jurassic), Veslefrikk Field, Norway. Geochimica et Cosmochimica Acta, 58(12): 2661-2675.

Mack, G.H., Cole, D.R., James, W.C., Giordano, T.H. and Salyards, S.L., 1994. Stable oxygen and carbon isotopes of pedogenic carbonate as indicators of Plio-Pleistocene paleoclimate in the Southern Rio Grande Rift, South-Central New Mexico. American Journal of Science, 294: 621-640.

Major, R.P. and Wilber, R.J., 1991. Crystal habit, geochemistry, and cathodoluminescence of magnesian calcite marine cements from the lower slope of Little Bahama Bank. Geological Society of America Bulletin, 103: 461-471.

Marshall, B.D., Whelan, J.F., Peterman, Z.E., Futa, K., Mahan, S.A., and Stuckless, J.S., 1992. Isotopic studies of fracture coatings at Yucca Mountain, Nevada, USA. In: Y.K. Kharaka and A.S. Maest (Editors), The Seventh International Symposium on Water-Rock Interaction. A. A. Balkema, Park City, Utah, USA, pp. 737-740.

Martinson, D.G., Pisias, N.G., Hays, J.D., Imbrie, J., Moore, T.C., Jr., and Shackleton, N.J., 1987. Age Dating and the Orbital Theory of the Ice Ages: Development of a High-Resolution 0 to 300,000-Year Chronostratigraphy. Quaternary Research, 27: 1-29.

McCrea, J.M., 1950. On the Isotopic Chemistry of Carbonates and a Paleotemperature Scale. The Journal of Chemical Physics, 18(6): 849-857.

McDermott, F., Ivanovich, M., Frape, S.K. and Hawkesworth, C.J., 1995. Palaeoclimatic Controls on Hydrological Systems: Evidence from U-Th dated calcite veins in the Fennoscandian and Canadian shields. In: I.A.E.A. (Editor), Isotopes in Water Resources Management. International Atomic Energy Agency, Vienna, pp. 401-416.

Menking, K.M., Bischoff, J.L., Fitzpatrick, J.A., Burdette, J.W. and Rye, R.O., 1997. Climatic/Hydrologic Oscillations since 155,000 yr B.P. at Owens Lake, California, Reflected in Abundance and Stable Isotope Composition of Sediment Carbonate. Quaternary Research, 48: 58-68.

Milton, G.M. and Brown, R.M., 1983. Uranium Series Disequilibrium in Rock/Water Systems of the Canadian Shield. In: I.A.E. Agency (Editor), Isotope Hydrology 1983. International Atomic Energy Agency, Vienna, pp. 433-445.

Milton, G.M., 1985. Uranium series disequilibrium in rock-water systems of the Canadian Shield. Ph. D. Thesis, University of Waterloo, Waterloo, Ontario, 233 pp.

Milton, G.M. and Brown, R.M., 1987. Uranium Series Dating of Calcite Coatings in Groundwater Flow Systems of the Canadian Shield. Chemical Geology (Isotope Geoscience Section), 65: 57-65.

Milton, G.M., 1987. Paleohydrological inferences from fracture calcite analyses: an example from the Stripa Project, Sweden. Applied Geochemistry, 2: 33-36.

Monger, H.C. and Adams, H.P., 1996. Micromorphology of Calcite-Silica Deposits, Yucca Mountain, Nevada. Soil Science Society of America Journal, 60: 519-530.

Muchez, P., Viaene, W. and Marshall, J.D., 1991. Origin of shallow burial cements in the Late Visean of the Campine Basin, Belgium. Sedimentary Geology, 73: 257-271.

Muhs, D.R. and Szabo, B.J., 1994. New uranium-series ages of the Waimanalo Limestone, Oahu, Hawaii: Implications for sea level during the last interglacial period. Marine Geology, 118: 315-326.

Muhs, D.R., Kennedy, G.L. and Rockwell, T.K., 1994. Uranium-Series Ages of Marine Terrace Corals from the Pacific Coast of North America and Implications for Last-Interglacial Sea Level History. Quaternary Research, 42: 72-87.

Noack, M.H., 1995. Estimating Groundwater Velocity for a Shallow Unconfined Aquifer using the $^{3}H/^{3}He^{*}$ Dating Technique: A Comparison to Other Hydrogeologic Methods. M. Sc. Thesis, Trent University, Peterborough, Ontario, 139 pp.

Nozaki, Y., Rye, D.M., Turekian, K.K. and Dodge, R.E., 1978. A 200 year record of carbon-13 and carbon-14 variations in a Bermuda coral. Geophysical Research Letters, 5(10): 825-828.

O'Neil, J.R., Clayton, R.N. and Mayeda, T.K., 1969. Oxygen Isotope Fractionation in Divalent Metal Carbonates. The Journal of Chemical Physics, 51(12): 5547-5558.

Ortec, 1996. MAESTRO™ for Windows: Software User's Manual, Version 3.0. EG&G Ortec, Oak Ridge, TN, 136 pp.

Pilvio, R. and Bickel, M., 1998. Separation of actinides from a bone ash matrix with extraction chromatography. Journal of Alloys and Compounds, 271-273: 49-53.

Quinn, T.M., 1991. Meteoric diagenesis of Plio-Pleistocene limestones at Enewetak Atoll. Journal of Sedimentary Petrology, 61(5): 681-703.

Rao, R.R. and Cooper, E.L., 1995. Separation of Low Levels of Actinides by Selective Oxidation/Reduction and Co-Precipitation with Neodymium Fluoride. Journal of Radioanalytical and Nuclear Chemistry, 197(1): 133-148.

Raven, K.G., 1980. Studies in fracture hydrology at Chalk River Nuclear Laboratories: 1977/78/79. AECL Report, TR-113.

Raven, K.G., 1986. Hydraulic Characterization of a Small Groundwater Flow System in Fractured Monzonitic Gneiss. AECL-9066, Whiteshell Nuclear Research Establishment, Pinawa, Manitoba.

Rea, D.K., Moore, T.C., Jr., Anderson, T.W., Lewis, C.F.M., Dobson, D.M., Dettman, D.L., Smith, A.J., and Mayer, L.A., 1994. Great Lakes paleohydrology: Complex interplay of glacial meltwater, lake levels, and sill depths. Geology, 22: 1059-1062.

Reyes, E., del Villar, L.P., Delgado, A., Cortecci, G., Nunez, R., Pelayo, M., and Cozar, J.S., 1998. Carbonation processes at the El Berrocal natural analogue granitic system (Spain): inferences from mineralogical and stable isotope studies. Chemical Geology, 150(3-4): 293-315.

Reynolds, P.H., 1992. Low Temperature Thermochronology by the 40Ar/39Ar Method. In: M. Zentilli and P.H. Reynolds (Editors), Short Course Handbook on Low Temperature Thermochronology. Mineralogical Association of Canada, Wolfville, Nova Scotia, pp. 3-19.

Richards, D.A., Smart, P.L. and Edwards, R.L., 1994. Maximum sea levels for the last glacial period from U-series ages of submerged speleothems. Nature, 367: 357-360.

Riggs, A.C., Carr, W.J., Kolesar, P.T. and Hoffman, R.J., 1994. Tectonic Speleogenesis of Devils Hole, Nevada, and Implications for Hydrogeology and the Development of Long, Continuous Paleoenviromental Records. Quaternary Research, 42: 241-254.

Roedder, E. (ed), 1984. Reviews in Mineralogy Volume 12: Fluid Inclusions, Mineralogical Society of America, 646 pages.

Saller, A.H. and Moore, C.H., Jr., 1991. Geochemistry of meteoric calcite cements in some Pleistocene limestones. Sedimentology, 38: 601-621.

Schwarcz, H. and Younge, C., 1980. Isotopic composition of palaeowaters as inferred from speleothem and its fluid inclusions. In: I.A.E. Agency (Editor), Palaeoclimates and Palaeowaters: A Collection of Environmental Isotope Studies. International Atomic Energy Agency, Vienna, pp. 115-133.

Schwarcz, H.P., and Blackwell, B., 1983. $^{230}Th/^{234}U$ age dating of a Mounterian Site in France. Nature, 301: 236-237.

Schwarcz, H.P., 1980. Absolute Dating of Travertines from Archaeological Sites. In: L.A. Currie (Editor), Nuclear and Chemical Dating Techniques: Interpreting the Environmental Record. ACS Symposium Series. American Chemical Society, Houston, Texas, pp. 475-490.

Seguin, A., 1994. Origin of Saline Groundwater in Torbolton Ward, Eastern Ontario. M.Sc. Thesis, University of Ottawa, Ottawa, Ontario, 112 pp.

Shepherd, T.J., Rankin, A.H. and Alderton, D.H.M., 1985. A Practical Guide to Fluid Inclusion Studies. Blackie and Son Limited, Glasgow, 239 pp.

Smith, J.E., Risk, M.J., Schwarcz, H.P. and McConnaughey, T.A., 1997. Rapid climate change in the North Atlantic during the Younger Dryas recorded by deep-sea corals. Nature, 386: 818-820.

Stuckless, J.S., Peterman, Z.E. and Muhs, D.R., 1991. U and Sr Isotopes in Ground Water and Calcite, Yucca Mountain, Nevada: Evidence Against Upwelling Water. Science, 254: 551-554.

Sultan, M., Sturchio, N., Hassan, F.A., Hamdan, M.A.R., Mahmood, A.M., Alfy, Z.E., and Stein, T., 1997. Precipitation Source Inferred from Stable Isotopic Composition of Pleistocene Groundwater and Carbonate Deposits in the Western Desert of Egypt. Quaternary Research, 48: 29-37.

Szabo, B.J. and Kyser, T.K., 1990. Ages and stable-isotope compositions of secondary calcite and opal in drill cores from Tertiary volcanic rocks of the Yucca Mountain area, Nevada. Geological Society of America Bulletin, 102: 1714-1719.

Szabo, B.J., Kolesar, P.T., Riggs, A.C., Winograd, I.J. and Ludwig, K.R., 1994a. Paleoclimatic Inferences from a 120,000-Yr Calcite Record of Water-Table Fluctuation in Browns Room of Devils Hole, Nevada. Quaternary Research, 41: 59-69.

Szabo, B.J., Ludwig, K.R., Muhs, D.R. and Simmons, K.R., 1994b. Thorium-230 Ages of Corals and Duration of the Last Interglacial Sea-Level High Stand on Oahu, Hawaii. Science, 266: 93-96.

Szabo, B.J., Bush, C.A. and Benson, L.V., 1996. Uranium-Series Dating of Carbonate (Tufa) Deposits Associated with Quaternary Fluctuations of Pyramid Lake, Nevada. Quaternary Research, 45: 271-281.

Szabo, B.J., 1997. Referred to as "in preparation" in Gascoyne et al, 1997.

Taylor, B.E., 1987. Stable Isotope Geochemistry of Ore-Forming Fluids. In: T.K. Kyser (Editor), Short Course in Stable Isotope Geochemistry of Low Temperature Fluids. Mineralogical Association of Canada, Saskatoon, pp. 337-445.

Veinott, G.I. and Cornett, R.J., 1998. Carbon isotopic disequilibrium in the shell of the freshwater mussel *Elliptio complanata*. Applied Geochemistry, 13: 49-57.

Vogel, J.C. and Kronfeld, J., 1997. Calibration of radiocarbon dates for the Late Pleistocene using U/Th dates on stalagmites. Radiocarbon, 39(1): 27-32.

Voltaggio, M., Barbieri, M., Branca, M., Castorina, F., Taddeucci, A., Tecce, F., Tuccimei, P., Turi, B., and Vesica, P., 1997. Calcite in fractures in a volcanic environment (Vulcano Island, Italy): contribution of geochronological and isotopic studies to volcanotectonics. Journal of Volcanology and Geothermal Research, 75: 271-282.

Wang, H. and Follomer, L.R., 1998. Proxy of monsoon seasonality in carbon isotopes from paleosols of the southern Chinese Loess Plateau. Geology, 26(11): 987-990.

Whittaker, S.G., James, N.P. and Kyser, T.K., 1994. Geochemistry of synsedimentary cements in Early Cambrian reefs. Geochimica et Cosmochimica Acta, 58(24): 5567-5577.

Winograd, I.J., Szabo, B.J., Coplen, T.B. and Riggs, A.C., 1988. A 250,000-Year Climatic Record from Great Basin Vein Calcite: Implications for Milankovitch Theory. Science, 242: 1275-1280.

Winograd, I.J., Coplen, T.B., Landwehr, J.M., Riggs, A.C., Ludwig, K.R., Szabo, B.J., Kolesar, P.T., and Revesz, K.M., 1992. Continuous 500,000-Year Climate Record from Vein Calcite in Devils Hole, Nevada. Science, 258: 255-260.

Winograd, I.J., Landwehr, J.M., Ludwig, K.R., Coplen, T.B. and Riggs, A.C., 1997. Duration and Structure of the Past Four Interglaciations. Quaternary Research, 48: 141-154.

Yakovlev, L.E., 1998. Isotopic Indications of the Genesis of Secondary Carbonates in the Muruntau Black Shale, Southern Tien Shan. Geochemistry International, 36(4): 318-328.

APPENDIX I - Radiochemical Calculations

Transforming α-spectrometry data into count rate and age data is a multi-step process. An overview of the calculations performed in this investigation is given here. The uncorrected count rate of each radio-nuclide is calculated as by equation AI-1.

$$A_{uncorrected} = \frac{Counts}{Time} \qquad (AI-1)$$

The count rate for each nuclide is then corrected for the background activity on the detector as well as the reagent blank and spike contribution in the α-decay energy range. The correction is represented by equation AI-2.

$$A_{corr} = A_{uncorrected} - A_{background} - A_{reagent} \qquad (AI-2)$$

It is easier to use the radio-chemical equations when the measurements are reported as count rates. Therefore, for the remainder of the appendix, unless otherwise stated, when a nuclide is listed, it is referring to the corrected count rate of that nuclide.

The principle radio-nuclides of interest (^{238}U, ^{234}U, ^{232}U, ^{232}Th, ^{230}Th, and ^{228}Th) were all corrected for both detector background and reagent blank. The reagent blank has two components, a contribution from the solutions used (water, acid etc.), and a contribution from the spike. The total spike contribution was different in each sample, as an attempt was made to spike each sample with a similar activity of the spike to the natural activity of the sample. As a result, different amounts of the spike were added to different samples throughout the investigation. This meant that the reagent correction had to be expressed in terms of the amount of the spike used (equation AI-3).

$$A_{reagent} = A_{solutions} + A_{spike}(/mL) * V_{spike}(mL) \qquad (AI-3)$$

The components of the spike (^{232}U and ^{228}Th) were only corrected for detector background and solution blanks, as their presence in the spike would not be considered contamination.

The count rate of the solution blank was determined by running through the extraction/separation protocol in the absence of either sample or spike. The solution blank was treated as though it were independent of the chemical yield. The solution blank was corrected for detector efficiency to create a blank that could be used in all detectors.

The contribution to the reagent blank from the spike was determined by running the extraction/separation protocol on solutions with different volumes of the spike. The solution blank component was assumed to be constant and the spike contribution to be linearly dependent on the volume of the spike used. The solution blank was also present in the measurement of the spike blank and had to be subtracted from the spike blank to determine the contribution of the spike on a per mL basis. The spike contribution to the blank was corrected for the detector efficiency and yield, to allow for its general application to each sample. The reagent blank correction required for each sample was expressed as a linear equation of the form y = mx + b, where y is the total correction, m is the spike contribution per mL, x is the volume of the spike used, and b is the solution blank. An idealized conception of the correction coefficients is given in Figure AI-1. The coefficients of the reagent blank correction for each of the radio-nuclides are summarized in Table AI-1. The coefficients must be corrected for the specific detector efficiency and

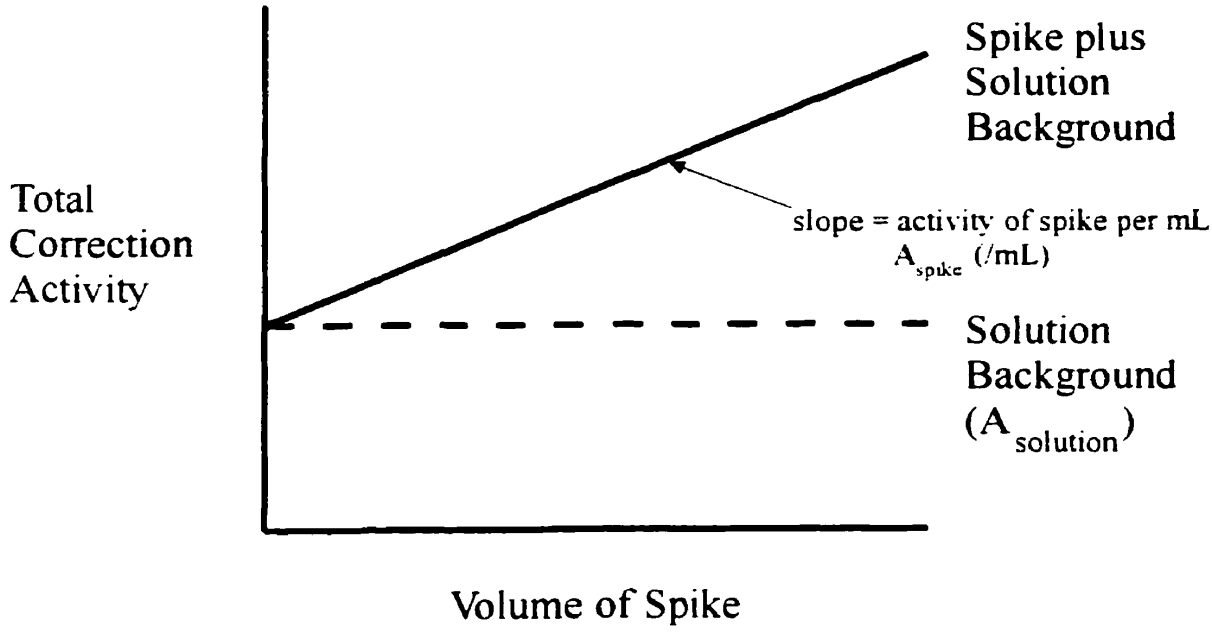

Figure AI-1 - An idealized representation of the co-efficients calculated to make the total reagent blank correction ($A_{reagent}$) from each of the nuclide activities measured. The constants from Table AI-1 are used in the following equation to determine the detector and sample specific reagent blank correction.

$$A_{reagent} = [A_{solution} * DE] + [A_{spike} * V_{spike} * DE * \frac{Yield}{100}]$$

DE = Detector efficiency (0 to 1)
Yield = U and Th yield
V_{spike} = volume of spike used (mL)

chemical yield prior to use (see Figure AI-1 and Table AI-1).

The concentrated spike was prepared by allowing ^{228}Th to in-grow from a ^{232}U source in solution. Once secular equilibrium had been achieved, the activity ratio of ^{228}Th/^{232}U in the spike was assumed constant at 1.027. This value is the transient equilibrium constant ($R_{A/B}$) for a short-lived daughter (^{230}Th) of a long-lived parent (^{234}U) and is calculated according to equation AI-4.

$$R_{B/A} = \frac{t_{1/2(A)}}{t_{1/2(A)} - t_{1/2(B)}} \qquad (AI\text{-}4)$$

$t_{1/2(A)}$ is the half-life of the long-lived parent and $t_{1/2(B)}$ is the half-life of the short-lived daughter. The ^{232}U/^{228}Th activity ratio is used to determine the activity of ^{228}Th in the spike. The ^{228}Th activity of the spike is crucial for the determination of Th in the sample.

The ^{228}Th measured by α-spectroscopy must be corrected for many factors. The first correction is for the spectral interference of ^{224}Ra which has ingrown since the Th was separated from the sample. As ^{224}Ra has a different chemistry, it will not be present in the Th fraction immediately after chemical extraction and separation of the Th from the sample; it accumulates as a result of ^{228}Th decay. To make the spectral correction, the theoretical total activity of ^{224}Ra generated in the sample since Th extraction and separation was calculated using equation AI-5.

TABLE AI-1 - The components of the reagent blank correction factor empirically determined from column runs of unspiked and spiked water. The count rates given are the total activities, and therefore, the solution contribution must be scaled down by the detector efficiency, and the spike contribution must be scaled down by the detector efficiency and the yield. The reagent blank correction for each nuclide is determined as;

$$A_{Reagent} = [A_{Solution} * DE] + [A_{Spike} * V_{Spike} * DE * \frac{Yield}{100}]$$

DE = Detector Efficiency
V_{spike} = volume of spike used (mL)
Yield = chemical yield of U or Th determined by yield tracer

Radio-nuclide	$A_{solution}$ (cpm) *	A_{spike} (cpm/mL)
^{238}U	0.005	0.013
^{234}U	0.004	0.034
^{232}U	0.052	**
^{232}Th	0.001	0.042
^{230}Th	0.000	0.092
^{228}Th	0.000	**

* - it is assumed that the solution contribution to the background is a constant and independent of the chemical yield
** - as ^{232}U and ^{228}Th are constituents of the spike, their presence in the spike fraction would not be treated as contamination

$$^{224}Ra_{theoretical} = {}^{228}Th_{corr} * [\frac{1 + e^{-\lambda_{Ra} * (t_{Th} - t_D)} - e^{-\lambda_{Ra} * t_D}}{\lambda_{Ra} * t_{Th}}] \qquad (AI-5)$$

λ_{Ra} = decay constant of Ra
t_{Th} = time of Th counting
t_D = time of delay between plating out and counting Th

The ^{228}Th activity was corrected by subtracting the possible ^{224}Ra contribution to the ^{228}Th peak measured. To make the correction, it was assumed that all the ^{224}Ra which decays with an α-particle energy of 5.447 MeV (5.4% of ^{224}Ra α-decay at 5.684 MeV; Ivanovich, 1992) contributes to the ^{228}Th peak at 5.427 MeV and must be removed. This correction was performed using equation AI-6.

$$^{228}Th_{Ra-corr} = {}^{228}Th_{Total} - (0.054 * {}^{224}Ra_{theoretical}) \qquad (AI-6)$$

The ^{228}Th was then corrected for the detrital (^{232}Th) component. In a "pristine" calcite, there should be negligible ^{232}Th present due to the low Th solubility in the calcite precipitating solution. As a result, any ^{232}Th present was assumed to be detrital in origin, and was treated as contamination introduced in nature or in the laboratory. ^{232}Th present in the calcite will decay to ^{228}Th at a rate that will eventually equal secular equilibrium. Thus, the maximum contribution from detrital Th to the ^{228}Th peak will equal the same activity as the ^{232}Th measured in the sample. This logic was used as the basis for the detrital Th correction (equation AI-7).

$$^{228}Th_{det-corr} = {}^{228}Th_{Ra-corr} - {}^{232}Th_{bkd-corr} \qquad AI-7)$$

The ^{228}Th activity was also corrected for decay of ^{228}Th during the time interval between plating out the Th for α-spectrometry and beginning the counting (equation AI-8).

$$^{228}Th_{final\text{-}corr} = {}^{228}Th_{det\text{-}corr} * e^{\lambda_{Th} \cdot t_D} \qquad (AI\text{-}8)$$

λ_{Th} = ^{228}Th decay constant
t_D = delay between plating out and α-counting

The percent yield of Th was calculated by comparing the $^{228}Th_{final\text{-}corr}$ to the ^{228}Th activity of the spike on the same detector (equation AI-9).

$$\%\ Yield\ Th = \frac{^{228}Th_{final\ corr}}{^{228}Th\ (/mL)_{corr\ for\ detector} * V_{spike}\ (mL)} * 100 \qquad (AI\text{-}9)$$

The activity of ^{232}Th was converted into a ^{232}Th concentration in ppm in the original sample. The concentration of Th in the sample was calculated using equation AI-10.

$$Th\ (ppm) = \frac{^{232}Th_{Total}}{^{232}Th\ (/\mu g)} * \frac{100}{\%\ Yield\ Th} \qquad (AI\text{-}10)$$

$^{232}Th_{Total}$ = Total ^{228}Th measured in the sample
^{232}Th (/μg) = the activity of 1 μg of ^{232}Th (0.246 dpm)

Equation AI-10 corrects the total ^{232}Th measured for the Th yield and then converts the activity to a mass of ^{232}Th. The uranium yield and concentration calculations are similar to the Th yield and concentration calculations (equations AI-11 and AI-12).

$$\%\ Yield\ U = \frac{^{232}U_{Total}}{^{232}U\ (/mL)_{corr\ for\ detector} * V_{spike}\ (mL)} * 100 \qquad (AI-11)$$

$$U\ (ppm) = \frac{\frac{^{238}U_{final-corr}}{^{238}U\ (/\mu g)} * \frac{100}{\%\ Yield\ U}}{Sample\ Weight\ (g)} \qquad (AI-12)$$

^{238}U (/μg) = the activity of 1 μg of ^{238}U (0.747 dpm)

The errors associated with the measurements and calculations were determined using the rules for error calculation of counting statistics and the associated rules of error propagation.

APPENDIX II - CALCULATION OF $^{230}Th/^{234}U$ AGES

The parent-daughter dating pair ^{234}U-^{230}Th is applicable to date any process that has chemically separated U and Th and formed a closed system. The general equation used for dating with the ^{234}U-^{230}Th pair is;

$$\frac{^{230}Th}{^{234}U} = 1 - e^{-\lambda_{230}t} \qquad (AII\text{-}1)$$

λ_{230} is the decay constant of ^{230}Th. However, equation AII-1 must be corrected for additional ^{234}U resulting from the decay of ^{238}U in the sample. A calcite which has been precipitated free of any initial Th can be dated by using the $^{230}Th/^{234}U$ ratio, and equation AII-2 (Kaufman and Broecker, 1965, in Gascoyne, 1992).

$$\frac{^{230}Th}{^{234}U} = \frac{1 - e^{-\lambda_{230}t}}{(\frac{^{234}U}{^{238}U})} + (1 - \frac{1}{(\frac{^{234}U}{^{238}U})}) * \frac{\lambda_{230}}{\lambda_{230} - \lambda_{234}} * (1 - e^{-(\lambda_{230} - \lambda_{234})t}) \qquad (AII\text{-}2)$$

λ_{230} = ^{230}Th decay constant
λ_{234} = ^{234}U decay constant

However, the calcite may co-precipitate detrital (^{232}Th) thorium. Aqueous Th exhibits the same chemical behaviour, regardless of whether it is ^{232}Th, ^{228}Th or ^{230}Th. Therefore, if the calcite precipitated ^{232}Th, it may have also precipitated ^{230}Th at the same time. If there is ^{232}Th present in the calcite, it cannot be assumed that all the ^{230}Th results from ingrowth during ^{234}U decay. To correct for any possible initial ^{230}Th, the $^{230}Th/^{232}Th$ ratio in the sample was calculated. If $^{230}Th/^{232}Th$ was less than 15, the sample was considered a "dirty

calcite," and the correction for the detrital Th of Ku and Laing (1984) (equation AII-3) was made.

$$^{230}Th_{calcite} = {}^{230}Th_{total} - R * ({}^{232}Th_{calcite} * e^{-\lambda_{230}t}) \qquad (AII\text{-}3)$$

λ_{230} = ^{230}Th decay constant
R = ratio of ^{232}Th to ^{230}Th initially, taken as 1.25 (Schwarcz and Blackwell, 1983)

In the dating equation (AII-2), the unknown, time (t), is in the exponent of two separate factors. This makes it impossible to isolate and directly solve for t. As a result, the equation is usually solved by use of an iterative program (Gascoyne, 1992). In this investigation, a spreadsheet was developed that determined a $(^{230}Th/^{234}U)_{calculated}$, given the $(^{234}U/^{238}U)_{measured}$ of the sample, and time at 100 year increments from 0 to 350 ka. The $(^{230}Th/^{234}U)_{calculated}$ was compared to the $(^{230}Th/^{234}U)_{measured}$ in the calcite, and the t which calculated the measured value was taken as the age of the calcite. This was repeated to calculate t for both the $(^{230}Th/^{234}U)_{measured}$ plus the error and $(^{230}Th/^{234}U)_{measured}$ minus the error (1-σ) calculated by the spike reduction program. This gave the upper and lower limits of the age respectively.

The algorithm designed to determine ages for this investigation also calculated the $^{230}Th_{calcite}$ using equation AII-3. In cases where the $(^{230}Th/^{232}Th)_{measured}$ of the calcite was greater than 15, the age calculated was recorded as the "uncorrected" age. If the $(^{230}Th/^{232}Th)_{measured}$ ratio was less than 15, the $^{230}Th_{calcite}$ activity was corrected by equation AII-3 and the process for determining t was repeated. The age calculated with the detrital ^{232}Th-corrected ratio was recorded as the "corrected" age.

APPENDIX III - DETECTION LIMIT AND REAGENT BLANK CONSTRAINTS ON THE APPLICABILITY OF THE TECHNIQUE TO $^{230}Th/^{234}U$ DATING

The applicability of the developed protocol to $^{230}Th/^{234}U$ dating of natural samples will be determined by the detection limit for U and Th. To determine a general lower limit of detection (LLD) for each of the nuclides, the average background across all detectors plus 2-σ, and the non-spiked reagent blank were summed. The total reagent blank is also a function of the volume of the spike used, therefore, the LLD for each nuclide is then expressed as an activity plus a spike contribution on a per mL basis. The LLD for each of the radio-nuclides is presented in Table AIII-1.

The age of the sample is recorded by ingrowth of ^{230}Th from decay of ^{234}U initially present in the sample. Thus, there is a minimum datable sample age as both the ^{234}U and the ^{230}Th in the sample have to be above the LLD. As a result, the applicability of the dating technique will be dependent upon both the concentration of U in the sample, and the sample's age. ^{230}Th activity can result from either a young sample with a high U concentration, or an old sample which has behaved as a closed system to U and Th since formation. To model the range of U concentrations and sample ages that this technique can be applied to, the ^{230}Th was fixed at the LLD and the ^{234}U activity was varied over a range of values. The general $^{230}Th/^{234}U$ dating equation (equation AII-2) was simplified and solved for t by assuming a $^{234}U/^{238}U$ activity ratio of 1. Using the LLD of ^{230}Th and varying ^{234}U, the minimum datable age was modelled as a function of the ^{234}U activity of the sample. The $^{234}U/^{238}U$ is used in the calculation of the $^{230}Th/^{234}U$ age, to correct for additional ^{234}U generated from ^{238}U decay in old calcites. As the minimum possible age

Table AIII-1 - Determination of the lower limit of detection (LLD) for each of the actinides measured in this study. These values were used to model the range of ages and U concentrations measurable in natural calcite by this technique. The LLD as a function of the volume of spike used was calculated as:

$$LLD_{spiked} = LLD_{unspiked} + A_{spike}(/mL) * V_{spike}(mL)$$

	Average Detector Background* (cpm)	2-σ (cpm)	LLD for an unspiked sample** (cpm)
^{238}U	0.001	0.002	0.008
^{234}U	0.003	0.003	0.010
^{232}U	0.020	0.033	0.105
^{232}Th	0.000	0.001	0.002
^{230}Th	0.001	0.001	0.002
^{228}Th	0.098	0.196	0.294

* - average of background across all detectors used was calculated to generate a LLD which could be applied to all samples, not a detector specific LLD

** - calculated as LLD = (avg background + 2-σ + $A_{solutions}$ (Table AI-1))

was being determined, it was unnecessary to correct for ^{238}U decay, and safe to set the $^{234}U/^{238}U$ activity ratio at 1 in the dating calculation. This assumes that all the ^{230}Th is present due to ^{234}U decay, and that there is no detrital Th correction. If there is a detrital Th correction, a younger age may be possible, but the error in the calculated age increases.

The datable range of ages in natural calcite as a function of the ^{234}U activity in the sample is represented graphically in Figure AIII-1. As the spike contribution to the LLD of both ^{230}Th and ^{234}U is dependent on the volume of the spike used, the range of datable ages is determined for three different volumes of spike, 0.10, 0.50 and 1.00 mL. From Figure AIII-1, it is evident that the minimum datable age is dependent on the ^{234}U activity of the sample, and that ages as young as 0 ka are obtainable, depending on the initial ^{234}U activity of the calcite and the volume of the spike used. The datable range of samples must lie on or above the line of minimum ages and to the right of the LLD of ^{234}U on Figure AIII-1. It can be seen in Figure AIII-1 that at volumes of the spike below 1 mL, the datable range of calcites by the protocol is limited by the LLD of ^{234}U, not by the LLD of ^{230}Th. If the ^{234}U activity in the sample is known, it is possible to use Figure AIII-1 to determine whether a reliable $^{230}Th/^{234}U$ age could be calculated, or as a check of the reliability of a calculated age.

To determine the range of sample U masses to which this protocol is applicable, the $^{234}U/^{238}U$ activity ratio in the sample must be characterized. Once the mass of U required to perform dating is established, it can serve as an indication of whether suitable samples or mass of sample are available. For example, 1 μg of U could be supplied by 1 g of a 1 ppm calcite or by 0.1 g of a 10 ppm calcite. ^{238}U is the most abundant isotope of U

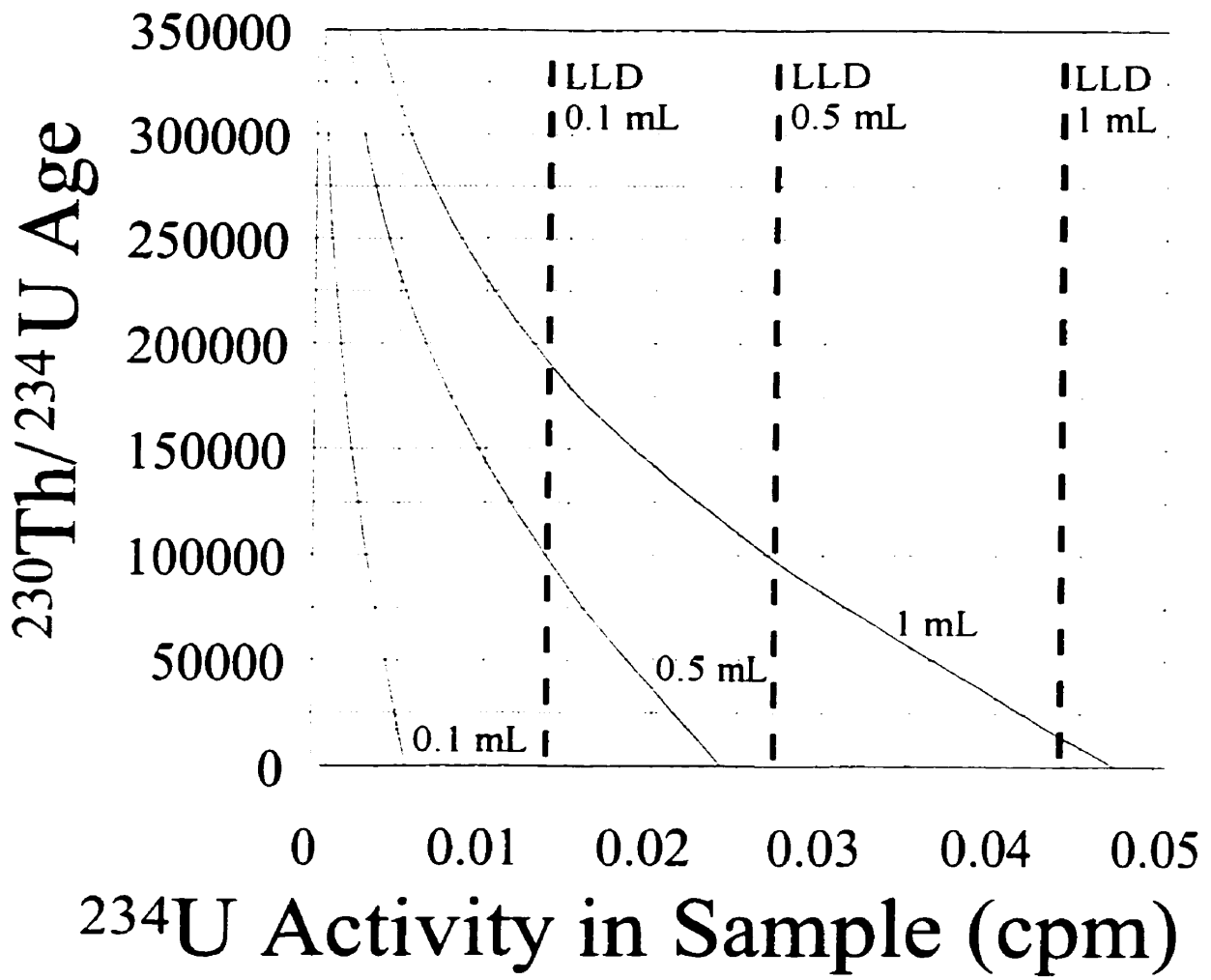

Figure AIII-1 - The minimum age calculable as a function of the ^{234}U activity in the calcite. The ^{230}Th activity was fixed at the LLD for three spike volumes, the ^{234}U activity was varied, the $^{234}U/^{238}U$ activity was fixed at 1, and the $^{230}Th/^{234}U$ age dating equation was solved for time. Below 1 mL of spike, the range of datable calcites is limited by the sample's ^{234}U activity, not the ^{230}Th activity in the sample.

(99.276% by mass), and as a result U concentration is expressed in terms of ^{238}U. The $^{234}U/^{238}U$ activity ratio can vary spatially and temporally in the natural environment. The $^{234}U/^{238}U$ activity ratio in natural waters can vary from 1 to 10 (Faure, 1991), although in most speleothems the ratio is between 0.8 and 2.6 (Gascoyne, 1977). The youngest datable calcites presented in terms of U mass in the calcite sample are a function of the LLD of ^{234}U, the LLD of ^{238}U, and the $^{234}U/^{238}U$ activity ratio. The minimum datable ranges of calcite U masses are presented as a function of the $^{234}U/^{238}U$ activity ratio in Figure AIII-2. The datable range of calcite U masses lies above both the line for minimum U mass, given the LLD of ^{234}U at the specific volume of the spike, and the spike volume specific LLD of ^{238}U. Assuming a $^{234}U/^{238}U$ activity in the low end of the range (in the range expected for speleothem), a minimum initial U mass of 0.075 μg is required to perform $^{230}Th/^{234}U$ dating with 1 mL of the spike, 0.05 μg for 0.5 mL of spike, and 0.025 μg for 0.1 mL spikes using the protocol developed in this investigation. Thus if the U concentration and the mass of calcite available are known, it can be determined using Figures AIII-1 and AIII-2 whether the sample could be effectively dated using the protocol developed in this investigation. The development of these figures allows for the possibility of using a technique such as ICP-MS to screen samples for suitability prior to analysis using the technique developed in this investigation.

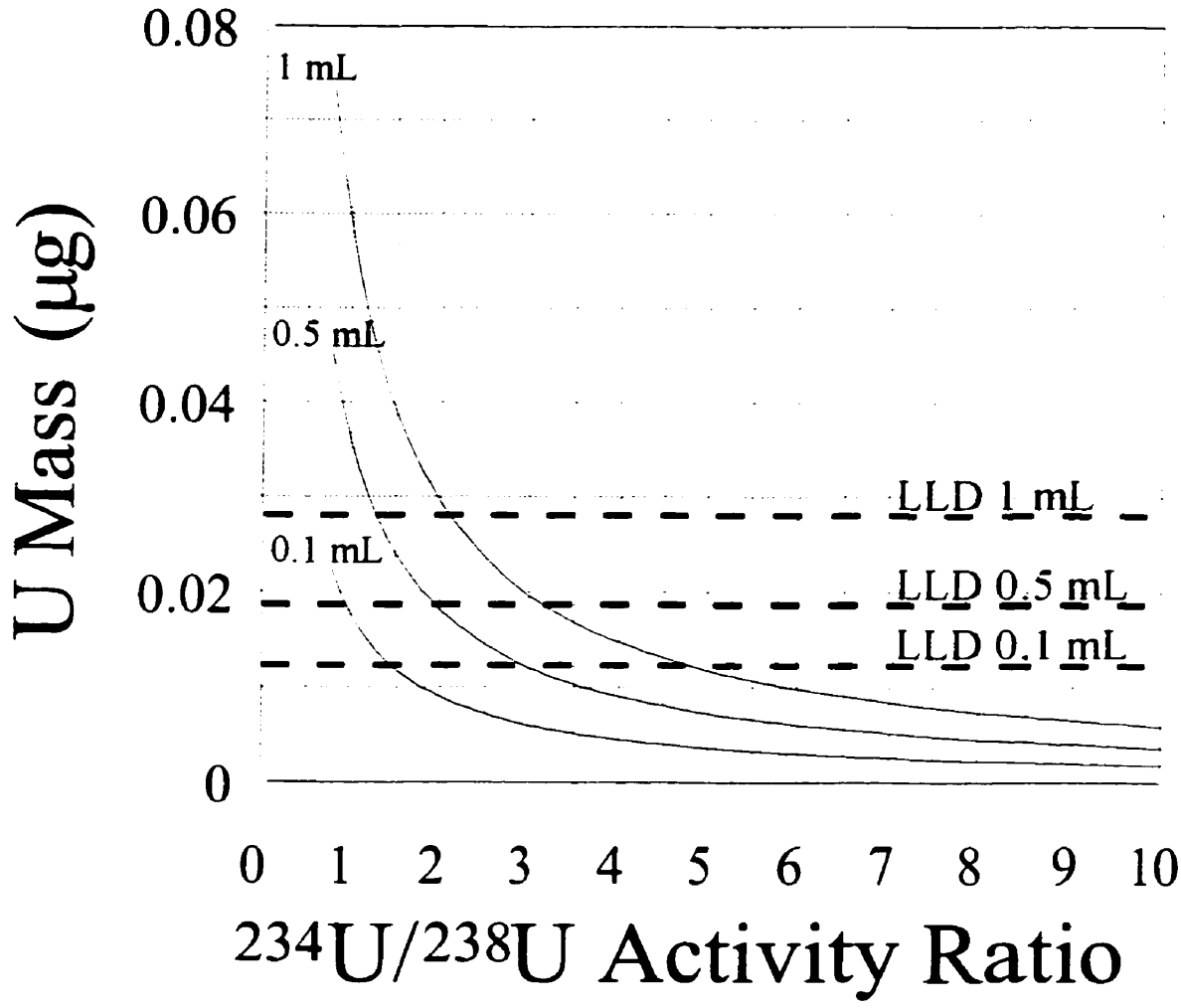

Figure AIII-2 - The mass of U required to date calcites using the method developed in this investigation as a function of the $^{234}U/^{238}U$ activity ratio and the volume of spike used in the sample. The curves represent the mass of ^{238}U in the sample with the specified $^{234}U/^{238}U$ activity ratio at the LLD of ^{234}U for three different volumes of spike (0.1, 0.5 and 1 mL). The horizontal lines represent the corresponding LLD's of ^{238}U for each volume of spike. A datable mass of U must lie above the LLD of ^{238}U and to the right of the curve representing the LLD of ^{234}U for the volume of spike used.

APPENDIX IV - SAMPLE DESCRIPTIONS

SAMPLE	DESCRIPTION
CR9-31.7	- sealed horizontal fracture - friable, looks cemented with very white calcite - looks old
CR9-161.0	- sub-vertical sealed fracture lined with calcite
CR9-167.5	- sub-vertical open fracture lined with platy calcite
CR9-179.5	- vertical fracture, possibly open, filled with thin platy calcite
CR9-350.9	- very open fractures - brecciated zone (like CR18-30) - many fractures filled with massive calcite
CR9-352.0	- sub-vertical fracture sealed with fine grained calcite - very old looking
CR9-468.65	- early horizontal fracture sealed with chlorite - no samples taken
CR9-522.9	- highly brecciated injurated fault zone (like CR18) - could be carbonate, very friable, small veins sealed with calcite
CR9-522.9B	- small piece of above, appears to be calcite, fine grained cement
CR9-528.7	- very fractured rock, water bearing zone, calcite contains a lot of hemetite
CR9-545.8	- calcite lining a possibly open fracture - very old looking
CR9-547.7	- open fracture next to sealed fracture (both sub-vertical) - massive calcite in open fracture, thin and platy calcite in sealed vein
CR18-30	- calcite cement sealing a highly fractured brecciated zone - fine grained
RH1-35.5	- intersection of 2 sub-vertical fractures - massive calcite in sealed vein (~ 1 mm)
RH1-45.4	- very fractured - small amount of fine grained (platy) calcite in open veins
RH1-69.3	- sub-vertical fracture sealed with fine grained to massive calcite

RH1-95.7	- platy calcite in water-bearing (open) sub-vertical fracture
RH1-99.4	- thin layer of fine grained calcite in an open fracture - highly brecciated zone
RH1-132.7	- sub-vertical fracture (possibly open) - contains thin layer of platy calcite
RH1-143.2	- sub-vertical fracture sealed with massive calcite
RH1-159.0	- sub-vertical sealed narrow fracture - contains massive calcite crystals
RH1-188.3	- sub-vertical open fracture containing platy and euhedral calcite
RH3-43	- large euhedral calcite crystals in open vein - young looking vertical fracture
RH3-54	- open vertical fracture lined by fine grained calcite
RH3-55	- large euhedral calcite crystals on sub-vertical open fracture
RH3-65.5	- sub-vertical open fracture with large euhedral calcite crystals - calcite is vuggy
RH3-87.7	- very fine grained calcite on horizontal fractures - looks old
RH3-102.2	- sub-vertical open fracture lined by thin platy calcite
RH3-180.6	- massive platy calcite on open horizontal fracture - horizontal fracture connects to a vertical fracture (also open)
RH3-181	- massive calcite in sealed vertical fracture
RH3-181.7	- sub-vertical open fracture - platy calcite coating walls of fracture
E1-26.5	- calcite crystals in sub-vertical open fracture - fell out of core
E1-59.7	- sub-vertical fractures sealed with calcite and chlorite - very fine grained
E1-63.25	- sub-vertical open fracture lined with massive euhedral calcite

E1-75.98	- horizontal calcite layer in chlorite host - very friable
E1-137.25	- vertical fracture sealed with massive calcite
E1-150.5	- sub-vertical fracture sealed with massive calcite
E1-170.5	- very small calcite crystals in large open vug in the host rock - not sampled for anything
E1-176.5	- thin platy calcite sealing a fracture
E1-190.2	- open vertical fracture with large euhedral calcite crystals

APPENDIX V - STABLE ISOTOPE DATA

Sample	Yield (%)	C-13 V-PDB	O-18 V-SMOW	Notes
E1-26.5	8.2	-10.0	22.6	
E1-63.25	8.4	-6.8	16.7	
E1-190.2	8.4	-7.2	15.6	
E1-59.7	4.5	-9.1	20.0	
E1-59.7	5.7	-8.8	19.4	re-run
E1-137.2	8.8	-7.4	18.9	
E1-150.5	7.5	-5.4	15.5	cc
E1-150.5	1.2	-5.3	16.7	cc + dol
E1-150.5	0.6	-5.5	17.2	dol
E1-176.5	8.5	-5.4	16.0	
RH3-43	7.9	-7.8	19.1	
RH3-54	8.7	-6.8	20.3	
RH3-55	8.6	-8.4	20.7	a
RH3-55	8.3	-8.3	20.4	b
RH3-65.5	8.1	-10.7	21.9	
RH3-102.	8.3	-5.7	15.4	
RH3-102.	8.2	-5.5	15.5	re-run
RH3-181	6.5	-6.7	17.7	
RH3-181	9.1	-7.0	18.1	re-run
CR18-30	4.8	-4.8	18.7	cc
CR18-30	3.7	-4.6	19.1	cc + dol
CR18-30	1.9	-4.7	19.3	dol
RH1-45.4	9.1	-6.9	17.9	
RH1-99.4	8.4	-6.7	15.7	
RH1-132.	5	-5.9	18.4	
RH1-188.	9.3	-6	17.3	
RH1-35.5	7.7	-6.6	16.3	

NOTE: cc = calcite, dol = dolomite
a, b, c, d represent multiple samples

APPENDIX V - Continued

Sample	Yield (%)	C-13 V-PDB	O-18 V-SMOW	Notes	
RH1-69.1	8.5	-6.4	17.4		
RH1-159	7.9	-5.7	19.2		
RH1-193.	6.7	-5.6	14.9		
E1-26.5	8.8	-9	23.1	quality control	
RH3-180.	5.9	-8.5	28.8		
RH3-181.	6.6	-6.7	15.5		
RH3-87.7	7.4	-7	20.3		
CR9-167.	8.9	-6.6	15.9		
CR9-172.	7.4	-6.9	16.6		
CR9-350.	8.2	-6.9	16.7		
CR9-545.	7	-6.4	16.9		
CR9-547.	8.9	-6.7	16.9		
CR9-161	6.7	-8.1	20.5		
CR9-352	6.7	-6.3	15.5		
RH1-193	8.2	-5.5	15.2	a	test homogeneity
RH1-193	8.3	-5.8	14.7	a-re-run	along calcite growth
RH1-193	8.8	-5.8	14.9	b	axis (a is closest to
RH1-193	7.9	-5.7	14.9	c	fracture wall, d is in
RH1-193	6.8	-5.8	14.9	d	the centre)
RH3-181	7.9	-6.3	15.9	a	test homogenaity
RH3-181	8.7	-5.7	15	b	along a fracture
RH3-181	8.6	-5.7	15.5	c	
RH3-181	5.9	-5.8	15.1	d	

NOTE: cc = calcite, dol = dolomite
a, b, c, d represent multiple samples

APPENDIX VI - FLUID INCLUSION DATA

Sample	Size (um)	F	Tm (C)	Th (C)	NOTES
RH3-55	17.5 * 17.5	0.95		88.4	
	3.5 * 10.5	0.95	-4.1	88.4	
	17.5 * 17.5	0.95	0	95.3	
	3.5 * 10.5	0.95	-4.1	78.5	
	17.5 * 17.5	0.95	-3	87.5	
	10.5 * 10.5	1	-0.1		Th < 50
	7.0 * 10.5	0.95	-18.7	86.2	
	7.0 * 10.5	0.95	-3	86.3	
	7.0 * 10.5	0.95	-19	87.6	
	7.0 * 10.5	0.95	-1.2	87.9	
	3.5 * 10.5	1	0	87.9	
E1-63.5	7.0 * 7.0	0.95	-1.8	85.6	
	5.3 * 10.5	0.95	-1.9	89.5	
	3.5 * 7.0	0.95	-1.8	87.2	
	8.8 * 8.8	0.95	-3.4	88.9	
	7.0 * 7.0	0.9	-1.8	85.2	
RH3-43	10.5 * 14.0	0.95		222	Th->222
	24.5 * 35.0	0.95	-0.4	222	
	24.5 * 35.0	0.95	-0.1	222	Th-leaked
RH3-65.3	14.0 * 17.5	0.95	-9.9	86.4	
	14.0 * 17.5	0.95	0.5		Tm-free motion
	5.3 * 8.8	0.95		103	
	14.0 * 17.5	0.95	-9.9	83.6	
RH1-69.2	3.5 * 10.5	0.95	0	79.4	Tm=-1 to +1
	8.8 * 10.5	0.95	0	83.9	
	8.8 * 10.5	0.95	0	82.4	
	14.0 * 28.0	0.95	0	88.6	
	17.5 * 35.0	0.95		88.9	
	17.5 * 26.3	0.95		100	Th>100
	10.5 * 24.5	0.95		137.4	

APPENDIX VI - Continued

Sample	Size (um)	F	Tm (C)	Th (C)	NOTES
CR18-30	3.5 * 10.5	0.95		59.9	
	7.0 * 10.5	0.95		100.5	Th>100.5
	7.0 * 10.5	0.95	-0.6	100.5	
	10.5 * 10.5	0.95		100.5	
	10.5 * 15.8	0.95	-0.9	89.2	
	7.0 * 8.8	0.95	0.2	117.3	Tm=-.5 to +1
	7.0 * 8.8	0.95	-0.4	48	Tm=-.6 to -.1
RH1-159	14.0 * 14.0	0.9	-0.1	125.1	Tm=-.4 to +.2 Th>125.1
	7.0 * 10.5	0.59		125.6	Th>125.6
	14.0 * 17.5	0.9		125.6	
	3.5 * 7.0	0.95		60	

APPENDIX VII - RADIOCHEMICAL DATA

SAMPLE	MEASURED RATIOS				CALCULATED RATIOS					
	Th230/ U234	U232/ Th228	Th230/ U238	Th230/ Th232	U234/ U238	error	Th230/ U238	error	Th230/ U238	error
76126-14	0.03	1.27	0.02	2.33	0.75	0.01	0.03	0.00	0.03	0.00
76126-14*	0.01	1.27	0.01		0.75	0.01	0.02	0.00	0.01	0.00
76126-15	0.02	1.14	0.01	3.39	0.74	0.01	0.02	0.00	0.02	0.00
76126-15*	0.01	1.14	0.01		0.74	0.01	0.01	0.00	0.01	0.00
76001-18	0.44	0.73	0.86	-17.16	1.97	0.07	0.33	0.01	0.64	0.02
76001-22	0.93	0.41	1.85	28.56	2.00	0.07	0.39	0.01	0.78	0.03
76001-23	0.37	0.90	0.73	-143.99	1.95	0.04	0.35	0.01	0.67	0.02
76001-42	0.43	0.73	0.93	-551.78	2.14	0.12	0.32	0.02	0.69	0.05
1000ppmU-17	0.00	1.01	0.00	0.32	0.40	0.00	0.00	0.00	0.00	0.00
RH1-193.2-30	2.06	0.87	2.20	-4.22	1.07	0.19	1.83	0.31	1.95	0.31
RH3-65.3-31	-0.01	2.19	-0.06	0.38	5.41	0.93	-0.02	-0.02	-0.13	-0.12
RH3-65.3-31*	0.00	2.19	0.00		5.41	0.93	0.00	0.02	0.00	0.11
RH3-65.3-31b	-0.04	1.99	-0.07	0.38	1.68	0.08	-0.09	-0.08	-0.14	-0.13
RH3-65.3-31b*	0.00	1.99	0.00		1.68	0.08	0.00	0.08	0.00	0.13
RH3-181-32	24.25	0.77	-14.94	3.09	-0.62	-0.85	19.29	14.55	-11.88	-13.83
RH3-181-32b	-5.67	0.60	4.72	2.66	-0.83	-1.17	-3.47	-2.00	2.89	3.80
CR9-547.7-33	0.16	0.89	0.60	-2.62	3.87	1.79	0.14	0.17	0.55	0.70
CR9-547.7-33b	0.61	0.91	1.12	-12.65	1.83	0.25	0.57	0.12	1.04	0.22
CR9-167.5-34	1.30	1.01	2.09	6.31	1.60	0.15	1.35	0.11	2.16	0.19
E1-150.5-35	1.28	0.64	2.28	1.86	1.78	0.17	0.85	0.07	1.51	0.14
E1-150.5-35*	1.09	0.64	1.93		1.78	0.17	0.72	0.07	1.27	0.12
CR9-172.5-36	1.10	0.66	1.71	3.16	1.56	0.04	0.74	0.02	1.16	0.04
CR9-172.5-36*	0.97	0.66	1.51		1.56	0.04	0.66	0.02	1.02	0.03
E1-176.5-37	1.52	0.71	2.10	3.81	1.38	0.05	1.10	0.04	1.53	0.06
RH3-102.2-38	1.37	1.24	1.58	16.67	1.16	0.13	1.74	0.17	2.02	0.20
CR18-30-39	1.03	0.50	2.64	-4.65	2.56	1.25	0.53	0.26	1.35	0.60
RH3-43-40	1.19	0.74	1.19	1.39	1.00	0.03	0.90	0.03	0.90	0.03
RH3-43-40*	1.09	0.74	1.09		1.00	0.03	0.83	0.02	0.82	0.02
E1-26.5-41	1.03	1.02	1.72	-392.35	1.67	0.17	1.08	0.10	1.80	0.18

NOTE - The components of the sample name are significant for data interpretation. The first group of numbers are used for sample identification, and the final number is the column used for U/Th extraction/separation. If the sample name ends with a 'b', the sample has been re-counted. If the sample name ends with an asterisk, the sample has been ^{232}Th corrected.

APPENDIX VII -Continued

SAMPLE	MASS (g)	SPIKE (mL)	U (ppm)	Th (ppm)	YIELD U (%)	Th (%)
76126-14	1.1508	1	12.99	0.59	91.09	72.61
76126-15	1.0505	1	12.41	0.36	82.49	79.31
76001-18	1.108	1	0.81	0.07	88.89	70.74
76001-22	1.0588	1	0.72	0.23	34.29	84.51
76001-23	1.0082	1	0.78	0.17	85.13	74.72
76001-42	0.1357	0.1	0.64	0.16	77.8	95.27
1000ppmU-17	0.06	1	1006.16	17.45	63.55	54.48
RH1-193.2-30	1.0366	1	0.07	0.08	79.07	79.26
RH3-65.3-31	0.977	1	0.12	0.07	89.84	43.87
RH3-65.3-31b	0.977	1	0.1	0.07	89.76	43.87
RH3-181-32	0.9501	1	0.01	0.08	58.19	77.31
RH3-181-32b	0.9501	1	0.01	0.21	53.08	100.48
CR9-547.7-33	0.4922	0.5	0.05	0.15	80.96	78.81
CR9-547.7-33b	0.4922	0.5	0.04	0.18	81.39	77.84
CR9-167.5-34	0.9257	0.1	0.05	0.08	82.8	89.15
E1-150.5-35	0.2619	0.1	0.15	0.46	78.94	102.63
CR9-172.5-36	0.4082	0.1	2.01	2.33	77.81	99.17
E1-176.5-37	0.9843	0.1	0.42	0.54	77.37	94.84
RH3-102.2-38	0.5227	0.2	0.13	0.13	76.86	67.18
CR18-30-39	1.5588	0.2	0.01	0.02	53.5	89.5
RH3-43-40	0.921	0.2	0.78	1.61	74.76	94.93
E1-26.5-41	0.383	0.1	0.13	0.06	79.91	75.95

NOTE - The components of the sample name are significant for data interpretation. The first group of numbers are used for sample identification, and the final number is the column used for U/Th extraction/separation. If the sample name ends with a 'b', the sample has been re-counted.

APPENDIX VIII - TRACE ELEMENT DATA

The trace element data was measured on the ICP-MS at the same time as the U and Th described in the methods. All values are given as ppm concentrations in the calcite, except for Ca and Mg which are given in percent.

SAMPLE	Ca (%)	Mg (%)	Al (ppm)	Mn (ppm)	Sr (ppm)	Fe (ppm)	Zn (ppm)	Th (ppm)	U (ppm)
RH1-159	27.0	10.3	265.4	5780.7	118.4	8180.7	6.14	0.195	0.027
CR18-30	25.8	11.5	48.8	3439.6	80.0	7888.6	1.19	0.005	0.000
RH1-69.2	30.8	0.3	2165.7	3453.3	108.3	3071.9	5.02	0.153	0.326
RH1-35.5	30.2	1.0	7129.5	3586.2	133.6	7674.3	40.10	5.155	0.703
CR9-547.7	30.1	0.8	1719.9	3649.8	139.9	2425.2	3.56	0.259	0.088
RH3-181.7	39.9	0.1	3621.5	1431.9	112.2	1728.6	4.12	3.103	0.442
CR9-172.5	29.7	0.6	7678.2	908.4	153.3	13338.9	29.85	6.250	1.095
CR9-161	35.0	0.8	4867.3	2411.4	190.1	7352.0	3598.89	0.105	0.099
E1-190.2	37.9	0.0	1.1	1132.7	43.6	426.7	0.49	0.173	0.064
RH3-54	32.4	0.1	207.5	5039.8	178.9	1745.6	2.13	0.054	0.358
CR9-545.8	34.5	0.5	9399.0	2731.6	184.0	4744.7	21.05	2.043	1.183
CR9-350.9	30.0	0.5	3845.6	2158.9	188.0	4865.2	11.28	0.457	0.534
RH1-45.4	33.5	0.2	1892.2	1533.9	138.5	2316.9	7.02	0.036	0.083
E1-176.5	32.6	0.2	1464.8	2575.3	130.9	1772.4	2.25	0.825	0.425
RH3-65.3	33.2	0.0	251.0	2177.1	109.1	547.0	0.75	0.014	0.091
E1-137.25	33.3	0.1	321.9	2502.6	115.6	1018.6	1.17	0.212	0.321
RH3 -181	34.2	0.0	40.7	2244.1	100.6	351.7	0.46	0.061	0.019
E1-150.5	33.4	1.6	2891.0	3149.0	216.4	5501.3	4.10	0.279	0.030
RH3-102.2	43.5	1.3	11536.9	2929.0	181.9	9366.3	5.73	0.153	0.160
RH1-132.7	45.7	1.1	9393.7	2629.6	176.4	11498.1	64.58	0.340	3.097
CR9-352	43.0	3.6	9989.6	5292.1	262.4	10980.0	11.42	1.005	0.163
E1-59.7	41.2	1.3	14081.8	2414.1	208.8	13274.5	11.51	0.167	1.238
CR9-167.5	32.5	0.1	233.9	1789.7	93.1	1020.1	1.11	0.127	0.068
RH3-65.3	31.3	0.0	121.9	1863.8	115.6	402.0	1.88	0.033	0.213
RH3-87.7	36.5	0.7	7097.7	4114.7	248.2	6166.9	93.73	0.239	0.592
RH1-99.4	36.3	0.1	1224.3	405.2	81.2	1948.0	5.90	0.074	0.102
RH1-45.4	37.4	0.2	1564.9	1853.6	149.2	3301.4	7.41	0.070	0.094
RH1-159	25.8	8.2	241.1	5324.0	125.7	10582.4	1.91	0.243	0.029